INAIA RHAVENE FREIRE FAGUNDES NACARATH

BIOCHEMICAL AND PHYSIOLOGICAL RESPONSES OF COMMON BEAN INFECTED BY *Sclerotinia sclerotiorum* MEDIATED BY OXALIC ACID AND PHOSPHITES AND DIAGRAMMATIC SCALE FOR ASSESSMENT OF WHITE MOLD SEVERITY

Tese apresentada à Universidade Federal de Viçosa, como parte das exigências do Programa de Pós-Graduação em Fitopatologia, para obtenção do título de *Doctor Scientiae*.

VIÇOSA
MINAS GERAIS – BRASIL
2018

Ficha catalográfica preparada pela Biblioteca Central da Universidade Federal de Viçosa - Câmpus Viçosa

T
F156b
2018

Nacarath, Inaia Rhavene Freire Fagundes, 1989-
Biochemical and physiological responses of common bean infected by *Sclerotinia sclerotiorum* mediated by oxalic acid and phosphites and diagrammatic scale for assessment of white mold severity / Inaia Rhavene Freire Fagundes Nacarath. – Viçosa, MG, 2018.
xii, 153f. : il. (algumas color.) ; 29 cm.

Orientador: Fabrício de Ávila Rodrigues.
Tese (doutorado) - Universidade Federal de Viçosa.
Inclui bibliografia.

1. *Phaseolus vulgaris*. 2. Feijão. 3. *Sclerotinia sclerotiorum. 4.* Fotossíntese. 5. Mofo branco. I. Universidade Federal de Viçosa. Departamento de Fitopatologia. Programa de Pós-graduação em Fitopatologia. II. Título.

CDD 22. ed. 632.47

INAIA RHAVENE FREIRE FAGUNDES NACARATH

BIOCHEMICAL AND PHYSIOLOGICAL RESPONSES OF COMMON BEAN INFECTED BY *Sclerotinia sclerotiorum* MEDIATED BY OXALIC ACID AND PHOSPHITES AND DIAGRAMMATIC SCALE FOR ASSESSMENT OF WHITE MOLD SEVERITY

Tese apresentada à Universidade Federal de Viçosa, como parte das exigências do Programa de Pós-Graduação em Fitopatologia, para obtenção do título de *Doctor Scientiae*.

APROVADA: 21 de março de 2018.

Dimas Mendes Ribeiro

Gleiber Quintão Furtado

José Eustáquio de Souza Carneiro

Paulo Cezar Cavatte

Fabrício de Ávila Rodrigues
(Orientador)

A Deus,

por iluminar meu caminho em todos os momentos.

Ao meu esposo Luciano,

por todo amor, companheirismo, incentivo e persistência.

Dedico

AGRADECIMENTOS

A Deus, por me abençoar com sua presença constante em minha vida.

Ao meu orientador, Professor Fabrício de Ávila Rodrigues pelo exemplo de disciplina e comprometimento; e por acreditar em mim, me apoiar e me mostrar os caminhos.

Ao meu coorientador, Dr. Daniel Debona por sua amizade e incontáveis momentos de contribuição, paciência e perseverança.

À Universidade Federal de Viçosa, onde, com orgulho e gratidão, concluo o meu doutorado. Ao Departamento de Fitopatologia por todo apoio ao desenvolvimento da minha tese. E ao Conselho Nacional de Desenvolvimento Científico e Tecnológico (CNPq), pela concessão da bolsa de estudos.

Aos Professores do Departamento de Fitopatologia pelos ensinamentos, amizade e pela sabedoria que não encontramos nos livros. E aos funcionários por toda ajuda, em especial ao Sr. Mário, Delfim e Daniel.

Aos companheiros do Laboratório da Interação Planta-Patógeno pela ótima convivência, em especial Patrícia, Caroline, Verônica e Aysla pelas valiosas contribuições na realização dos experimentos.

Ao meu primeiro orientador, Professor Edson Mizobutsi pela amizade, conselhos e pelos inesquecíveis ensinamentos em fitopatologia durante a iniciação científica.

À minha família, pelo carinho e incentivo. Em especial a minha mãe, maior incentivadora e apoiadora dos meus estudos. Meu pai que, desde a minha infância, em suas atividades a campo, despertou em mim preceitos de trabalho, coragem e interesse pela agricultura. E aos meus irmãos Inael, Ítalo, Luiz, Miguel, Maria Fernanda e Marcelo, pelo companheirismo, apoio e torcida.

Aos meus amigos que se tornaram parte da minha família: Danielle, Daniel, Iana, Igor, Maria Izabel, Sabrina e Vanessa; obrigada pelo companheirismo, palavras de incentivo e pela amizade fundamental. Vocês são pessoas maravilhosas e muito especiais para minha vida!

E a todos que contribuíram de alguma maneira para que eu realizasse este sonho, obrigada!

BIOGRAFIA

Inaia Rhavene Freire Fagundes Nacarath, filha de Nelson Freire de Alkimin e Maria Iromá Fagundes, nasceu em 21 de setembro de 1989, em Montes Claros, Estado de Minas Gerais (MG).

Em 2008, ingressou no curso de agronomia da Universidade Estadual de Montes Claros (MG), onde graduou-se em julho de 2013. Em agosto deste mesmo ano, iniciou o curso de Mestrado em Fitopatologia na Universidade Federal de Viçosa (MG), defendendo a sua dissertação em julho de 2015.

Em agosto de 2015, ingressou no curso de Doutorado em Fitopatologia na Universidade Federal de Viçosa (MG).

SÚMARIO

ABSTRACT

FAGUNDES-NACARATH, Inaia Rhavene Freire, D.Sc., Universidade Federal de Viçosa, March, 2018. **Biochemical and physiological responses of common bean infected by *Sclerotinia sclerotiorum* mediated by oxalic acid and phosphites and diagrammatic scale for assessment of white mold severity**. Adviser: Fabrício Avila Rodrigues. Co-adviser: Daniel Debona.

White mold, caused by *Sclerotinia sclerotiorum*, is one of the most devastating diseases of common bean worldwide. The wide range of hosts (>400 species) and the fungus' ability to survive for many years on the soil as sclerotia make disease management very difficult. Despite the importance of white mold, many aspects of the host-fungus interaction remain elusive. Here, a series of experiments was conducted to assess the biochemical and physiological changes mediated by oxalic acid (OA, the main pathogenic material secreted by *S. sclerotiorum*), phosphites in the common bean-*S. sclerotiorum* interaction as well as a diagrammatic scale for assessment of white mold severity (WMS). Firstly, we performed biochemical and physiological analyses to investigate the role of oxalic acid (OA) during *S. sclerotiorum* infection. To this end, common bean plants were sprayed with water or OA (referred to as –OA and +OA plants, respectively) and either challenged or not with a wild type (WT) and an OA-defective mutant (A4) of *S. sclerotiorum*. Irrespective of OA spray, WT isolate was more aggressive than A4 isolate, and spraying OA increased OA concentration in the leaflets and the aggressiveness of both isolates. Biochemical limitations were found to be behind *S. sclerotiorum*-induced photosynthetic impairments, notably for the +OA plants inoculated with WT isolate. Inoculated plants were not able to fully capture and exploit the collected energy as a result photochemical dysfunctions, which were potentiated by OA. With exception of catalase activity (CAT), there were increases in the activities of antioxidant enzymes, remarkably for plants that were inoculated with WT isolate. OA attenuated most of such increases, thereby increasing generation of superoxide and hydrogen peroxide and the concurrent damage to the host cell membranes, as evidenced by the increases in malondialdehyde (MDA) concentration. In the second experiment, we investigated physiological changes in common bean plants that were sprayed with water, zinc (Zn) or copper (Cu) phosphites and challenged or not with

S. sclerotiorum. *In vitro* assays revealed that Zn and Cu phosphites inhibited fungal growth in a dose-dependent manner, but the latter was more fungitoxic. Lesion area and white mold severity were reduced by Zn and Cu phosphites, but the former was more effective. *Sclerotinia sclerotiorum* infection dramatically impaired plant photosynthesis, but such impairments were greatly abrogated in the Zn and Cu phosphite-treated plants. Concentrations of chlorophyll *a* + *b* and carotenoids were decreased in inoculated plants, but lower decreases were recorded in the presence of Zn and Cu phosphites. In the last study, we investigated whether Zn and Cu phosphites potentiate biochemical defenses of common bean against white mold. Histopathological analysis showed fewer fungal hyphae and less collapse of the mesophyll cells in the Zn and Cu phosphite-treated plants relative to the control. The *S. sclerotiorum*-triggered accumulation of reactive oxygen species, OA and MDA were constrained as a result of Zn and Cu phosphites sprays. In general, the activities of the antioxidant and defense enzymes at early stages of pathogen infection were higher in Zn- and Cu-sprayed plants than in their non-sprayed counterparts. Concentrations of total soluble phenols and lignin-thioglycolic acid derivatives in the inoculated plants were not affected by the Cu phosphite treatment, but they were higher and lower, respectively, in the Zn phosphite treatment at 60 hai than in the control. In conclusion, our results showed that OA enhance biochemical limitations to photosynthesis, photochemical dysfunctions and oxidative stress in common bean leaflets during the infection process of *S. sclerotiorum*. Additionally, we provide novel evidences of the potential of Zn and Cu phosphites in attenuate the physiological impairments and shed light on the biochemical defense mechanisms involved in the Zn and Cu phosphites-mediated suppression of white mold in common bean. In the fourth experiment, we develop SADs consisting of eight color images of diseased leaflets with severity values that ranged from 0.4 to 53.7%. Twenty raters [10 experienced (ER) and 10 inexperienced (IR)] validated the SADs by assessing the same set of 50 images twice, the first without SADs and the second using it as an aid. The SADs significantly improved both accuracy and precision for IR, whereas for ER only precision (*r*) was improved by SADs. The SWM estimates were also more reliable because inter-rater reliability (coefficient of determination, R^2) was significantly increased for both ER and IR by using SADs. Therefore, the SADs presented is thought to be a valuable tool to provide accurate, precise and reliable estimates of the SWM on common bean.

RESUMO

FAGUNDES-NACARATH, Inaia Rhavene Freire, D.Sc., Universidade Federal de Viçosa, março de 2018**. Respostas bioquímicas e fisiológicas do feijoeiro infectado por *Sclerotinia sclerotiorum* mediada pelo ácido oxálico e fosfitos e escala diagramática para avaliação da severidade do mofo branco.** Orientador: Fabrício Avila Rodrigues. Coorientador: Daniel Debona.

O mofo branco, causado por *Sclerotinia sclerotiorum*, é uma das doenças mais devastadoras do feijoeiro em todo o mundo. A ampla gama de hospedeiros (> 400 espécies) e a capacidade do fungo de sobreviver por muitos anos no solo, como escleródios, dificultam muito o manejo da doença. Apesar da importância do mofo branco, muitos aspectos da interação fungo-hospedeiro permanecem elusivos. Aqui, uma série de experimentos foi conduzida para avaliar as alterações bioquímicas e fisiológicas mediadas por ácido oxálico (OA, o principal material patogênico secretado por *S. sclerotiorum*), fosfitos na interação feijão-*S. sclerotiorum*, bem como desenvolver uma escala para a quantificação da severidade do mofo branco (WMS). Primeiramente, realizamos análises bioquímicas e fisiológicas para investigar o papel do ácido oxálico (OA) durante a infecção por *S. sclerotiorum*. Para este fim, plantas de feijoeiro foram pulverizadas com água ou OA (referidas como plantas -OA e + OA, respectivamente) e desafiadas ou não com um tipo selvagem (WT) e um mutante deficiente na produção do OA (A4) de *S. sclerotiorum*. Independentemente do spray OA, o isolado WT foi mais agressivo que o isolado A4, e a pulverização da OA aumentou a concentração de OA nos folhetos e a agressividade de ambos os isolados. Verificou-se que as limitações bioquímicas estavam envolvidas nas deficiências fotossintéticas induzidas por *S. sclerotiorum*, nomeadamente para as plantas + OA inoculadas com o isolado WT. As plantas inoculadas não foram capazes de capturar e explorar completamente a energia coletada como resultado de disfunções fotoquímicas, que foram potencializadas pela OA. Com exceção da atividade da catalase (CAT), houve aumento nas atividades de enzimas antioxidantes, notavelmente para plantas que foram inoculadas com o isolado WT. A OA atenuou a maioria desses aumentos, aumentando assim a geração de superóxido e peróxido de hidrogênio e o dano concomitante às membranas da célula hospedeira, como evidenciado pelos aumentos na concentração de aldeído

malônico (MDA). No segundo experimento, investigamos mudanças fisiológicas em plantas de feijoeiro que foram pulverizadas com fosfitos de água, zinco (Zn) ou cobre (Cu) e desafiadas ou não por *S. sclerotiorum*. Ensaios *in vitro* revelaram que os fosfitos de Zn e Cu inibiram o crescimento fúngico de maneira dose-dependente, mas o último foi mais fungitóxico. A área da lesão e a severidade do mofo branco foram reduzidas pelos fosfitos de Zn e Cu, mas o primeiro foi mais efetivo. A infecção por *S. sclerotiorum* prejudicou dramaticamente a fotossíntese das plantas, mas tais deficiências foram muito anuladas nas plantas tratadas com fosfito de Zn e Cu. Concentrações de clorofila *a* + *b* e carotenoides foram reduzidas em plantas inoculadas, mas menores decréscimos foram registrados na presença de fosfitos de Zn e Cu. No último estudo, investigamos se os fosfitos de Zn e Cu potencializam as defesas bioquímicas do feijoeiro contra mofo branco. A análise histopatológica mostrou menos hifas fúngicas e menos colapso das células do mesofilo nas plantas tratadas com fosfito de Zn e Cu em relação ao controle. O acúmulo de espécies reativas de oxigênio, OA e MDA desencadeadas por *S. sclerotiorum* foi restrito como resultado da pulverização com os fosfitos de Zn e Cu. Em geral, as atividades das enzimas antioxidativas e de defesa nos estágios iniciais da infecção pelo patógenos foram maiores em plantas pulverizadas com Zn e Cu do que em suas contrapartes não pulverizadas. Concentrações de fenóis solúveis totais e lignina derivado do ácido tioglicólico nas plantas inoculadas não foram afetadas pelo tratamento com fosfito de Cu, mas foram maiores e menores, respectivamente, no tratamento com fosfito de Zn a 60 hai do que no controle. Em conclusão, nossos resultados mostraram que OA aumenta as limitações bioquímicas à fotossíntese, disfunções fotoquímicas e estresse oxidativo em folhetos de feijoeiro durante o processo de infecção de S. sclerotiorum. Adicionalmente, nós fornecemos novas evidências do potencial dos fosfitos de Zn e Cu em atenuar as deficiências fisiológicas e lançar luz sobre os mecanismos de defesa bioquímica envolvidos na supressão mediada por fosfitos de Zn e Cu do mofo branco no feijoeiro. No quarto experimento, desenvolvemos SADs que consistiram em oito imagens coloridas de folíolos de feijoeiro doentes com valores de WMS variando de 0,4 a 53,7%. Vinte avaliadores [10 experientes (ER) e 10 inexperientes (IR)] validaram os SADs avaliando o mesmo conjunto de 50 imagens duas vezes, o primeiro sem SADs e o segundo usando-o. Os SADs melhoraram significativamente a acurácia e a precisão para IR, enquanto que para ER apenas a precisão (*r*) foi melhorada por SADs. As

estimativas de WMS também foram mais confiáveis para repetibilidade inter-avaliador (coeficiente de determinação, R^2) foi significativamente maior para ER e IR usando SADs. Portanto, os SADs apresentados são uma ferramenta valiosa para fornecer estimativas acuradas, precisas e repetíveis da WMS do feijoeiro.

GENERAL INTRODUCTION

White mold, caused by *Sclerotinia sclerotiorum* (Lib.) De Bary, is a yield-limiting disease of common bean (*Phaseolus vulgaris* L.) in several countries (Boland and Hall, 1994), including Argentina, Brazil, Canada and the USA. In Brazil, the world's leading producer and consumer of common bean, white mold is widespread and yield losses can reach up to 100% (Schwartz and Singh, 2013).

White mold symptoms include water-soaked spots that are brown in color and soft in consistency; such spots progress quickly given rise to necrotic lesions over which a white cottony mycelium can be seen (Steadman, 1983). The symptoms can be observed in all above ground organs regardless of the plant growth stage, though flowering is the most susceptible phase since senescing flowers represent the primary via for *S. sclerotiorum* infection (Purdy, 1979). White mold epidemics are favored by mild temperatures (< 20°C), high humidity (>70%), high planting density and prostrate plant growth habit (Schwartz and Singh, 2013; Steadman, 1983).

There are different lines of evidence showing that the *S. sclerotiorum*-produced OA has a key role in fungal infection (Godoy et al., 1990; Cessna et al., 2000). OA has been demonstrated to play multiple roles during infection process of *S. sclerotiorum*; however, information regarding photosynthetic performance and antioxidant system of common bean leaflets as a result of exogenously administered OA upon *S. sclerotiorum* infection is still missing.

There are few strategies for controlling white mold in common bean and resistant cultivars are not available to growers. Phosphite-based compounds are marketed as foliar fertilizers and disease resistance inducers; in addition, their metal salts are effective in controlling diseases caused by *Phytophthora* spp. (Adaskaveg et al., 2015; Dalio et al., 2014) and fungi, including *Rhizoctonia solani*, *Alternaria*

alternata and *Fusarium* spp. (Cerqueira et al., 2017; Lobato et al., 2010; Reuveni et al., 2003; Sharaf et al., 2004) in several plant species.

To assess the efficacy of methods for disease control, disease quantification plays a critical role (Madden et al., 2007) and must be accurate, precise and reliable (Nutter and Schultz, 1995; Madden et al., 2007). The standard area diagram (SAD) is a standardized method to disease quantification and it has been used as a tool to estimate disease severity, an essential variable in phytopathometry (Del Ponte et al., 2017). The use of the SADs has demonstrated that inexperienced raters are more benefited in terms of accuracy and precision when compared with estimates made without SADs (Braido et al., 2014; Vieira et al., 2014; Debona et al., 2015; Dolinski et al., 2017).

In the first chapter of this study, we performed detailed analysis at both biochemical (activities of antioxidant enzymes and ROS content) and physiological (leaf gas exchange and chlorophyll *a* fluorescence) levels to investigate OA's role during *S. sclerotiorum* infection in common bean leaflets. To this end, common bean plants were or were not sprayed with OA and either challenged or not with a wild type and an OA-defective mutant of *S. sclerotiorum*. In the second chapter, we performed detailed leaf gas exchange, chlorophyll *a* fluorescence and concentration of photosynthetic pigments analyses to examine the effect of zinc (Zn) and copper (Cu) phosphites in the photosynthetic performance of common bean plants that were either challenged or not with *S. sclerotiorum*. In the third chapter, biochemical assays (antioxidant and defense enzyme activities, concentrations of reactive oxygen species, oxalic acid, TSP and LTGA) were performed to elucidate whether phosphites potentiate host defenses against *S. sclerotiorum* infection. Ultimately, the fourth chapter of this study aimed at developing SADs to quantify WMS in common bean leaflets and to determine the effect of SADs and rater experience in accuracy, precision and reliability of the estimates of WMS.

References

Adaskaveg JE, Hao W, Förster H, 2015. Postharvest strategies for managing phytophthora brown rot of citrus using potassium phosphite in combination with heat treatments. Plant Disease **99**, 1477–1482.

Boland G, Hall R, 1994. Index of plant hosts of *Sclerotinia sclerotiorum*. *Canadian of Journal of Plant Pathology* **16**, 93–108.

Braido R, Gonçalves-Zuliani AMO, Nocchi PTR, Belasque Júnior J, Janeiro V, Bock CH, Nunes WMC, 2014. Development and validation of standard area diagrams as assessment aids for estimating the severity of citrus canker on unripe oranges. Plant Disease **98**,1543–1550.

Cessna SG, Sears VE, Dickman MB, Low PS, 2000. Oxalic acid, a pathogenicity factor for *Sclerotinia sclerotiorum*, suppresses the oxidative burst of the host plant. *Plant Cell* **12**, 2191–2199.

Dalio RJD, Fleischmann F, Humez M, Osswald W, 2014. Phosphite protects *Fagus sylvatica* seedlings towards *Phytophthora plurivora* via local toxicity, priming and facilitation of pathogen recognition. *PLoS ONE* **9**, e87860.

Debona D, Nascimento KJT, Rezende D, Rios JA, Bernardeli AMA, Silva LC, Rodrigues FA, 2015. A set of standard area diagrams to assess severity of frogeye leaf spot on soybean. European Journal Plant Pathology **142**, 603–614.

Del Ponte EM, Pethybridge SJ, Bock C, Michereff SJ, Machado FJ, Spolti P, 2017. Standard area diagrams for aiding severity estimation: scientometrics, pathosystems and methodological trends in the last 25 years. Phytopathology **10**, 1161–1174.

Dolinski MA, Duarte HSS, Silva JB, May De Mio LL, 2017. Development and validation of a standard area diagram set for assessment of peach rust. European Journal Plant Pathology **148**, 817–824.

Godoy G, Steadman JR, Dickman MB, Dam R, 1990. Use of mutants to demonstrate the role of oxalic acid in pathogenicity of *Sclerotinia sclerotiorum* on *Phaseolus vulgaris*. *Physiological and Molecular Plant Pathology* **37**, 179–191.

Lobato MC, Olivieri FP, Daleo GR, Andreu AB, 2010. Antimicrobial activity of phosphites against different potato pathogens. *Journal of Plant Diseases and Protection* **117**, 102–109.

Madden, L. V., Hughes, G., van den Bosch, F., 2007. The study of plant disease epidemics. St. Paul: APS Press. 421 pp.

Nutter FW, Schultz PM, 1995. Improving the accuracy and precision of disease assessments: selection of methods and use of computer-aided training programs. Canadian Journal Plant Pathology **17**, 174–184.

Purdy LH, 1979. *Sclerotinia sclerotiorum*: History, diseases and symptomatology, host ranges, geographic distribution and impact. Phytopathology **69**, 875–880.

Reuveni M, Sheglov D, Cohen Y, 2003. Control of moldy-core decay in apple fruits by *β*-aminobutyric acids and potassium phosphites. *Plant Disease* **87**, 933–936.

Schwartz HF, Singh SP, 2013. Breeding common bean for resistance to diseases: a review. Crop Science **53**, 1832–1844.

Sharaf EF, Farrag AA, 2004. Induced resistance in tomato plants by IAA against *Fusarium oxysporum* f. sp. *Lycopersici*, Polish Journal of Microbiology **53**, 111–116.

Steadman JR, 1983. White mold – a serious yield – limiting disease of bean. Plant Disease **67**, 346–350.

Vieira RA, Mesquini RM, Silva CN, Hata FT, Tessmann DJ, Scapim CA, 2014. A new diagrammatic scale for the assessment of northern corn leaf blight. Crop Protection **56**, 55–57.

CHAPTER 1

Oxalic acid-mediated biochemical and physiological changes in the common bean-*Sclerotinia sclerotiorum* interaction

Abstract

The success of *Sclerotinia sclerotiorum* infection relies largely on the production of the non-host selective toxin named oxalic acid (OA). This toxin is known to play multiple roles in host infected by the fungus, but its effect on photosynthesis and on the antioxidant system of common bean plants remain elusive. Therefore, we performed detailed analysis of leaf gas exchange, chlorophyll *a* fluorescence, activities of antioxidant enzymes, concentrations of reactive oxygen species and photosynthetic pigments to investigate the OA's role during the *S. sclerotiorum* pathogenesis. To achieve this goal, common bean plants were sprayed with water or with oxalic acid (referred to as –OA and +OA plants, respectively) and either non-challenged or challenged with a wild type (WT) or an OA-defective mutant (A4) of *S. sclerotiorum*. Irrespective of OA spray, the WT isolate was more aggressive than the A4 isolate and spraying OA increased OA concentration in the leaflets as well as the aggressiveness of both isolates. Biochemical limitations were behind *S. sclerotiorum*-induced photosynthetic impairments notably for the +OA plants inoculated with the WT isolate. Inoculated plants were not able to fully capture and exploit the collected energy due to the degradation of photosynthetic pigments. Photoinhibition of photosynthesis and photochemical dysfunctions were potentiated by OA. Higher activities of superoxide dismutase, peroxidase and ascorbate peroxidase besides reductions on catalase activity were noticed for plants inoculated with the WT isolate. OA was able to counteract most of the increases in the activities of antioxidant enzymes thereby increasing the generation of superoxide and hydrogen peroxide and the concurrent damage to the membranes of host cells as evidenced by the high malondialdehyde concentration. In conclusion, OA was found to enhance biochemical limitations to photosynthesis, photochemical dysfunctions and oxidative stress in the leaflets of common bean plants infected by *S. sclerotiorum*.

Keywords: *Phaseolus vulgaris*, antioxidant system, chlorophyll *a* fluorescence, leaf gas exchange, photosynthesis, white mold.

Introduction

Sclerotinia sclerotiorum (Lib.) De Bary, causal agent of white mold, is one of the most devastating and worldwide spread plant pathogens (Bolton *et al*., 2006). This fungus specie infects over 400 plant species including economically important crops such as common bean (Boland & Hall, 1994). A non-host-selective toxin, named oxalic acid (OA), is released by *S. sclerotiorum* during its necrotrophic phase with enormous ability to macerate the host tissues (Andrew *et al*., 2012). The OA occurs widely in nature and can being found in animals, bacteria, fungi, plants, rocks, soils and sometimes as free acid, but more commonly as soluble potassium or sodium oxalate or as insoluble calcium oxalate (Ferrar & Walker, 1993; Guimarães & Stotz, 2004).

There are different lines of evidence showing that the *S. sclerotiorum*-produced OA play a key role in fungal infection (Godoy *et al*., 1990; Cessna *et al*., 2000). Firstly, mutants of the fungus defective in the OA biosynthesis were non-pathogenic to plants of commom bean (Godoy *et al*., 1990) and *Arabidopsis* (Dickman & Mitra, 1992). Moreover, OA-defective mutants of *S. sclerotiorum* caused smaller lesions on plant tissue of several hosts (Cessna *et al*., 2000; Kim *et al*., 2008; Williams *et al*., 2011; Liang *et al*., 2015). Additionally, the overexpression of an oxalate oxidase, which is involved in OA catabolism, in oilseed rape and soybean plants increased their resistance against white mold (Liu *et al*., 2015; Davidson *et al*., 2016). Besides pathogenicity, OA biosynthesis may also affect *S. sclerotiorum* growth and development. For instance, ultraviolet-light-induced mutants (mutants 'A') displayed reduced growth, aberrant development, produced soft hyphae and lost their ability to produce sclerotia (Rollins & Dickman, 2001; Rollins, 2003).

It has been demonstrated that OA plays multiple roles during the infection process of *S. sclerotiorum*. This toxin is able to manipulate the programmed cell death in plants (Errakhi *et al*., 2008; Kim *et al*., 2008), compromise the structure of pectin by chelating

calcium ions (Ca^{2+}) (Bateman & Beer, 1965) and counteract abscisic acid (ABA)-induced stomatal closure (Guimarães & Stotz, 2004). Furthermore, *S. sclerotiorum*-released OA was shown to decrease the oxidative burst and other host defense responses (Cessna *et al*., 2000). On the other hand, decreasing OA accumulation by using fungal mutants or the overexpression of oxalate oxidase lead to reactive oxygen species (ROS) generation allowing, therefore, the plant to activate some defense responses (Cessna *et al*., 2000; Hu *et al*., 2003; Dong *et al*., 2008). Interestingly, the manipulation of ROS metabolism by OA seems to be biphasic: initially, OA prevents ROS accumulation, then activating their production at advance stages of pathogen infection (Williams *et al*., 2011). The OA was also found to induce wilting symptoms in *S. sclerotiorum*-infected plants (Noyes & Hancock, 1981; Kolkman & Kelly, 2000).

Although there are reports that *S. sclerotiorum* is capable to manipulate both plant physiology and metabolism, information regarding the changes occurring on the photosynthetic performance and on the antioxidant system of common bean plants exposed to exogenous OA application upon *S. sclerotiorum* infection is still missing in the literature. Here, we performed detailed analysis at both biochemical (activities of antioxidant enzymes and ROS concentration) and physiological (measurements of leaf gas exchange and chlorophyll *a* fluorescence parameters) levels to investigate the OA's role during *S. sclerotiorum* infection in common bean leaflets non-sprayed or sprayed with OA and challenged or not with a wild type or an OA-defective fungal mutant.

Material and methods

Plant growth and oxalic acid spraying

Five seeds of common bean from cultivar Pérola, susceptible to *S. sclerotiorum*, were sown in plastic pots of 2 liters containing 2 kg of Tropstrato® substrate (Vida

Verde, Mogi Mirim, São Paulo, Brazil) composed of a mixture of pine bark, peat and expanded vermiculite (1:1:1). Each pot was thinned to three seedlings seven days after emergence. Plants were kept in a greenhouse (30 ± 5ºC temperature, 65 ± 5% relative humidity and 900 ± 15 µmol photons m^{-2} s^{-1} natural photosynthetically active radiation). Plants were fertilized weekly with 100 mL of a modified nutrient solution based on Clark (1975) as follows: 0.8 mM KNO_3, 0.069 mM $NH_4H_2PO_4$, 1 mM NH_4NO_3, 1 mM $Ca(NO_3).4H_2O$, 0.9 mM KCl, 0.6 mM $MgSO_4$ $7H_2O$, 0.5 µM $CuSO_4$ $5H_2O$, 2 µM $ZnSO_4$ $7H_2O$, 19 µM H_3BO_3, 7 µM $MnCl_2$ $4H_2O$, 0.6 µM Na_2MoO_4 $4H_2O$, 60 µM $FeSO_4$ $7H_2O$ and 90 µM disodium ethylenediaminetetraacetic acid (EDTA). Plants were watered with deionized water as needed.

The oxalic acid (OA) (Sigma-Aldrich, São Paulo, Brazil) solution was prepared by using distilled sterile water (DSW) to obtain the concentration of 20 mM (pH 5.8 adjusted with 1 M KOH). The OA solution was sprayed at 2 h before inoculation of common bean plants (15 ml per plant at the V3 growth stage) with *S. sclerotiorum*. Plants were sprayed using a CO_2 pressurized backpack sprayer equipped with a flat fan nozzle (XR 110 02®, Teejet, Glendale Heights, IL, USA) at a 200,000-Pa pressure to deliver a spray volume of 200 L ha^{-1}. Plants sprayed with DSW served as the control treatment.

Fungal growth and plant inoculations

Isolates of a wild-type (WT) (1980) and an OA-defective mutant (A4) of *S. sclerotiorum* (Godoy *et al*., 1990) were grown on potato dextrose agar and kept in a growth chamber (24°C and 12 h photoperiod) for seven days. An agar plug (5 mm in diameter) containing the advancing edge of growing fungal mycelia was removed and used to inoculate the adaxial surface of leaflets from common bean plants (three leaflets per plant and one agar plug per leaflet). Inoculated plants were transferred to a plastic

mist growth chamber (MGC) inside a greenhouse for the duration of the experiment. The MGC was made of wood (2 m wide, 15 m high, 5 m long) and covered with 100 µm thick transparent plastic. The temperature inside the MGC ranged from 20 ± 2°C (day) to 17 ± 2°C (night). The relative humidity was maintained at 92 ± 3% using a misting system with nozzles (model NEB-100; KGF Co.) that sprayed mist every 30 min above the plant canopy. The relative humidity and temperature were measured with a thermohygrograph (TH-508; Impac). The maximum natural photon flux density at plant canopy height was approximately 900 µmol m^{-2} s^{-1}.

Determination of lesion area (LA) and white mold severity (WMS)

Inoculated leaflets of each plant were collected at 36, 60 and 84 hours after inoculation (hai) and lesion were measured in two orthogonal directions using a digital caliper to obtain the LA. The leaflets were also scanned at 300 dpi resolution and the obtained images were further processed using the software QUANT (Vale *et al*. 2003) to quantify the WMS.

Evaluation of the leaf gas exchange parameters

Leaf gas exchange parameters were determined in one leaflet of the third leaf of each plant (four leaflets per treatment) at 36, 60 and 84 hai. The net carbon assimilation rate (A), stomatal conductance to water vapor (g_s), internal CO_2 concentration (C_i) and transpiration rate (E) were estimated from 09:00 to 12:00 h under artificial and saturating photon irradiance (1,200 µmol m^{-2} s^{-1}) and an external CO_2 concentration of 400 µmol mol^{-1} using a portable open-system infrared gas analyzer (LI-6400, LI-COR Inc., Lincoln, NE, USA). All measurements were performed by setting the block temperature at 25°C.

Chlorophyll (Chl) *a* fluorescence imaging

The Imaging-PAM fluorometer and the Imaging Win software MAXI version (Heinz Walz GmbH, Effeltrich, Germany) were used to obtain the images and parameters of Chl *a* fluorescence in one leaflet of the third leaf of each plant (four leaflets per treatment) at 36, 60 and 84 hai. Plants were dark-adapted for 1 h and leaflets were placed individually in the CCD ("charge-coupled device") camera to obtain the images at the resolution of 640 × 480 pixels in a support at a distance of 18.5 cm from the CCD camera that was used to capture the Chl *a* fluorescence emission. The leaflets were illuminated with a weak modulated measuring beam (0.5 μmol m^{-2} s^{-1}, 100 μs, 1 Hz) to obtain the initial fluorescence (F_0). A saturating white light pulse of 2,400 μmol m^{-2} s^{-1} (10 Hz) was emitted for 0.8 s to determine the maximum fluorescence emission (F_m). Based on these initial measurements, the maximum photosystem II (PSII) photochemical efficiency of the dark-adapted leaflets was estimated through the variable-to-maximum Chl *a* fluorescence ratio, $F_v/F_m = [(F_m - F_0)/F_m)]$. Next, the leaflets were exposed to actinic photon irradiance (531 μmol m^{-2} s^{-1}) for 120 s to obtain the steady-state fluorescence yield (F_s), after which a saturating white light pulse (2,400 μmol m^{-2} s^{-1}; 0.8 s) was applied to achieve the light-adapted maximum fluorescence (F_m'). The light-adapted initial fluorescence (F_0') was estimated according to Oxborough & Baker (1997). Based on Kramer *et al*. (2004), the energy that was absorbed by the PSII for the following three yield components for dissipative processes was calculated as follows: the photochemical yield [$Y(II) = (F_m' - F_s)/F_m')$], the yield for dissipation by down-regulation [$Y(NPQ) = (F_s/F_m') - (F_s/F_m)$] and the yield for other non-photochemical (non-regulated) losses [$Y(NO) = F_s/F_m$]. The apparent electron transport rate was calculated as ETR = Y(II) × PPFD × f × α according to Baker (2008).

Determination of the concentration of photosynthetic pigments

Five squared leaflet areas (1 cm^2) were punched from each leaflet of the third leaflet of each plant per replication of each treatment at 36, 60 and 84 hai to determine the concentrations of Chl *a*, Chl *b* and carotenoids. Leaflet samples were immersed in glass tubes containing 5 mL of dimethyl sulfoxide (DMSO) solution (saturated with calcium carbonate ($CaCO_3$), 5 g L^{-1}) and kept in the dark at room temperature for 24 h. The absorbance of the extracts was read at 480, 649 and 665 nm in a spectrophotometer using the $CaCO_3$ saturated solution of DMSO as a blank. Concentrations of Chl *a*, Chl *b* and carotenoids were calculated according to Wellburn (1994).

Biochemical assays

For all biochemical assays, the third leaves, from base to the top, of each plant per replication of each treatment were collected at 36, 60 and 84 hai. Leaf samples were kept in liquid nitrogen during samplings and stored at -80°C until further analysis.

Determination of antioxidant enzymes activities

To determine the activities of ascorbate peroxidase (APX) (EC 1.11.1.11), catalase (CAT) (EC 1.11.1.6), peroxidase (POX) (EC 1.11.1.7) and superoxide dismutase (SOD) (EC 1.15.1.1), a total of 0.2 g of leaf tissue was ground into a fine powder with liquid nitrogen in a mortar and pestle. The fine powder was homogenized in a 2 ml solution containing 50 mM potassium phosphate buffer (pH 6.8), 0.1 mM EDTA, 1 mM phenylmethyl-sulphonyl fluoride (PMSF) and 2% (w/v) polyvinylpyrrolidone (PVP). The homogenized material was centrifuged at 12,000 × *g* at 4°C for 15 min and the supernatant was used for enzymes determination. SOD activity was determined by measuring its ability to inhibit the photochemical reduction of nitroblue tetrazolium (NBT) as described by Beauchamp & Fridovich (1971) by adding 50 µl of the crude enzyme extract to 1.95 ml of a mixture containing 50 mM potassium phosphate buffer

(pH 7.8), 13 mM methionine, 75 µM NBT, 0.1 mM EDTA and 2 µM riboflavin. Samples were light-exposed for 10 min and the production of formazan blue, resulting from the photoreduction of NBT, was measured at 560 nm. Samples kept in the dark for 10 min served as a blank. One unit of SOD was defined as the amount of enzyme necessary to inhibit NBT photoreduction by 50%. Activity of CAT was determined after addition of 50 µl of the crude enzyme extract to 1.95 ml of a reaction mixture containing 50 mM potassium phosphate buffer (pH 7.0) and 20 mM hydrogen peroxide (Havir & McHale 1989). The absorbance was recorded at 240 nm for 1 min. POX activity was assayed by determining the pyrogallol oxidation as proposed by Kar & Mishra (1976). The reaction was started after the addition of 15 µl of the crude enzyme extract to 1.98 ml of a reaction mixture containing 25 mM potassium phosphate (pH 6.8), 20 mM pyrogallol and 20 mM H_2O_2. The activity was determined through the absorbance of colored purpurogallin recorded for 1 min at 420 nm (Chance & Maehly 1955). The APX activity assay followed that described by Nakano & Asada (1981). A total of 15 µl of the crude enzyme extract was added to 1.98 ml of a mixture containing 50 mM phosphate buffer (pH 7.0), 1 mM H_2O_2 and 1 mM sodium ascorbate. The rate of ascorbate oxidation was measured by recording the absorbance at 290 nm for 1 min. Enzyme activity was expressed in a protein-basis whose concentration was determined according to the method of Bradford (1976).

Determination of malondialdehyde (MDA) concentration

Oxidative damage in the leaf cells was assessed based on lipid peroxidation and expressed as equivalents of MDA according to Cakmak & Horst (1991). A total of 100 mg of leaf tissue was ground into a fine powder using a mortar and pestle with liquid nitrogen and homogenized in 2 ml of 0.1% (w/v) trichloroacetic acid (TCA) solution in ice bath and the homogenate was centrifuged at 12,000 × *g* for 15 min at 4°C. After

centrifugation, 0.5 ml of the supernatant was added to 1.5 ml of TBA solution (0.5% in 20% TCA) and held for 30 min in a boiling water bath at 95°C. After this period, the reaction was stopped in ice bath. The samples were centrifuged at 9,000 × *g* for 10 min and the absorbance of the supernatant was read at 532 nm and discounting the non-specific absorbance at 600 nm (Heath & Packer 1968).

Determination of superoxide (O_2^-) concentration

A total of 0.2 g of leaf tissue was ground into a fine powder in a mortar and pestle with liquid nitrogen. The fine powder was homogenized in 2 ml of a solution containing 100 mM sodium phosphate buffer (pH 7.2) and 1 mM sodium diethyl dithiocarbamate (SDD). The homogenate was centrifuged at 22,000 × *g* for 20 min at 4°C. After centrifugation, 0.1 ml of the supernatant was reacted with 1.9 ml of a solution containing 100 mM sodium phosphate buffer (pH 7.2), 1 mM SDD and 0.25 mM NBT. The O_2^- concentration was determined by subtracting the absorbance of the final product from the initial absorbance at 540 nm (Chaitanya & Naithani 1994).

Determination of hydrogen peroxide (H_2O_2) concentration

A total of 0.2 g of leaf tissue was ground into a fine powder in liquid nitrogen and homogenized in 2 ml of a mixture containing 50 mM potassium phosphate buffer (pH 6.5) and 1 mM hydroxylamine. The homogenate was centrifuged at 10,000 × *g* for 15 min at 4°C (Kuo & Kao 2003) and the supernatant was used as the crude extract. A total of 100 µl of the supernatant was then added to a reaction mixture containing 100 µM ferric ammonium sulphate ($FeNH_4[SO_4]$), 25 mM sulphuric acid, 250 µM xylenol orange and 100 mM sorbitol in a final volume of 2 ml (Gay & Gebicki 2000). After 30 min of dark incubation at room temperature, the absorbance of the samples was determined at 560 nm. Blanks were prepared under the same conditions and subtracted

from the samples. A standard curve for H_2O_2 (Sigma-Aldrich, São Paulo, Brazil) was used to determine the H_2O_2 concentration.

Determination of oxalic acid (OA) concentration

A catalytic kinetic spectrophotometric method (Liu *et al*. 2015) was used to determine OA concentration. A total of 0.2 g of leaf tissue was ground into in 0.9% NaCl solution and the homogenized was centrifuged at 1,000 × *g* for 10 min. A total of 100 µL aliquot of the supernatant, 120 µL sulphuric acid (1 M) and 40 µL methylene blue were mixed and distilled sterile water was added to achieve a final volume of 980 mL. The mixture was heated in water bath (40°C) for 5 min and 20 µL of 0.1 M potassium dichromate was added to the tube. After 5 min, 200 µL sodium carbonate (2 M) was added to terminate the reaction and the absorbance was measured at 660 nm and recorded as A_s. Absorbance at 660 nm was read again and recorded as A_b when the aliquot of the supernatant was replaced with water. The difference between A_s and A_b ($\Delta A = A_s - A_b$) corresponded to OA concentration. A calibration curve was generated by measuring ΔA for different and known OA concentrations.

Experimental design and data analysis

A 3 × 2 factorial experiment, consisting of three inoculation conditions (IC) (non-inoculated leaflets and inoculated leaflets with both WT and A4 isolates) and plants spray (PS) (non-sprayed or sprayed with OA and referred to as –OA and +OA plants, respectively), was arranged in a completely randomized design with four replications. Each replication corresponded to a plastic pot containing three plants. Data were subjected to analysis of variance (ANOVA) and means were compared based on Tukey's test ($P \leq 0.05$). For LA and WMS, ANOVA was considered to be a 2 × 2 × 3 factorial experiment with two IC (WT and A4 isolates), two PS and three evaluation

times (ET) (36, 60 and 84 hai). For Chl *a* fluorescence parameters, concentration of photosynthetic pigments and biochemical assays, ANOVA was considered to be a 3 × 2 × 3 factorial experiment consisting of three IC, two PS and three ET (36, 60 and 84 hai). Principal components analysis (PCA) technique was used to determine the relationship among the variables and parameters evaluated. Data were analyzed using the Minitab software (version 18; Minitab Corporation).

Results

Analysis of variance

The factors IC and ET and their interaction were significant for LA and WM. Most of the factors and double interactions were significant for all variables, whereas IC × PS × ET interaction was significant for APX, CAT and POX activities (Table 1).

LA and WMS

Regardless of OA spray, white mold lesions were larger at 36, 60 and 84 hai on the leaflets inoculated with the WT isolate (Fig. 1A, B, E, F, I and J) than on those inoculated with the A4 isolate (Fig. 1C, D, G, H, K and L). The OA spray resulted in more severe white mold symptoms for both isolates (Fig. 1B, D, F, H, J and L). LA was significantly lower by 82-97% and 75-86% for leaflets inoculated with the A4 isolate for –OA and +OA plants, respectively, compared to the WT isolate (Fig. 1M and N). On the other hand, OA spray increased LA by 17-21% and 56-664% for leaflets inoculated with WT and A4 isolates, respectively (Fig. 1N). Leaflets inoculated with the A4 isolate showed lower WMS (by 83-94% and 75-87% for –OA and +OA plants, respectively) than their WT-inoculated counterparts (Fig. 1O and P). WMS was significantly

increased by 36-76% and 29-661% due to OA spray for leaflets inoculated with WT and A4 isolates, respectively (Fig. 1P).

Leaf gas exchange parameters

The –OA plants displayed significant decreases in A, g_s and E in response to *S. sclerotiorum* infection (60-90% and 22-38%, 52-79% and 25-43%, 49-72% and 24-34% for WT and A4 isolates, respectively) overall the experiment time-course (Fig. 2A, C and G). For the leaflets of +OA plants, A was reduced by 70-98% and 32-62%, g_s by 68-90% and 34-60% and E by 62-86% and 34-56% for plants inoculated with the WT and A4 isolates, respectively, compared to the non-inoculated leaflets (Fig. 2B, D and H). C_i was increased by 7 and 12% at 60 hai and by 13 and 27% at 84 hai for the –OA and +OA plants, respectively, when inoculated with the WT isolate. Similarly, C_i increased by 12% at 84 hai for +OA plants inoculated with the A4 isolate (Fig. 2E and F). The +OA plants that were inoculated with the WT isolate showed decreases in A (32-86%) and g_s (35-60%) from 36 to 84 hai and in E (50%) at 84 hai relative to their –OA counterparts (Fig. 2A, B, C, D, G and H). For the A4 isolate, OA spray also decreased A (20-41%) in all evaluation times as well as g_s (33-38%) and E (32-31%) at 60 and 84 hai, respectively (Fig. 2A, B, C, D, G and H). C_i was significantly increased by 6 and 9% for the WT isolate and by 6 and 13% for the A4 isolate at 60 and 84 hai, respectively, upon OA spray (Fig. 2E and F).

Chl *a* fluorescence parameters

Irrespective of OA spray, images of Chl *a* fluorescence evidenced changes in all parameters starting on 36 hai in the leaflets inoculated either with WT and A4 isolates. A progressive loss of the photosynthetic capacity was evidenced as the evaluation time progressed, especially for the +OA inoculated plants as indicated by the dark areas in

the images (Fig. 3). The –OA plants inoculated with the WT isolate displayed significant reductions in F_v/F_m (6-38%), Y(II) (23-62%) and ETR (25-85%) values besides increases in Y(NPQ) (45-56%) throughout the evaluation times and Y(NO) (56%) at 84 hai compared to non-inoculated plants. Similarly, decreases in F_v/F_m (11%) and Y(II) (26%) values at 84 hai and in ETR (16-31%) at 60 and 84 hai as well as increases in Y(NPQ) (48%) at 84 hai occurred for plants inoculated with the A4 isolate relative to their non-inoculated counterparts (Fig. 4A, C, E, G and I). For +OA plants, inoculation with the WT isolate resulted in significant decreases in the F_v/F_m (10-58%), Y(II) (37-87%) and ETR (39-95%) values as well as increases in both Y(NPQ) (42-61%) for all evaluation times and Y(NO) (26-67%) at 60 and 84 hai. Similarly, lower F_v/F_m (11-20%) and Y(II) (30-48%) values at 60 and 84 hai and ETR (43-50%) throughout the evaluation times besides higher Y(NPQ) (45-60%) at 60 and 84 hai and Y(NO) (19%) at 84 hai were observed for plants inoculated with the A4 isolate relative to their non-inoculated counterparts (Fig. 4B, D, F, H and J). In the absence of *S. sclerotiorum* inoculation, neither OA spray impacted the Chl *a* parameters nor the IC affected the Y(NPQ). Conversely, the +OA plants inoculated with the WT isolate showed significant decreases in Y(II) (15-68%) and ETR (15-69%) values throughout the evaluation times; F_v/F_m was also reduced (13-63%) and Y(NO) was increased (13-34%) at 60 and 84 hai, respectively, compared to the –OA plants. For plants inoculated with the A4 isolate, OA spray resulted in decreases in F_v/F_m (11%), Y(II) (22-32%) at 60 and 84 hai and in ETR (16-34%) values for all evaluation times as well as an increase in Y(NO) (35%) at 84 hai (Fig. 4A-J).

Concentration of photosynthetic pigments

For the –OA plants, there was significantly decreases in the concentrations of photosynthetic pigments upon *S. sclerotiorum* infection; for the WT isolate, the

concentration of Chl *a* + *b* (18-38%) and carotenoids (49-60%) decreased at 60 and 84 hai whereas for the A4 isolate the Chl *a* + *b* concentration decreased by 14% at 84 hai (Fig. 7A and C). For +OA plants, Chl *a* + *b* and carotenoids concentrations were reduced by 23-52% and 34-85% for plants inoculated with the WT isolate from 36 to 84 hai and by 13-28% at 60 and 84 hai and by 14-24% from 36 to 84 hai for plants inoculated with the A4 isolate, respectively, relative to the non-inoculated plants. Chl *a* + *b* and carotenoids concentrations were reduced by 16-28% and 37-63% at 60 and 84 hai, respectively, for plants inoculated with the WT isolate and by 17-21% and 13-19% at 60 and 84 hai, respectively, for plants inoculated with the A4 isolate upon OA spray (Fig. 5 B and D).

Antioxidant enzymes activities

For –OA plants inoculated with the WT isolate there were significantly increases in the activities of SOD (41-59%), POX (139-264%) and APX (35-83%) at 60 and 84 hai and a decrease in CAT (30%) at 84 hai compared with their non-inoculated counterparts (Fig. 6A-H). For plants inoculated with the A4 isolate, there were significantly increases for activities of POX (73%) and APX (38%) at 84 hai (Fig. 6A, C, E and G). For +OA plants inoculated with the WT isolate there were significantly increases in POX (12-100%) and decreases in CAT (18-47%) throughout the evaluation times whereas for plants inoculated with the A4 isolate CAT activity (19-23%) decreased at 60 and 84 hai (Fig. 6D and F). For +OA inoculated plants, there were lower activities of CAT, POX and APX (by 20-50% and 26-28%, by 25-37% and 34-35% and by 23-29% and 12-25% for WT and A4 isolates, respectively) and of SOD (by 24-34% for WT isolate) at 60 and 84 hai in comparison to the –OA counterparts (Fig. 6 A-H).

Concentrations of OA, O_2^-, H_2O_2 and MDA

For –OA plants, there were significantly increases in the concentrations of OA (45-67%), O_2^- (282-336%), H_2O_2 (51-91%) and MDA (46-49%) at 60 and 84 hai when inoculated with the WT isolate whereas for the A4 isolate there were increases for O_2^- (103-156%) and H_2O_2 (27-48%) at 60 and 84 hai, respectively, and of MDA (22%) at 84 hai in comparison to non-inoculated plants (Fig. 7A, C, E and G). For +OA inoculated plants, there were higher concentrations of O_2^-, H_2O_2 and MDA than for non-inoculated counterparts (by 491-567% and 274-331%, by 57-95% and 20-45% and by 87-101% and 41-42% for WT and A4 isolates, respectively). In addition, OA concentration was significantly higher (65-68%) at 60 and 84 hai for +OA plants inoculated with the WT isolate in comparison to non-inoculated plants (Fig. 7B, D, F and H). For +OA plants, the OA concentration increased for non-inoculated plants (26-41%) as well as for plants inoculated with the WT (32-43%) and A4 (29-48%) isolates. For +OA plants, the concentrations of O_2^-, H_2O_2 and MDA were higher (increases of 31-40% and 51-60%, of 20-25% and 14-15% and of 14-38% and 20-19% for WT and A4 isolates, respectively) than for the –OA plants (Fig. 7A-H).

Principal component analysis (PCA)

Besides univariate analysis, data were further subjected to PCA to gain more insights of the role played by the OA on biochemical and physiological changes using the first two PCs, which covered most of the variation of the dataset (Fig. 8, PC1 and PC2 explained 79 and 9% of the total variance, respectively). The PCA revealed that either -–OA and +OA plants clustered together indicating, therefore, that OA spray did not caused biochemical and physiology changes in the absence of *S. sclerotiorum* infection (Fig. 8A). The A4 mutant was also clustered to them confirming, therefore, that mutation in the oxalacetate acetylhydrolase gene abrogates *S. sclerotiorum*-induced biochemical and physiological dysfunctions. By contrast, for –OA plants inoculated

with the WT and for +OA plants either inoculated with WT and A4 isolates formed separate groups indicating that for OA spray: i) helped the A4 isolate to manipulate plant' metabolism for WMS development and ii) potentiated biochemical and physiological changes induced by the WT isolate. The PC1 showed positive scores for LA, WMS, C_i, Y(NPQ), Y(NO), SOD, APX, POX, OA, O_2^-, H_2O_2 and MDA (which were clustered together) and negative scores for A, g_s, E, CAT, F_v/F_m, Y(II), ETR, Chl *a+b* and CAR (Fig. 8B).

Discussion

In the present study, we provide novel insights of OA's role in the *S. sclerotiorum* pathogenesis on the leaflets of common bean plants. This non-host selective toxin is capable to enhance *S. sclerotiorum*-induced oxidative stress and physiological impairments on the leaflets of common bean plants, which were greatly attenuated when they were inoculated with a OA-defective mutant of *S. sclerotiorum* (isolate A4) in the absence of OA spray. As expected, both LA and WMS were higher in the leaflets inoculated with the WT isolate in comparison to the A4 isolate, whereas spraying OA enhanced disease symptoms caused by both isolates. The OA concentration was found to be higher for +OA plants than for the –OA ones irrespective of fungus inoculation, notably for those that were inoculated with the WT isolate. On the other hand, though OA spray had increased either WMS as well as the OA content in the leaflets, it was not able to recover the aggressiveness of A4 isolate in comparasion to level of aggressiveness of the WT isolate. This finding is most likely due to the fact that we have done only one OA spray, whereas the toxin is continuously produced during infection process of *S. sclerotiorum*. In agreement with our findings, the OA concentration in an isolate defective on its production was reduced in comparison to the WT isolate (Guimarães & Stotz, 2004; Kim *et al*., 2008; Williams *et al*., 2011; Liang *et*

al., 2015). Indeed, OA-defective mutants of *S. sclerotiorum* were found to be non-pathogenic to plants of common bean (Godoy *et al*., 1990) and *Arabidopsis* (Dickman & Mitra, 1992) or caused lesions of reduced size in different hosts (Cessna *et al*., 2000; Kim *et al*., 2008; Williams *et al*., 2011; Liang *et al*., 2015).

The –OA plants displayed notable decreases in the values of A, g_s and E as a result of *S. sclerotiorum* infection; however, OA spray enhanced such decreases. It is well-known that pathogens infection on common beans may depresses photosynthesis as reported for the diseases bacterial common blight (Díaz *et al*., 2001) anthracnose (Polanco *et al*., 2014; Rodrigues *et al*., 2014) as well as angular leaf spot and rust (Jesus Júnior *et al*., 2001). The progressive decreases in A observed in the leaflets of common bean plants infected by *S. sclerotiorum* were associated with stomatal closure (reduction in g_s the values), which may have constrained CO_2 influx into the mesophyll indicating, therefore, that diffusive limitations could have played a role in the decreases in photosynthesis. From 60 hai onwards, however, C_i was found to be higher for plants inoculated with the WT isolate than for their non-inoculated counterparts favoring a scenario in which decreases in A stemmed from *S. sclerotiorum* infection were governed by biochemical limitations at the chloroplasts level. Moreover, the finding that, irrespective of OA spray, C_i values were higher for plants inoculated with the WT isolate than for those inoculated with the A4 isolate and that OA spray increased C_i values for plants inoculated with both isolates is a clear indicative that OA exacerbated *S. sclerotiorum*-induced biochemical constrains to photosynthesis in the leaflets of common bean plants. Accordingly, spraying of OA was able to compromise the photosynthetic performance of tobacco plants by repressing carbon assimilation (Yang *et al*., 2014). The *S. sclerotiorum*-induced decreases in g_s and E values were more evident for the +OA plants, particularly for those that were inoculated with the WT. This finding explain the desiccation symptoms noticed on the leaflets as the white mold

development, notably from 60 hai onwards. Thus, our results show that besides OA production had played a key role in *S. sclerotiorum* infection in the leaflets of common bean plants, this toxin also enhanced fungus-induced physiological impairments. Therefore, the progressive loss of the photosynthetic capacity of *S. sclerotiorum*-infected leaflets is thought to be governed chiefly by the degradative action of OA in host tissues. In contrast to our findings, OA was capable to manipulate the guard cells to promote stomatal opening and increase *E* values on plants of fava bean plants (Guimaraes & Stotz, 2004). Such discrepancy may be attributed, among other factors, to the place where pathogen was inoculated (stem *versus* leaflet), differences in hosts as well as the time-course during which the leaf gas exchange parameters were measured.

Irrespective of OA spray, analysis of Chl *a* fluorescence revealed changes for all parameters since 36 hai in the leaflets inoculated with the WT isolate. A progressive loss of the photosynthetic performance was evidenced over the time-course evaluated, especially for +OA inoculated plants. Moreover, the photochemistry in the *S. sclerotiorum*-infected leaflets was dramatically depressed as the white mold developed. The infected leaflets displayed clear adjustments in light capture and dissipation; *S. sclerotiorum* infection was showed to diminish the maximum photochemical efficiency of the PSII as indicated by the F_v/F_m values suggesting, therefore, the occurrence of photoinhibition of photosynthesis. The decreases in Y(II) values (a relative measure of PSII performance) indicated that the energy absorbed by the photosynthetic pigments in the *S. sclerotiorum*-infected leaflets was not directed to the photochemical process, probably due to the pathogen-induced photooxidative damage, which was more evident for the +OA plants. In fact, the increases in Y(NPQ) values (thermal regulated dissipation of energy that occurs in the PSII reaction centers through xanthophyll cycle and it is induced by light and proton gradient across thylakoid membrane), associated with decreases in the F_v/F_m values, suggest that thermal dissipation of the energy was

not sufficient to prevent photooxidative damages. This can also be depicted from the progressive increases in Y(NO) values (ratio between heat and fluorescence dissipated energy, mainly when the PSII reaction centers are closed), evidencing that photoprotection mechanisms became ineffective (Klughammer & Schreiber, 2008), culminating in reductions in ETR values. Photochemical dysfunctions were found to be enhanced by OA since decreases in the F_v/F_m, Y(II) and ETR values and increases in Y(NO) values were larger for plants inoculated with the WT than for those inoculated with the A4 isolate and for the +OA plants than for their –OA counterparts suggesting that OA played a key role in the photosynthetic impairments on the leaflets of common bean plants infected by *S. sclerotiorum*. Yang *et al*. (2014) reported that spraying OA dramatically compromised the PSII activity in tobacco leaves as evidenced by reductions in F_v/F_m and ETR values and increases in Y(NPQ) values corroborating which the results of the present study.

Concurrently with decreases in F_v/F_m, Y(II) and ETR values and increases in Y(NPQ) and Y(NO) values, the concentration of photosynthetic pigments was negatively impaired due to *S. sclerotiorum* infection that was linked with a decrease on the photosynthetic performance. Regardless of OA spray, for plants inoculated with the WT isolate the decrease on the concentration of photosynthetic pigments was more affected than for the A4 isolate; such decreases, however, were boosted by OA for both isolates. Therefore, our findings shed light on the action of OA through the degradation of photosynthetic pigments upon *S. sclerotiorum* infection. Accordingly, OA has been shown to macerate the tissues of common bean plants causing chloroplasts degeneration. Moreover, the action of cell wall degrading enzymes released by pathogens has also been reported (Bateman & Beer, 1965; Cessna *et al*., 2000; Tariq & Jefferies, 1985) and may have contributed to reduce the concentrations of Chl *a*+*b* and carotenoids as the infection of *S. sclerotiorum* took place.

The activities of antioxidant enzymes changed due to either *S. sclerotiorum* and OA spray. SOD represents the first line of defense against the ROS and is responsible for O_2^- removal through its conversion to H_2O_2 and O_2 (Malencic *et al*., 2010). Other enzymes such as CAT, POX and APX detoxify H_2O_2 generated spontaneously or from O_2^- dismutation via SOD. In general, the –OA plants inoculated with the WT isolate displayed higher SOD, POX and APX activities relative to their non-inoculated counterparts, whereas CAT activity was reduced. By contrast, enzymes' activities usually remained unchanged when the leaflets were inoculated with the A4 isolate indicating, therefore, that OA played a key role in manipulating the host antioxidant system in order to favor *S. sclerotiorum* infection. In another study, *S. sclerotiorum* infection was also demonstrated to increase activities of SOD, POX, APX and decrease those of CAT in common bean plants (Leite *et al*., 2014). The increased activities of SOD, POX and APX recorded for the –OA plants inoculated with the WT isolate were most likely an attempt of the plants to constrain fungal-induced ROS production. Conversely, spraying OA resulted in lower activities of CAT, POX and APX for plants inoculated with both isolates and of SOD for WT isolate from 60 hai onwards confirming, therefore, the potential of OA to induced a decrease in SOD activity as reported for sunflower (Malencic *et al*., 2004). These results favor a scenario in which OA, by reducing the activities of antioxidant enzymes, is able to trigger ROS accumulation thereby facilitating the colonization of leaflets tissue by *S. sclerotiorum* which is in line with the more severe symptoms of white mold for +OA plants.

The generation of ROS, including O_2^- and H_2O_2, at the attempted sites of pathogens penetration is one of the earliest biochemical responses of host resistance observed after their recognition (Cessna *et al*., 2000; Yarden *et al*., 2014). The manipulation of ROS balance by *S. sclerotiorum* has been shown to play a pivotal role for the successful fungal infection. Initially, *S. sclerotiorum* is able to suppress the ROS production in

plants to prevent the activation of defense responses; then, ROS accumulation is triggered to induce oxidative stress in the host cells to favor fungal colonization. These changes have been linked to the OA that is produced *S. sclerotiorum* on the infected tissues (Godoy *et al*., 1990; Cessna *et al*., 2000; Willian *et al*., 2011; Zhou *et al*., 2013). Our findings provide additional support for the OA's role in inducing oxidative stress in the *S. sclerotiorum*-infected leaflets of common bean plants at advanced stages of fungal infection when ROS accumulation was induced. For –OA plants, notable increases for O_2^- and H_2O_2 generation from 60 hai onwards occurred in response to infection by the two isolates of *S. sclerotiorum*; nevertheless, these increases were more pronounced for plants inoculated with the WT isolate which is directly related to the higher OA concentration obtained for these plants. The finding that ROS level was also increased for –OA plants inoculated with the A4 isolate indicated that despite OA playing a major role in the ROS generation, other effectors secreted by *S. sclerotiorum* (*e.g*., cell wall degrading enzymes) may also trigger ROS production. The O_2^- and H_2O_2 accumulation was enhanced due to OA spray irrespective of the isolate used, which most likely potentiated the *S. sclerotiorum*-induced oxidative stress. Indeed, *S. sclerotiorum* triggered striking cellular damage in the host cells, mainly for the plants that were inoculated with WT isolate based on the high MDA concentration. This finding is believed to be a result of the direct action of OA on membrane destabilization since increases in MDA concentration were more prominent for +OA plants than for the –OA ones regardless of the fungal isolate used. In agreement with our results, ROS and MDA contents were also found to be increased in the leaflets of soybean plants infected by *S. sclerotiorum* (Malencic *et al*., 2010).

Taking together, the results from the present study demonstrate that OA has a key role in enhancing *S. sclerotiorum*-triggered biochemical and physiological impairments on the leaflets of common bean plants. Fungal-induced decreases in photosynthesis

were governed chiefly by biochemical limitations, which were higher for plants inoculated with the WT isolate exposed to OA. Moreover, the concentration of photosynthetic pigments was more impacted on plants infected with the compromising, therefore, their ability to fully capture and exploit the collected light energy than for those infected with the A4 isolate, especially if they exposed to OA. Although plants infection by the WT isolate showed increased activities of the antioxidant enzymes in the absence of exogenous OA, it was greatly or completely abrogated in the presence of OA resulting, therefore, in increased oxidative stress and consequently exacerbating white mold symptoms for +OA plants.

Acknowledgments

Professor F. A. Rodrigues thanks the Conselho Nacional de Desenvolvimento Científico e Tecnológico (CNPq) for his fellowship. Mrs. I. R. F. Fagundes-Nacarath was supported by CNPq. We thank Professor Martin Dickman (Texas A&M University, USA) for providing the strains of *S. sclerotiorum* used in this study. This study was supported by grants from CAPES, CNPq and FAPEMIG to Prof. F. A. Rodrigues.

References

Andrew M, Barua R, Short SM, Kohn LM, 2012. Evidence for a common toolbox based on necrotrophy in a fungal lineage spanning necrotrophs, biotrophs, endophytes, host generalists and specialists. *PLOS One* **7**, e29943.

Baker NR, 2008. Chlorophyll fluorescence: A probe of photosynthesis *in vivo*. *Annual Review of Plant Biology* **59**, 89-113.

Bateman DF, Beer SV, 1965. Simultaneous production and synergistic action of oxalic acid and polygalacturonase during pathogenesis by *Sclerotium rolfsii*. *Phytopathology* **55**, 204–211.

Beauchamp C, Fridovich I, 1971. Superoxide dismutase: improved assays and an assay applicable to acrylamide gels. *Analytical Biochemistry* **44**, 276–287.

Boland G, Hall R, 1994. Index of plant hosts of *Sclerotinia sclerotiorum*. *Canadian of Journal Plant Pathology* **16**, 93–108.

Bolton MD, Thomma BPHJ, Nelson BD, 2006. Pathogen profile *Sclerotinia sclerotiorum* Lib. de Bary: biology and molecular traits of a cosmopolitan pathogen. *Molecular Plant Pathology* **7**, 1–16.

Bradford MN, 1976. A rapid and sensitive method for the quantitation of microgram quantities of protein utilizing the principle of protein-dye binding. *Analytical Biochemistry* **72**, 248–254.

Cakmak I, Horst WJ, 1991. Effect of aluminum on lipid peroxidation, superoxide dismutase, catalase, and peroxidase activities in root tips of soybean (*Glycine max*). *Physiologia Plantarum* **83**, 463–468.

Cessna SG, Sears VE, Dickman MB, Low PS, 2000. Oxalic acid, a pathogenicity factor for *Sclerotinia sclerotiorum*, suppresses the oxidative burst of the host plant. *Plant Cell* **12**, 2191–2199.

Chaitanya KSK, Naithani SC, 1994. Role of superoxide lipid peroxidation and superoxide 370 dismutase in membrane perturbation during loss of viability in seeds of *Shorea robusta* 371 Faertn. *New Phytologist* **126**, 623–627.

Chance B, Maehley AC, 1955. Assay of catalases and peroxidases. *Methods in Enzymology* **2**, 764–775.

Clark RB, 1975. Characterization of phosphates in intact maize roots. *Journal of Agricultural Food Chemistry* **23**, 458–460.

Davidson AL, Blahut-Beatty L, Itaya A, Zhang Y, Zheng S, Simmonds D, 2016. Histopathology of *Sclerotinia sclerotiorum* infection and oxalic acid function in susceptible and resistant soybean. *Plant Pathology* **65**, 878–887.

Díaz CG, Bassanezi RB, Godoy CV, Lopes DB, Bergamin Filho A, 2001. Quantificação do efeito do crestamento bacteriano comum na eficiência fotossintética e na produção do feijoeiro. *Fitopatologia Brasileira* **26**, 71–76.

Dickman MB, Mitra A, 1992. *Arabidopsis thaliana* as a model for studying *Sclerotinia sclerotiorum* pathogenesis. *Physiological and Molecular Plant Pathology* **41**, 255–263.

Dong X, Ji R, Guo X, Foster SJ, Chen H, Dong C, Liu Y, Hu Q, Liu S, 2008. Expressing a gene encoding wheat oxalate oxidase enhances resistance to *Sclerotinia sclerotiorum* in oilseed rape (*Brassica napus*). *Planta* **228**, 331–340.

Errakhi R, Meimoun P, Lehner A, Vidal G, Briand J, Corbineau F, Rona JP, Bouteau F, 2008. Anion channel activity is necessary to induce ethylene synthesis and programmed cell death in response to oxalic acid. *Journal of Experimental Botany* **59**, 3121–3129.

Ferrar PH, Walker JRL, 1993. o-Diphenol oxidase inhibition - an additional role for oxalic acid in the phytopathogenic arsenal of *Sclerotinia sclerotiorum* and *Sclerotium rolfsii*. *Physiological and Molecular Plant Pathology* **43**, 415–422.

Gay C, Gebicki JM, 2000. A critical evaluation of the effect of sorbitol on the ferric-xylenol orange hydroperoxide assay. *Analytical Biochemistry* **284**, 217–220.

Godoy G, Steadman JR, Dickman MB, Dam R, 1990. Use of mutants to demonstrate the role of oxalic acid in pathogenicity of *Sclerotinia sclerotiorum* on *Phaseolus vulgaris*. *Physiological and Molecular Plant Pathology* **37**, 179–191.

Guimaraes RL, Stotz HU, 2004. Oxalate production by *Sclerotinia sclerotiorum* deregulates guard cells during infection. *Plant Physiology* **136**, 3703–3711.

Havir EA, MChale NA, 1989. Enhanced-peroxidatic activity in specific catalase isozymes of tobacco, barley, and maize. *Plant Physiology* **91**, 812–815.

Heath RL, Packer L, 1968. Photoperoxidation in isolated chloroplast. I Kinetics and stoichometry of fatty acid peroxidation. *Archives of Biochemistry and Biophysics* **125**, 189–198.

Hu X, Bidney DL, Yalpani N, Duvick JP, Crasta O, Folkerts O, Lu G, 2003. Overexpression of a gene encoding hydrogen peroxide-generating oxalate oxidase evokes defense responses in sunflower. *Plant Physiology* **133**, 170–181.

Jesus Junior WC, Vale FXR, Martinez CA, Coelho RR, Costa LC, Hau B, Zambolim L, 2001. Effects of angular leaf spot and rust on leaf gas exchange and yield of common bean (*Phaseolus vulgaris*). *Photosynthetica* **39**, 603–606.

Kar M, Mishra D, 1976. Catalase, peroxidase, and polyphenol oxidase activities during rice leaf senescence. *Plant Physiology* **57**, 315–319.

Kim KS, Min J-Y, Dickman MB, 2008. Oxalic acid is an elicitor of plant programmed cell death during *Sclerotinia sclerotiorum* disease development. *Molecular Plant–Microbe Interactions* **21**, 605–612.

Klughammer C, Schreiber U, 2008. Complementary PSII quantum yield calculated from simple fluorescence parameters measured by PAM fluorometry and saturation pulse method. *PAM Application Notes* **1**, 27–35.

Kolkman JM, Kelly JD, 2000. An indirect test using oxalate to determine physiological resistance to white mold in common bean. *Crop Science* **40**, 281–285.

Kramer DM, Johnson G, Kiirats O, Edwards GE, 2004. New fluorescence parameters for the determination of QA redox state and excitation energy fluxes. *Photosynthesis Research* **79**, 209-218.

Kuo MC, Kao CH, 2003. Aluminum effects on lipid peroxidation and antioxidative enzyme activities in rice leaves. *Biologia Plantarum* **46**, 149–152.

Leite ME, Santos JB, Ribeiro Júnior PM, Souza DA, Castro LA, Resende MLV, 2014. Biochemical responses associated with common bean defence against *Sclerotinia sclerotiorum*. *European Journal of Plant Pathology* **138**, 391–404.

Liang X, Liberti D, Li M, Kim YT, Hutchens A, Wilson R, Rollins JA, 2015. Oxaloacetate acetylhydrolase gene mutants of *Sclerotinia sclerotiorum* do not accumulate oxalic acid, but do produce limited lesions on host plants. *Molecular Plant Pathology* **16**, 559–571.

Liu F, Wang M, Wen J, Yi B, Shen J, Ma C, Tu J, Fu T, 2015. Overexpression of barley oxalate oxidase gene induces partial leaf resistance to *Sclerotinia sclerotiorum* in transgenic oilseed rape. *Plant Pathology* **64**, 1407–1416.

Malencic D, Kiprovski B, Popovic M, Prvulovic D, Miladinovic J, Djordjevic V, 2010. Changes in antioxidant systems in soybean as affected by *Sclerotinia sclerotiorum* (Lib.) de Bary. *Plant Physiology and Biochemistry* **48**, 903–908.

Malencic D, Vasic D, Popovic M, Devic D, 2004. Antioxidant systems in sunflower as affected by oxalic acid. *Biologia Plantarum* **48**, 243–247.

Nakano Y, Asada K, 1981. Hydrogen peroxidase is scavenged by ascorbate specific peroxidases in spinach chloroplasts. *Plant and Cell Physiology* **22**, 867–880.

Noyes RD, Hancock JG, 1981. Role of oxalic acid in the *Sclerotinia* wilt of sunflower. *Physiological Plant Pathology* **18**, 123–132.

Oxborough K, Baker NR, 1997. An instrument capable of imaging chlorophyll *a* fluorescence from intact leaves at very low irradiance and at cellular and subcellular levels of organization. *Plant, Cell & Environment* **20**, 1473–1483.

Polanco LR, Rodrigues FA, Nascimento KJT, Cruz MFA, Curvelo CRS, DaMatta FM, Vale FXR, 2014. Photosynthetic gas exchange and antioxidative system in common bean plants infected by *Colletotrichum lindemuthianum* and supplied with silicon. *Tropical Plant Pathology* **39**, 35–42.

Rodrigues FA, Polanco LR, Duarte HSS, Resende RS, Vale FXR, 2014. Photosynthetic gas exchange in common bean submitted to foliar sprays of potassium silicate, sodium molybdate and fungicide and infected with *Colletotrichum lindemuthianum*. *Journal of Phytopathology* **163**, 554–559.

Rollins JA, 2003. The *Sclerotinia sclerotiorum* pac1 gene is required for sclerotial development and virulence. *Molecular Plant–Microbe Interactions* **16**, 785–795.

Rollins JA, Dickman MB, 2001. pH signaling in *Sclerotinia sclerotiorum*: identification of a pacC/RIM1 homolog. *Applied and Environmental Microbiology* **67**, 75–81.

Tariq VN, Jeffries P, 1985. Changes occurring in chloroplasts of *Phaseolus* following infection by *Sclerotinia*: A cytochemical study. *Journal of Cell Science* **75**, 195–295.

Vale FXR, Fernandes Filho EI, Liberato JR, 2003. QUANT: a software plant disease severity assessment. In: R. Close, M. Braithwaite & I. Havery (Eds.), *Proceedings of the 8th International Congress of Plant Pathology* (pp. 105). New Zealand.

Wellburn AR, 1994. The spectral determination of chlorophylls *a* and *b*, as well as total carotenoids, using various solvents with spectrophotometers of different resolution. *Journal of Plant Physiology* **144**, 307-313.

Williams B, Kabbage M, Kim HJ, Britt R, Dickman MB, 2011. Tipping the balance: *Sclerotinia sclerotiorum* secreted oxalic acid suppresses host defenses by manipulating the host redox environment. *PLOS Pathogens* **7**, e1002107.

Yang C, Zhang Z, Gao H, Liu M, Fan X, 2014. Mechanisms by which the infection of *Sclerotinia sclerotiorum* (Lib.) de Bary affects the photosynthetic performance in tobacco leaves. *BMC Plant biology* **14**, 1–11.

Yarden O, Veluchamy S, Dickman MB, Kabbage M, 2014. *Sclerotinia sclerotiorum* catalase SCAT1 affects oxidative stress tolerance, regulates ergosterol levels and controls pathogenic development. *Physiological and Molecular Plant Pathology* **85**, 34–41.

Zhou J, Sun A, Xing D, 2013. Modulation of cellular redox status by thiamine-activated NADPH oxidase confers *Arabidopsis* resistance to *Sclerotinia sclerotiorum. Journal of Experimental Botany* **64**, 3261–3272.

List of Tables and Figures

Table 1. Analysis of variance of the effects of inoculation conditions (IC), plants non-sprayed or sprayed with oxalic acid (PS), evaluation time (ET) and their interactions for white mold severity (WMS), lesion area (LA), leaf gas exchange parameters (net CO_2 assimilation rate (A), stomatal conductance to water vapor (g_s), internal CO_2 concentration (C_i) and the transpiration rate (E)), chlorophyll *a* fluorescence parameters (maximum PSII quantum efficiency (F_v/F_m), photochemical yield (Y(II)), yield for dissipation by down-regulation (Y(NPQ)) and yield for other non-photochemical (non-regulated) losses (Y(NO)) as well as electron transport rate (ETR)), concentrations of chlorophyll *a*+*b* (Chl *a*+*b*) and carotenoids (CAR), activities of superoxide dismutase (SOD), catalase (CAT), peroxidase (POX), ascorbate peroxidase (APX) as well as the concentrations of oxalic acid (OA), superoxide (O_2^-), hydrogen peroxide (H_2O_2) and malondialdehyde (MDA).

Variables/ Parameters	IC	PS	ET	IC ×PS	IC × ET	PS × ET	IC × PS × ET
LA	<0.001	-	<0.001	-	<0.001	-	-
WMS	<0.001	-	<0.001	-	<0.001	-	-
A	<0.001	<0.001	<0.001	<0.001	<0.001	0.973	0.121
g_s	<0.001	<0.001	<0.001	0.099	0.002	0.145	0.545
C_i	<0.001	<0.001	<0.001	0.011	<0.001	0.013	0.038
E	<0.001	<0.001	<0.001	0.002	0.038	0.901	0.809
F_v/F_m	<0.001	<0.001	<0.001	<0.001	<0.001	<0.001	0.009
Y(II)	<0.001	<0.001	<0.001	<0.001	<0.001	0.002	0.169
Y(NPQ)	<0.001	0.091	0.001	0.169	<0.001	0.407	0.448
Y(NO)	<0.001	0.015	<0.001	0.027	<0.001	0.003	0.024
ETR	<0.001	<0.001	<0.001	<0.001	<0.001	0.010	0.651
Chl *a*+*b*	<0.001	<0.001	<0.001	0.009	<0.001	0.005	0.549
CAR	<0.001	<0.001	<0.001	0.001	<0.001	0.213	0.812
SOD	<0.001	0.160	0.432	<0.001	0.001	0.012	0.007
CAT	<0.001	<0.001	<0.001	<0.001	0.001	<0.001	0.001
POX	<0.001	<0.001	<0.001	<0.001	<0.001	<0.001	<0.001
APX	0.001	0.696	<0.001	<0.001	<0.001	<0.001	<0.001
OA	<0.001	<0.001	<0.001	0.053	<0.001	0.422	0.140
O_2^-	<0.001	<0.001	<0.001	<0.001	<0.001	0.028	0.058
H_2O_2	<0.001	<0.001	<0.001	0.070	<0.001	0.232	0.711
MDA	<0.001	0.001	<0.001	<0.001	<0.001	<0.001	0.090

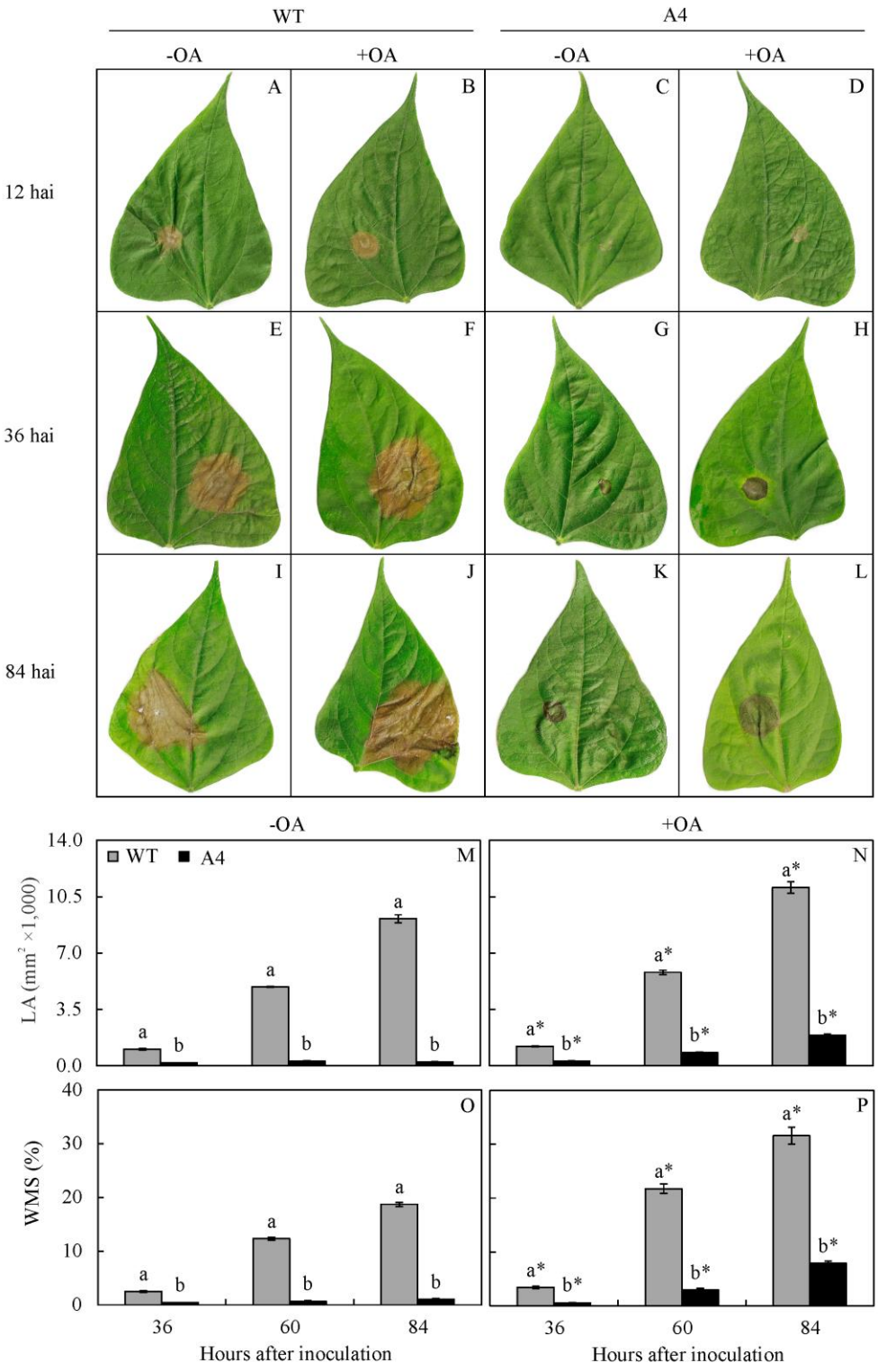

Figure 1. White mold symptoms (A-L), lesion area (M and N) and severity (O and P) on the leaflets of common bean plants sprayed with water (–OA) (A, C, E, G, I, K, M and O) or oxalic acid (+OA) (B, D, F, H, J, L, N and P) and either inoculated with the wild type (WT) (A, B, E, F, I and J) or an oxalic acid-defective mutant (A4) (C, D, G,

H, K and L) of *Sclerotinia sclerotiorum*. For each evaluation time, means for each isolate followed by different letters and from -OA and +OA treatments followed by an asterisk (*) are significantly different ($P \leq 0.05$) according to Tukey's test. Bars represent the standard error of the means. $n = 4$.

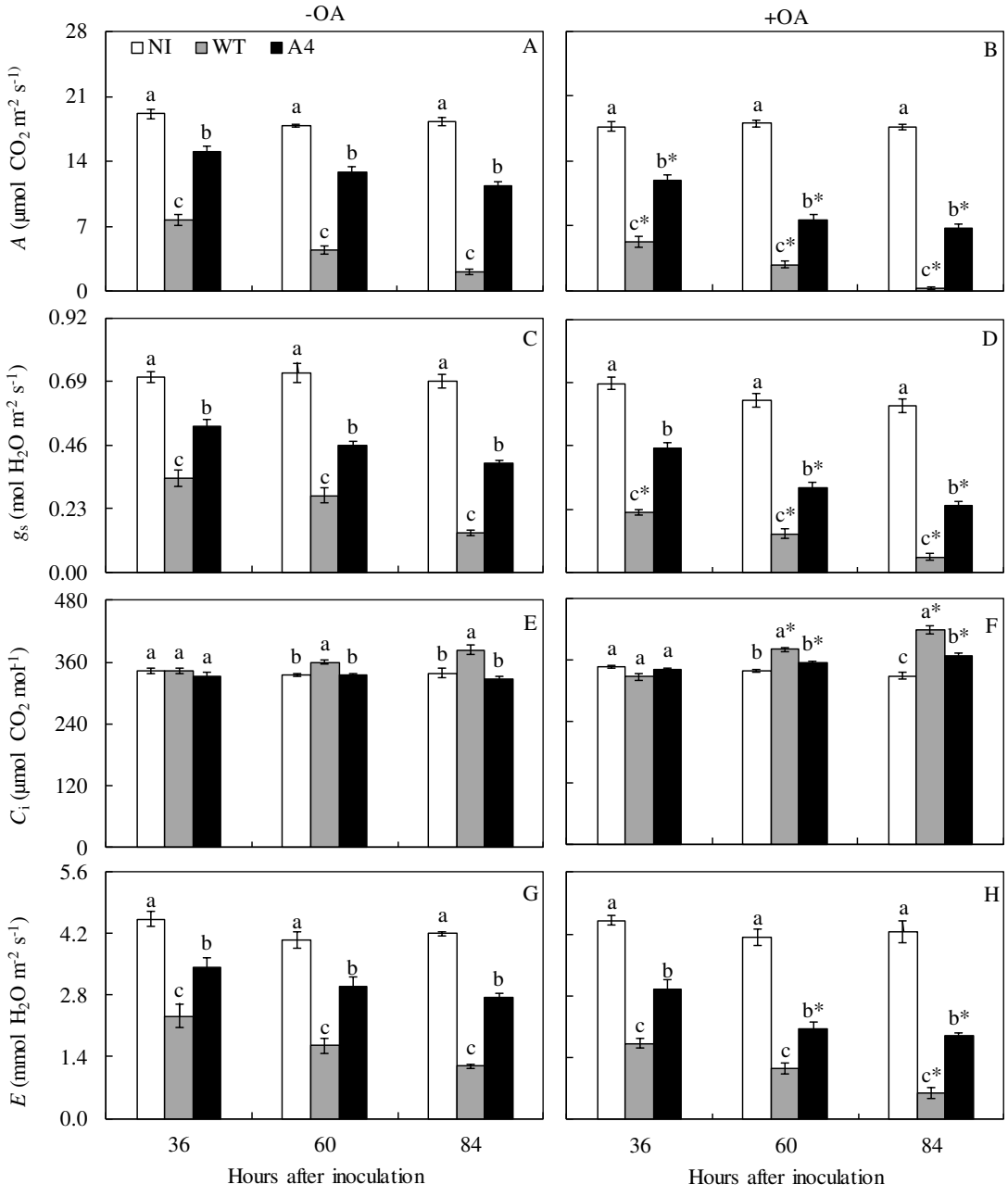

Figure 2. Leaf gas exchange parameters net carbon assimilation rate (*A*) (A and B), stomatal conductance to water vapor (g_s) (C and D), internal CO_2 concentration (C_i) (E and F) and transpiration rate (*E*) (G and H) determined on the leaflets of common bean

plants sprayed with water (–OA) (A, C, E and G) or oxalic acid (+OA) (B, D, F and H) and non-inoculated (NI) or either inoculated with the wild type (WT) or an oxalic acid-defective mutant (A4) of *Sclerotinia sclerotiorum*. For each evaluation time, means for each isolate followed by different letters and from -OA and +OA treatments followed by an asterisk (*) are significantly different ($P \leq 0.05$) according to Tukey's test. Bars represent the standard error of the means. n = 4.

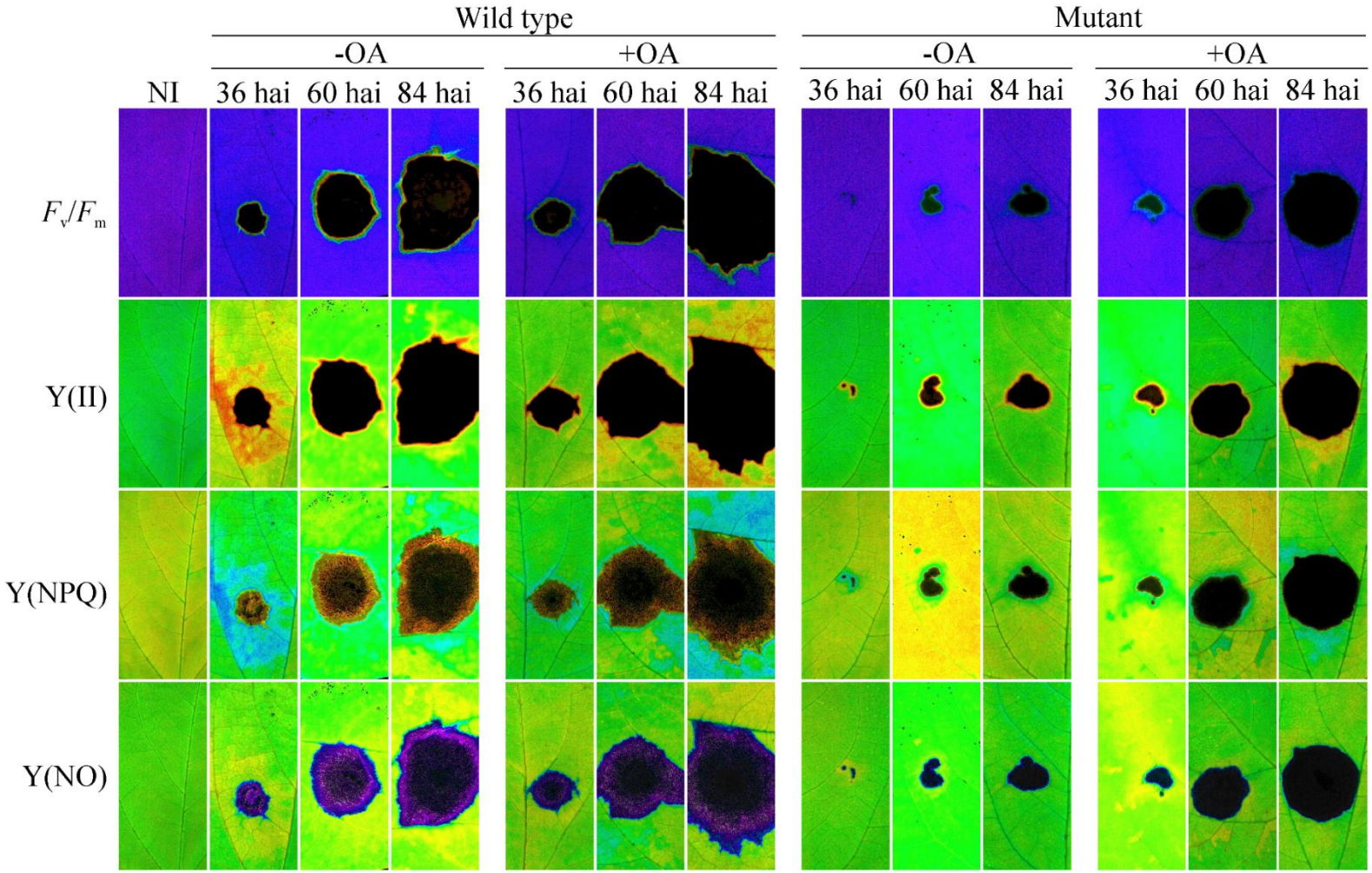
Wild type
Mutant
-OA
+OA
-OA
+OA
NI
36 hai
60 hai
84 hai
36 hai
60 hai
84 hai
36 hai
60 hai
84 hai
36 hai
60 hai
84 hai
F_v/F_m
Y(II)
Y(NPQ)
Y(NO)

Figure 3. Images of the chlorophyll *a* fluorescence parameters maximum PSII quantum efficiency (F_v/F_m), photochemical yield (Y(II)), yield for dissipation by down-regulation (Y(NPQ)) and yield for other non-photochemical (non-regulated) losses (Y(NO)) on the leaflets of common bean plants sprayed with water (–OA) or oxalic acid (+OA) and non-inoculated (NI) or either inoculated with the wild type (WT) or an oxalic acid-defective mutant (A4) of *Sclerotinia sclerotiorum*.

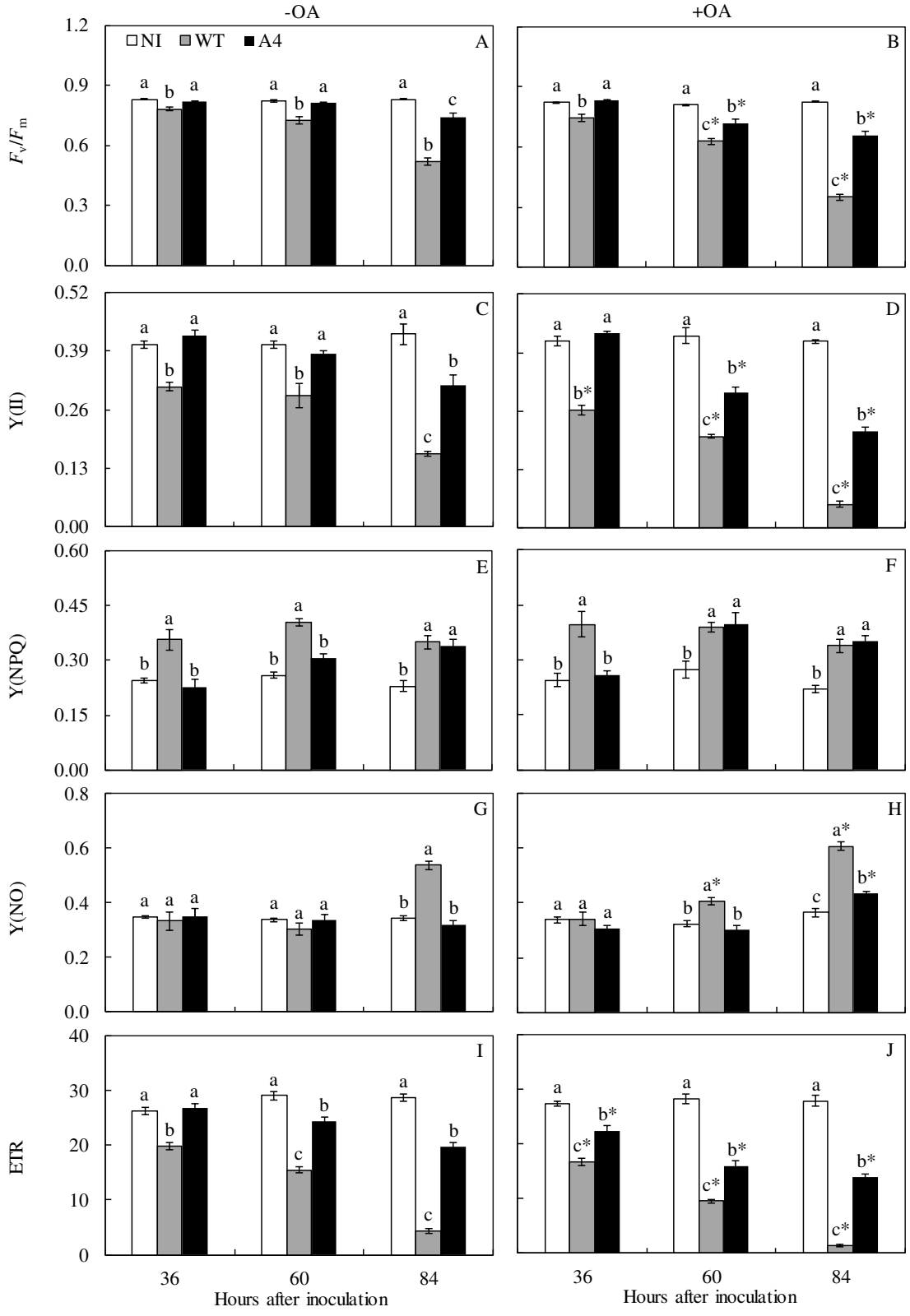

Figure 4. Chlorophyll *a* parameters variable-to-maximum chlorophyll *a* fluorescence ratio (F_v/F_m) (A and B), photochemical yield (Y(II)) (C and D), yield for dissipation by down-regulation (Y(NPQ)) (E and F), yield for other non-photochemical (non-regulated) losses (Y(NO)) (G and H) and electron transport rate (ETR) (I and J)

determined on the leaflets of common bean plants sprayed with water (–OA) (A, C, E, G and I) or oxalic acid (+OA) (B, D, F, H and I) and non-inoculated (NI) or either inoculated with the wild type (WT) or an oxalic acid-defective mutant (A4) of *Sclerotinia sclerotiorum*. For each evaluation time, means for each isolate followed by different letters and from -OA and +OA treatments followed by an asterisk (*) are significantly different ($P \leq 0.05$) according to Tukey's test. Bars represent the standard error of the means. $n = 4$.

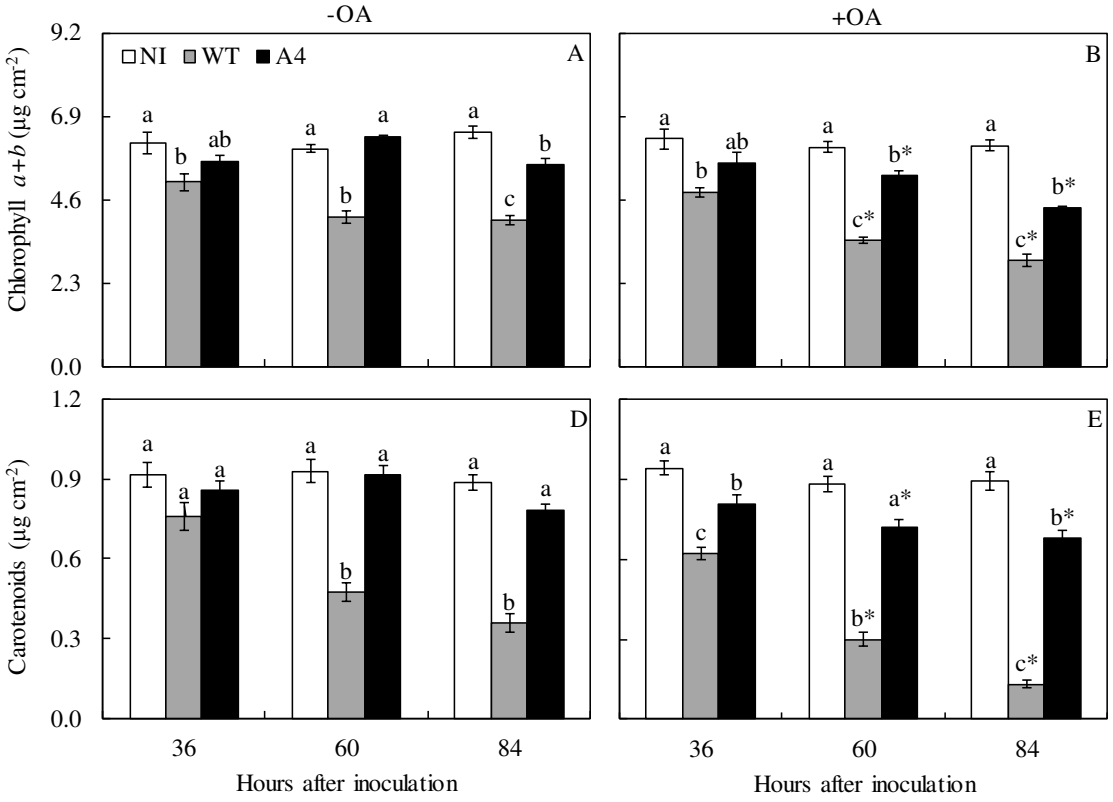

Figure 5. Concentrations of chlorophyll *a*+*b* (A and B) and carotenoids (C and D) on the leaflets of common bean plants sprayed with water (–OA) (A and C) or oxalic acid (+OA) (B and D) and non-inoculated (NI) or either inoculated with the wild type (WT) or an oxalic acid-defective mutant (A4) of *Sclerotinia sclerotiorum*. For each evaluation time, means for each isolate followed by different letters and from -OA and +OA treatments followed by an asterisk (*) are significantly different ($P \leq 0.05$) according to Tukey's test. Bars represent the standard error of the means. $n = 4$.

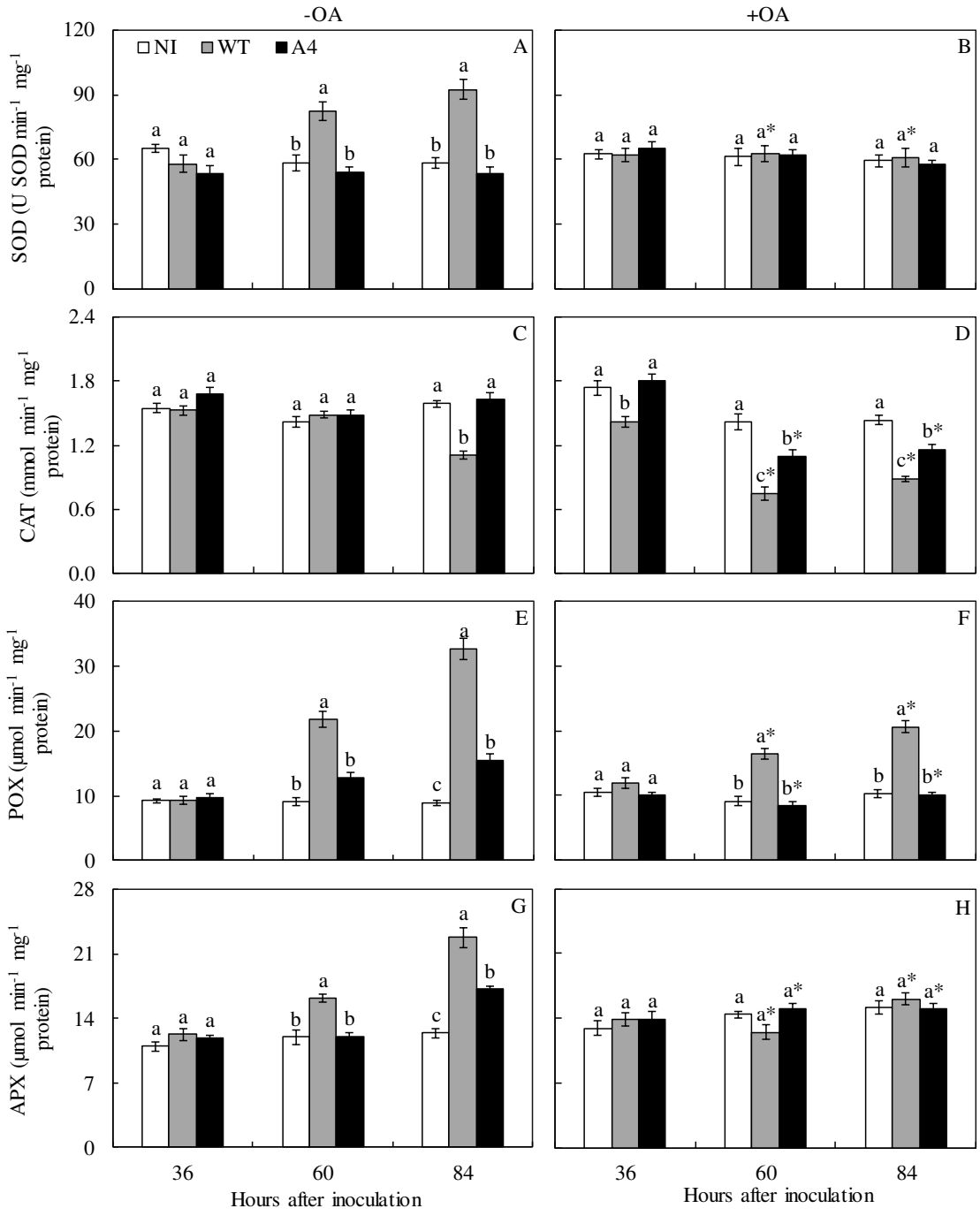

Figure 6. Activities of superoxide dismutase (SOD) (A and B), catalase (CAT) (C and D), peroxidase (POX) (E and F) and ascorbate peroxidase (APX) (G and H) on the leaflets of common bean plants sprayed with water (–OA) (A, C, E and G) or oxalic acid (+OA) (B, D, F and H) and non-inoculated (NI) or either inoculated with the wild type (WT) or an oxalic acid-defective mutant (A4) of *Sclerotinia sclerotiorum*. For each evaluation time, means for each isolate followed by different letters and from -OA and

+OA treatments followed by an asterisk (*) are significantly different ($P \leq 0.05$) according to Tukey's test. Bars represent the standard error of the means. $n = 4$.

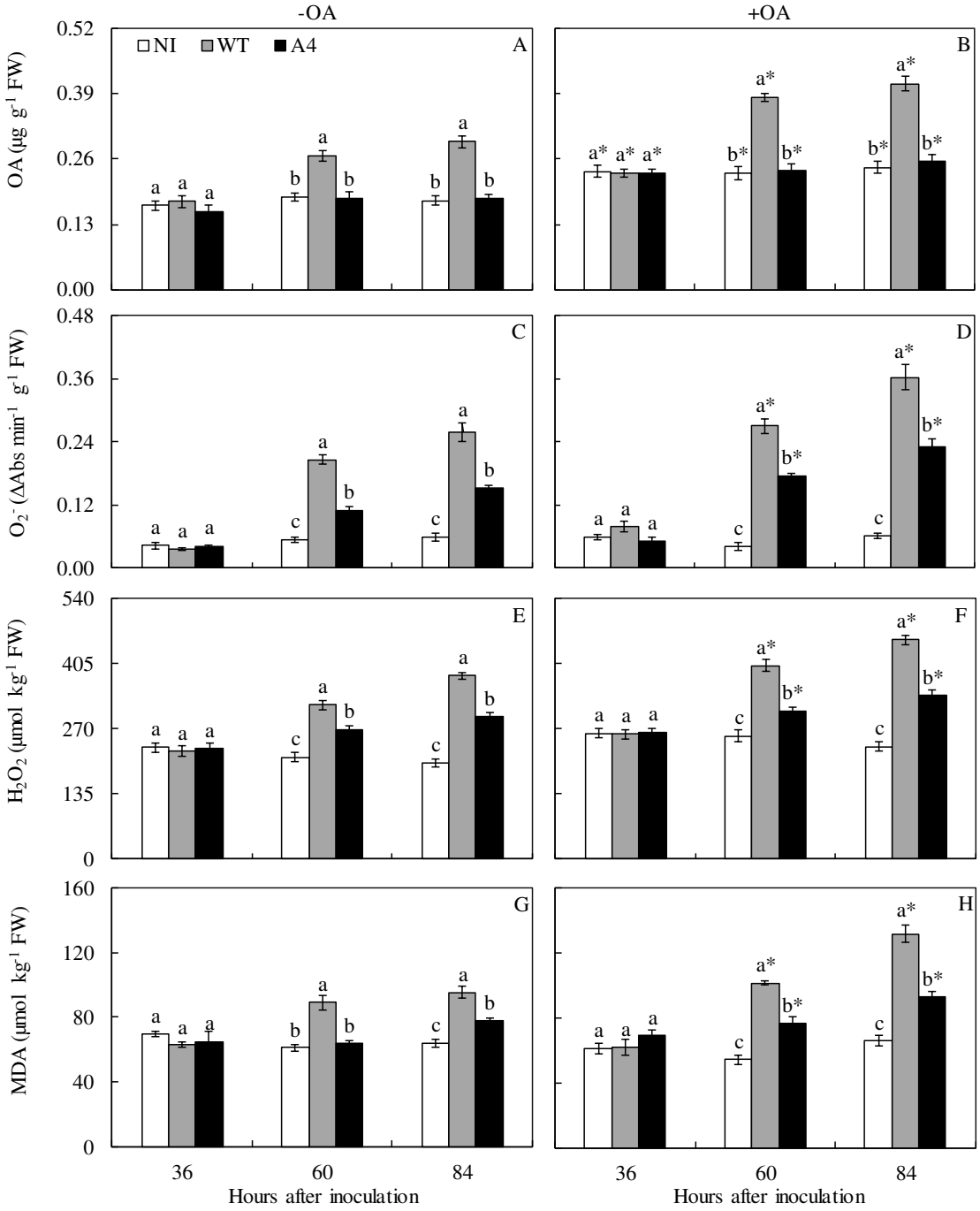

Figure 7. Concentrations of oxalic acid (OA) (A and B), superoxide (O_2^-) (C and D), hydrogen peroxide (H_2O_2) (E and F) and malondialdehyde (MDA) (G and H) on the leaflets of common bean plants sprayed with water (–OA) (A, C, E and G) or oxalic acid (+OA) (B, D, F and H) and non-inoculated (NI) or either inoculated with the wild

type (WT) or an oxalic acid-defective mutant (A4) of *Sclerotinia sclerotiorum*. For each evaluation time, means for each isolate followed by different letters and from –OA and +OA treatments followed by an asterisk (*) are significantly different ($P \leq 0.05$) according to Tukey's test. FW = fresh weight. Bars represent the standard error of the means. $n = 4$.

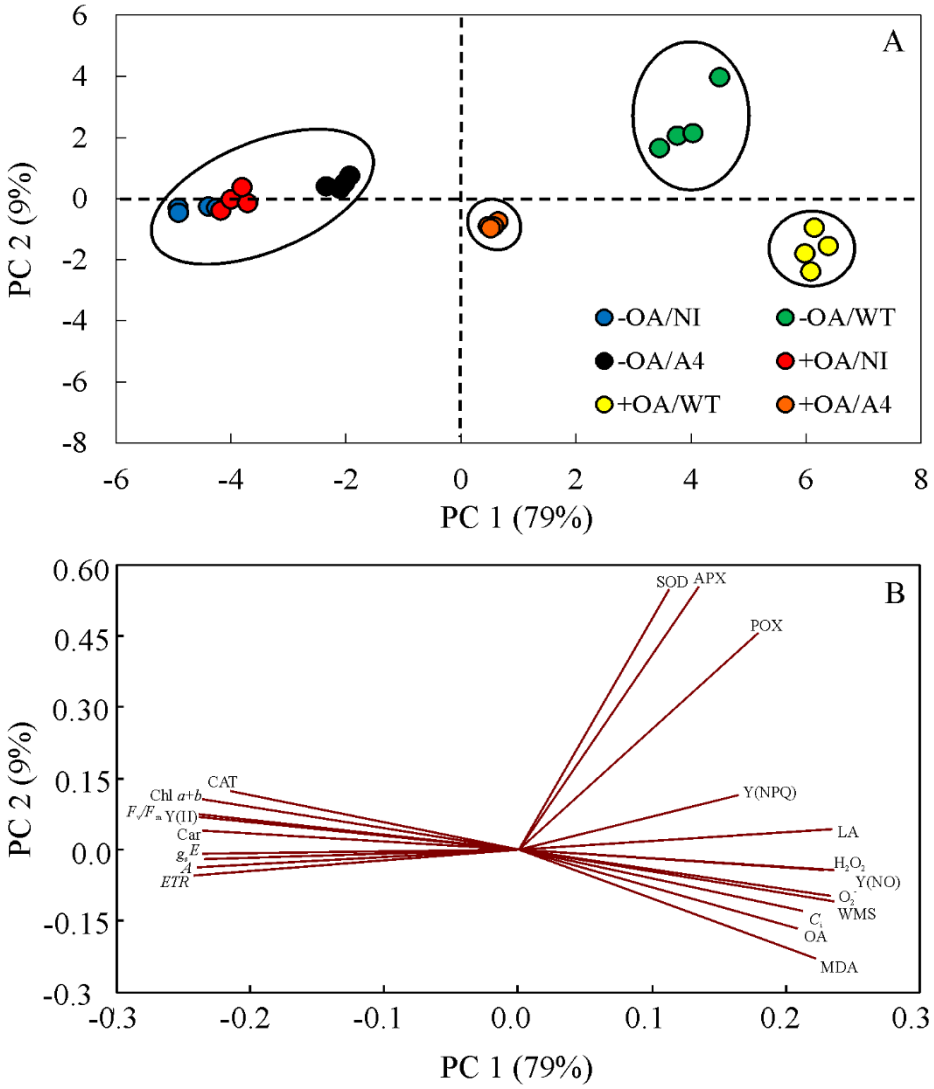

Figure 8. Score (A) and loading (B) plots of the principal component analysis comparing lesion area (LA), white mold severity (WMS), leaf gas exchange parameters (net CO_2 assimilation rate (A), stomatal conductance to water vapor (g_s), internal CO_2 concentration (C_i) and the transpiration rate (E)), chlorophyll *a* fluorescence parameters

(maximum PSII quantum efficiency (F_v/F_m), photochemical yield (Y(II)), yield for dissipation by down-regulation (Y(NPQ)), yield for other non-photochemical (non-regulated) losses (Y(NO)) and electron transport rate (ETR)), concentrations of chlorophyll *a* + *b* (Chl *a*+*b*) and carotenoids (Car), activities of superoxide dismutase (SOD), catalase (CAT), peroxidase (POX), ascorbate peroxidase (APX) as well as concentrations of oxalic acid (OA), superoxide (O_2^-), hydrogen peroxide (H_2O_2) and malondialdehyde (MDA) on the leaflets of common bean plants sprayed with water (–OA) or oxalic acid (+OA) and non-inoculated (NI) or either inoculated with the wild type (WT) or an oxalic acid-defective mutant (A4) of *Sclerotinia sclerotiorum*.

CHAPTER 2

Phosphites attenuate S*clerotinia sclerotiorum*-induced physiological impairments in common bean

Abstract

Phosphites, marketed as foliar fertilizers and resistance activators, have been shown to be effective for the control of diseases in many profitable crops. Despite the importance of white mold, caused by *Sclerotinia sclerotiorum*, to reduce common bean yield, knowledge of the phosphites´ effect on disease control at the physiological level is still missing. In this study, the leaf gas exchanges and chlorophyll *a* parameters as well as the concentrations of photosynthetic pigments in common bean plants that were sprayed with zinc (Zn) or copper (Cu) phosphites and challenged or not with *S. sclerotiorum* were determined. Based on the *in vitro* assays, Zn and Cu phosphites inhibited fungal mycelial growth in a dose-dependent manner, but the Cu phosphite showed to be more fungitoxic. Lesion area and white mold severity were reduced by Zn and Cu phosphites, but the Zn phosphite was more effective. Fungal infection dramatically decreased the values of net carbon assimilation rate, stomatal conductance to water vapor and transpiration rate on non-sprayed plants. Increases in internal CO_2 concentration indicated that fungal-induced photosynthetic impairments were chiefly governed by biochemical limitations, but these impairments were greatly abrogated in the Zn and Cu phosphite-sprayed plants. Similarly, the photochemical dysfunctions stemmed from *S. sclerotiorum* infection were limited in the Zn and Cu phosphite-sprayed plants. Concentrations of chlorophyll *a+b* and carotenoids decreased on inoculated plants, but lower reductions were recorded on Zn and Cu phosphites-sprayed plants. In conclusion, the potential of Zn and Cu phosphites in attenuate the *S. sclerotiorum*-induced physiological impairments in common bean leaflets was demonstrated and may be an effective mean for managing this disease under field conditions.

Keywords: *Phaseolus vulgaris*, chlorophyll *a* fluorescence, leaf gas exchange, photosynthesis, white mold.

Introduction

White mold, caused by *Sclerotinia sclerotiorum* (Lib.) De Bary, is a yield-limiting disease of common bean (*Phaseolus vulgaris* L.) in many countries [1], including Argentina, Brazil, Canada and the USA. In Brazil, the world's leading producer and consumer of common bean, white mold is wide spread and caused yield losses up to 100% [2].

White mold symptoms include water-soaked spots that are brown in color and soft in consistency; such spots progress quickly and turn into necrotic lesions over which a white cottony mycelium can be seen [3]. The symptoms can be noticed in all above ground organs regardless of the plant growth stage; flowering is the most susceptible growth phase since senescing flowers represent the primary plant organ for infection by for *S. sclerotiorum* [4]. White mold epidemics are favored by mild temperatures (< 20°C), high humidity (> 70%), high sowing density and prostrate plant growth habit [3, 2].

There are few strategies for controlling white mold of common bean and resistant cultivars are very difficult to obtain [5]. Rotation with non-host crops, control of irrigation, selection of upright cultivars [6] and biological control [7] are among the alternatives that are used for white mold management, but such measures have a limited efficiency due to *S. sclerotiorum* fungal aggressiveness and its wide host range [1]. Despite fungicides being a major strategy for disease control [5,8,9], they have potential negative impacts in human health and the environment, thus limiting their use [10]. In addition, an isolate of *S. sclerotiorum* from common bean showing resistance to a commonly used fungicide (methyl thiophanate) was recently found in Brazil [11].

In view of the challenge to control white mold, novel alternatives need to be urgently investigated. Phosphite-based compounds are marketed as foliar fertilizers and disease resistance inducers, being their metal salts effective in controlling diseases caused by *Phytophthora* spp. [12-14] and fungi such as *Rhizoctonia solani*, *Alternaria alternata* and *Fusarium* spp. [15-18] in several plant species. Phosphites can have a direct action against pathogens inhibiting mycelial growth and leading to hyphal rupture as well as affecting the plant's physiology under absence or presence of the pathogen [19-21]. Phosphites sprays attenuate the pathogen-induced photosynthetic dysfunctions in the *Fagus sylvatica-Phytophthora plurivora*, *Aesculus hippocastanum-Pseudomonas syringae* pv. *aesculi* e *Pinus-Fusarium circinatum* interactions [13,22,18]. The effect of phosphites however on the physiological performance of *S. sclerotiorum*-infected common bean has never been performed.

Considering the lack of information in the literature regarding the physiological changes in common bean sprayed with phosphites and infected with *S. sclerotiorum*, the present study aimed to examine the effect of zinc and copper phosphites on the photosynthetic performance of common bean plants challenged or not with *S. sclerotiorum* by examining the leaf gas exchange and chlorophyll *a* fluorescence parameters as well as the concentration of photosynthetic pigments.

Material and methods

Plant growth

Five seeds of common bean from cultivar Pérola, susceptible to *S. sclerotiorum*, were sown in plastic pots of 2 liters containing 2 kg of Tropstrato® substrate (Vida Verde, Mogi Mirim, São Paulo, Brazil) composed of a mixture of pine bark, peat and expanded vermiculite (1:1:1). Each pot was thinned to three seedlings seven days after emergence. Plants were kept in a greenhouse (30 ± 5ºC temperature, 65 ± 5% relative humidity and 900 ± 15 μmol photons m^{-2} s^{-1} natural photosynthetically active radiation). Plants were fertilized weekly with 100 mL of a modified nutrient solution based on [23] as follows: 0.8 mM KNO_3, 0.069 mM $NH_4H_2PO_4$, 1 mM NH_4NO_3, 1 mM $Ca(NO_3).4H_2O$, 0.9 mM KCl, 0.6 mM $MgSO_4$ $7H_2O$, 0.5 μM $CuSO_4$ $5H_2O$, 2 μM $ZnSO_4$ $7H_2O$, 19 μM H_3BO_3, 7 μM $MnCl_2$ $4H_2O$, 0.6 μM Na_2MoO_4 $4H_2O$, 60 μM $FeSO_4$ $7H_2O$ and 90 μM disodium ethylenediaminetetraacetic acid (EDTA). Plants were watered with deionized water as needed.

Inoculum production, inoculation procedure and treatments

The isolate CMES 1465 of *S. sclerotiorum* obtained from common bean, provided by EMBRAPA Soybean (Londrina, Paraná State, Brazil), was used for plant inoculations. The isolate was preserved as sclerotia; for their production, carrots were washed, peeled, cut in cubes of approximately 1 × 1 × 1 cm, transferred to Erlenmeyer flasks and autoclaved at 121°C for 20 min [24]. For inoculum production, a sclerotium was transferred to each Petri dish containing potato dextrose agar (PDA) medium and kept in a growth chamber (20°C and 12 h photoperiod) for seven days.

The three leaflets of the third leaf, from the base to the top, of each plant (V3 growth stage) were inoculated with a plug (5 mm in diameter) of PDA medium obtained

from the edge of three-day-old actively growing colonies of *S. sclerotiorum*. Each PDA plug was placed between the main vein and the edge of the leaflet and gently pressed with the forefinger. Inoculated plants were transferred to a plastic mist growth chamber (MGC) inside a greenhouse for the duration of the experiment. The MGC was made of wood (2 m wide, 15 m high, 5 m long) and covered with 100 µm thick transparent plastic. The temperature inside the MGC ranged from 20 ± 2°C (day) to 17 ± 2°C (night). The relative humidity was maintained at 92 ± 3% using a misting system with nozzles (model NEB-100; KGF Co.) that sprayed mist every 30 min above the plant canopy. The relative humidity and temperature were measured with a thermohygrograph (TH-508; Impac). The maximum natural photon flux density at plant canopy height was approximately 900 µmol m^{-2} s^{-1}.

At 48 h before *S. sclerotiorum* inoculation, plants were sprayed with water (control treatment), zinc (Zn) phosphite (5 mL L^{-1}, Phytogard® Zn (40% P_2O_5 and 10% Zn), Stoller do Brasil S.A., Cosmópolis, Brazil) or copper (Cu) phosphite (2.5 mL L^{-1}, Strong (20% P_2O_5 and 4% Cu), Giro Produtos Agrícolas LTDA, Machado, Brazil). Plants were sprayed using a CO_2 pressurized backpack sprayer equipped with a flat fan nozzle (XR 110 02®, Teejet, Glendale Heights, IL, USA) at a 200,000-Pa pressure to deliver a spray volume of 200 L ha^{-1}.

In vitro *assays*

The sensitivity of *S. sclerotiorum* to both Zn and Cu phosphites was evaluated *in vitro* using different concentrations of the products as following: 0, 0.625, 1.25, 2.5, 5 and 10 mL L^{-1} of PDA medium. Melted PDA medium was amended with each rate of phosphite and then poured into Petri plates (20 mL per plate). Then, one PDA plug (5 mm in diameter), containing fungal mycelia obtained from the edge of a three-days old *S. sclerotiorum* colony, was placed in the center of Petri dishes, which were kept in a

growth chamber (20°C and 12 h photoperiod). Fungal colony in each Petri dish was measured to obtain its diameter in two orthogonal directions at 24, 36, 48 and 60 h using a digital caliper.

Disease evaluation

Inoculated leaflets of each plant were collected at 12, 36, 60 and 84 h after inoculation (hai) to determine lesion area (LA) by measuring the perpendicular directions using a digital caliper. Leaflets were also scanned at 300 dpi resolution to obtain images that were further processed using the software QUANT [25] to determine the white mold severity (WMS).

Evaluation of the leaf gas exchange parameters

Leaf gas exchange parameters were determined in one leaflet from the third leaf of each plant (four leaflets per treatment) at 12, 36 and 60 hai. The net carbon assimilation rate (A), stomatal conductance to water vapor (g_s), internal CO_2 concentration (C_i) and transpiration rate (E) were estimated from 09:00 to 12:00 h under artificial and saturating photon irradiance (1,200 μmol m^{-2} s^{-1}) and an external CO_2 concentration of 400 μmol mol^{-1} using a portable open-system infrared gas analyzer (LI-6400, LI-COR Inc., Lincoln, NE, USA). All measurements were performed by setting the block temperature at 25°C.

Chlorophyll (Chl) a fluorescence imaging

The Imaging-PAM fluorometer and the Imaging Win software MAXI version (Heinz Walz GmbH, Effeltrich, Germany) were used to obtain the images and parameters of chlorophyll *a* fluorescence in one leaflet from the third leaf of each plant (four leaflets per treatment) at 12, 36, 60 and 84 hai. Plants were dark-adapted for 1 h

and leaflets were placed individually in the CCD ("charge-coupled device") camera to obtain the images at the resolution of 640 × 480 pixels in a support at a distance of 18.5 cm from the CCD camera that was used to capture the chlorophyll *a* fluorescence emission. The leaflets were illuminated with a weak modulated measuring beam (0.5 μmol m^{-2} s^{-1}, 100 μs, 1 Hz) to obtain the initial fluorescence (F_0). A saturating white light pulse of 2,400 μmol m^{-2} s^{-1} (10 Hz) was emitted for 0.8 s to determine the maximum fluorescence emission (F_m). Based on these initial measurements, the maximum photosystem II (PSII) photochemical efficiency of the dark-adapted leaflets was estimated through the variable-to-maximum chlorophyll *a* fluorescence ratio, $F_v/F_m = [(F_m - F_0)/F_m)]$. Next, the leaflets were exposed to actinic photon irradiance (531 μmol m^{-2} s^{-1}) for 120 s to obtain the steady-state fluorescence yield (F_s), after which a saturating white light pulse (2,400 μmol m^{-2} s^{-1}; 0.8 s) was applied to achieve the light-adapted maximum fluorescence (F_m'). The light-adapted initial fluorescence (F_0') was estimated according [26]. Based on [27], the energy that was absorbed by the PS II for the following three yield components for dissipative processes was calculated as follows: the photochemical yield [$Y(II) = (F_m' - F_s)/F_m')$], the yield for dissipation by down-regulation [$Y(NPQ) = (F_s/F_m') - (F_s/F_m)$] and the yield for other non-photochemical (non-regulated) losses [$Y(NO) = F_s/F_m$]. The apparent electron transport rate was calculated as ETR = Y(II) × PPFD × *f* × α and it was estimated according to [28].

Determination of the concentration of photosynthetic pigments

Five squared leaflet areas (1 cm^2) were punched from each leaflet of the third leaflet of each replication and treatment at 12, 36, 60 and 84 hai to determine the concentrations of chlorophyll (Chl) *a* + *b* and carotenoids. Leaflet samples were immersed in glass tubes containing 5 mL of dimethyl sulfoxide (DMSO) solution

[saturated with calcium carbonate ($CaCO_3$), 5 g L^{-1}] and kept in the dark at room temperature for 24 h. The absorbance of the extracts was read at 480, 649 and 665 nm in a spectrophotometer using the $CaCO_3$ saturated solution of DMSO as a blank. Concentrations of Chl *a* + *b* and carotenoids were calculated according to [29].

Experimental design and data analysis

A 3 × 2 factorial experiment, consisting of three foliar treatments (FT) [water (control treatment), Zn and Cu phosphites] and non-inoculated or inoculated plants, was arranged in a completely randomized design with four replications. Each replication corresponded to a plastic pot containing three plants. Experiments were repeated once. All parameters and variables were subjected to analysis of variance (ANOVA) and means were compared by Tukey's test ($P \leq 0.05$). For WMS and LA, ANOVA was considered to be a 3 × 4 factorial experiment with three FT and four evaluation times (12, 36, 60 and 84 hai). For leaf gas exchange parameters, ANOVA was considered to be a 3 × 2 × 3 factorial experiment consisting of three FT, non-inoculated and inoculated plants and three evaluation times (12, 36 and 60 hai). For the chlorophyll *a* fluorescence parameters and concentration of photosynthetic pigments, ANOVA was considered to be a 3 × 2 × 4 factorial experiment consisting of three FT, non-inoculated and inoculated plants and four evaluation times (12, 36, 60 and 84 hai). Principal components analysis (PCA) technique was used to determine the relationship among the parameters and variables studied. Data were analyzed using the Minitab software (version 18; Minitab Corporation).

Results

Analysis of variance

The factor FT was significant for LA and WM and the factor ET and the FT × ET interaction were significant for WMS. Most of the factors and double interactions were significant whereas FT × PI × ET interaction was significant for the parameters A, C_i, E and F_v/F_m and the concentration of Chl a+b (Table 1).

In vitro *assays*

Fungal mycelial growth was affected by the concentrations of Zn and Cu. Inhibition of mycelial growth started at the concentrations of 1.25 and 0.625 mL L^{-1} of Zn and Cu phosphites, respectively (Fig. 1C and H). At 10 mL L^{-1}, Zn phosphite dramatically reduced mycelial growth whereas no growth was observed for the Cu phosphite. EC_{50} values were 0.85 and 0.69 mL L^{-1} for the Zn and Cu phosphites, respectively, indicating a higher fungitoxic effect of the latter (Fig. 2).

Disease evaluation

White mold symptoms were reduced at 36, 60 and 84 hai on the leaflets of plants sprayed with both Zn phosphite (Fig. 3F-H) and Cu phosphite (Fig. 3J-L) in constrat to the leaflets of plants sprayed with water (Fig. 3B-D). Decreases in LA were 67-82% for Zn phosphite and 44-60% for Cu phosphite compared to the control treatment (Fig. 3M). WMS was reduced by 60-78% and 43-62% for Zn and Cu phosphites, respectively (Fig. 3N).

Leaf gas exchange parameters

For non-inoculated plants, there was no significant effect of FT for A, g_s, C_i and E regardless of the evaluation time (Fig. 4A, C, E and G). For the Zn phosphite-sprayed and inoculated plants, values of A, g_s and E were significantly higher by 131 and 813%, by 151 and 500% and by 114 and 358% at 36 and 60 hai, respectively, in comparison to

the control treatment (Fig. 4B, D, F and H). Similarly, for Cu phosphite-sprayed and inoculated plants, values of *A* (73 and 605%), g_s (64 and 362%) and *E* (71 and 192%) were significantly higher at 36 and 60 hai, respectively, relative to their control counterparts (Fig. 4B, D and H). Values of C_i were significantly lower by 9 and 11% at 60 hai, respectively, for both Zn and Cu phosphite-sprayed and inoculated plants compared to the control plants (Fig. 4F). The deleterious effect of *S. sclerotiorum* on the leaf gas exchange was confirmed by significant decreases in *A* (74 and 95%), g_s (72 and 92%) and *E* (61 an 88%), respectively, at 36 and 60 hai for the control plants in comparison to the non-inoculated plants (Fig. 4A, B, C, D, G and H). C_i was significantly increased by 14% at 60 hai (Fig. 4E and F).

Chl a fluorescence parameters

The quantitative analysis and images of Chl *a* fluorescence parameters did not show any change among treatments for the non-inoculated plants (Fig. 5, Fig. 6A, C, E, G and I). By contrast, inoculated plants from the control treatment displayed alterations in Chl *a* fluorescence as early as 12 hai and a progressive loss of photosynthetic capacity was evident over time as indicated by the dark areas in the images, whereas that Zn and Cu phosphite-sprayed plants showed alterations only from 36 hai onwards (Fig. 5).

Inoculated plants showed significant decreases in the values of F_v/F_m (12-43%), Y(II) (24-86%) and ETR (45-92%) and increases in the values of Y(NPQ) (21-68%) and Y(NO) (12-136%) from 12 to 84 hai in comparison to the non-inoculated plants regardless of the treatment (Fig. 6). However, higher values of F_v/F_m (12-43%), Y(II) (52-146%) and ETR (30-198%) and lower values of Y(NO) (18-27%) were recorded for Zn phosphite-sprayed plants relative to their non-sprayed counterparts. For the Cu phosphite-sprayed plants, higher values of F_v/F_m (13-30%), Y(II) (28-75%) and ETR

(17-115%) and lower values of Y(NO) (13-18%) were also observed compared to plants from the control treatment.

Photosynthetic pigments

Phosphite sprays did not affect the concentration of photosynthetic pigments either for non-inoculated plants regardless of evaluation time (Fig. 7A and C) or for inoculated plants (Fig. 7B and D) at 12, 36 and 60 hai, except for Chl *a* + *b* at 60 hai. For inoculated plants, the concentration of Chl *a* + *b* was reduced by 30 and 42% at 60 and 84 hai, respectively (Fig. 7A and B) and that of carotenoids by 26% at 84 hai (Fig. 7C and D). Concentration of Chl *a* + *b* was significantly higher by 42 and 46% for Zn phosphite and by 20 and 29% for Cu phosphite-sprayed plants at 60 and 84 hai, respectively, compared to non-sprayed plants (Fig. 7). Moreover, Zn and Cu phosphite-sprayed plants showed concentration of carotenoids that was higher by 30 and 20% in comparison to plants from the control treatment.

Principal component analysis (PCA)

To explore in more detail the effect of the Zn and Cu phosphites on plant physiology, the dataset obtained from the present study was analyzed using PCA of the first two PCs, which cover the major variance of the dataset (Fig. 8; PC1 and PC2 cover 83 and 8% of the total variance, respectively). This fingerprint analysis revealed that for non-inoculated plants, the physiological parameters were not apparently affected by Zn and Cu phosphites since such treatments were clustered together with plants from the control treatment (Fig. 8A). In sharp contrast, a clear trend of physiological re-adjustment was observed for inoculated plants. Plants from the control treatment formed a single group, whereas there was no segregation between plants sprayed either with Zn or Cu phosphites confirming, therefore, their similar potential in constraining the *S.*

sclerotiorum-induced physiological impairments. The first PC, characterized by positive scores for A, g_s, E, F_v/F_m, Y(II), ETR, Chl $a+b$ and carotenoids (which were clustered together), had negative correlations with LA, WMS, C_i, Y(NPQ) and Y(NO) (Fig. 8B).

Discussion

Previous studies demonstrated that phosphites were effective in controlling several economically important diseases including diseases in potato [17], Ceratocystis wilt in mango [30], pine pitch canker [18], coffee leaf rust [31] and anthracnose on common bean [32]. Additionally, phosphites have been particularly effective in controlling diseases caused by oomycetes in a wide range of horticultural crops and native ecosystems [33,13]. Despite these reports, there is a paucity of studies examining the photosynthetic apparatus of phosphite-treated plants. In this regard, based on data from the present study, the potential of Zn and Cu phosphites to control white mold development on common bean was partially based on the plants having a better photosynthetic performance.

Mycelial growth of *S. sclerotiorum* was inhibited as the concentrations of Zn and Cu phosphites increased, suggesting that there may have been a direct action on fungal physiology. This could be caused by the cations and not PO_3. The EC_{50} values were 0.85 and 0.69 mL L^{-1} for the Zn and Cu phosphites, respectively, indicating that the latter was more fungitoxic. Moreover, Zn and Cu phosphites decreased both LA and WMS. Therefore, the reduction in white mold symptoms noticed on leaflets sprayed with Zn or Cu phosphites can be explained, at least partially, to their direct action on *S. sclerotiorum*. Despite being less fungitoxic, Zn phosphite was more efficient than Cu phosphite in white mold control suggesting that other mechanisms, besides direct action, may be involved in the decrease of white mold symptoms. Some studies have shown that phosphites have a direct effect on pathogen growth as well as able to

activate plant defense mechanisms [34,13,35]. Further studies should be performed to elucidate the effect of phosphites in common bean resistance induction to white mold.

The A, g_s and E values were lower from 36 hai for inoculated plants. Similar observations have been reported for other pathogens infecting common bean plants such as *Xanthomonas axonopodis* pv. *phaseoli* [36], *Colletotrichum lindemuthianum* [37,38], *Uromyces appendiculatus* and *Pseudocercospora griseola* [39] and other host-parasite interactions such as rice-*Bipolaris oryzae* [40] and corn-*Stenocarpella macrospora* [41]. The progressive decreases in A observed in *S. sclerotiorum*-infected leaflets may be related to stomatal closure (reduction in the g_s values), which constrained the CO_2 influx into the mesophyll cells. The concurrent decreases in the g_s and E values may also explain the symptoms of desiccation of the leaflets over symptom development, which were more evident at 60 hai. By contrast, [42] found that oxalic acid, the main non-host selective toxin produced by *S. sclerotiorum*, manipulated the guard cells on the leaves of fava beans by promoting stomatal opening and increasing transpiration. Such observed discrepancies maybe a result of differences in plant species, inoculation method and disease symptom evaluations. The authors evaluated the leaf gas exchange parameters on stem and non-wilting leaves while in the present study leaflets were inoculated which showed intense wilting as the white mold progressed. In spite of stomatal closure, that most likely reduced CO_2 influx, C_i was found to be increased in non-sprayed and inoculated plants at 60 hai. Therefore, decreases in A values were probably governed by biochemical limitations at the chloroplastic level even though mesophyll constrains cannot be ruled out. Oxalic acid results in host tissue maceration and is considered a factor of pathogenicity for *S. sclerotiorum* [43,44]. In line with the results from the present study, [45] concluded that infection of leaves from tobacco plants by *S. sclerotiorum* compromised their photosynthetic performance due to the action of oxalic acid. By contrast, the reduction in white mold symptoms mediated by

Zn and Cu phosphites limited the pathogen-induced decreases in A, g_s and E values compared to non-sprayed leaflets. Accordingly, potassium phosphite was demonstrated to have either a direct and indirect action on *Phytophthora plurivora*, inhibiting its mycelial growth, as well as the product was able to preserve the photosynthetic machinery of the pathogen-infected *Fagus sylvatica* plants [13]. Thus, the results from the present study suggests that phosphites, noteworthy the Zn phosphite, attenuated the physiological plant dysfunctions caused by *S. sclerotiorum* infection.

The photochemical performance of *S. sclerotiorum*-infected leaflets was progressively reduced as LA and WMS increased. The decreases in the maximum photochemical efficiency of PSII, F_v/F_m, as indicated by the occurrence of photoinhibition of the photosynthesis, was due to *S. sclerotiorum* infection. Y(II), which is a relative measure of PSII performance, was decreased for infected leaflets suggesting that light energy that was absorbed by the photosynthetic pigments was not allocated to the photochemical process probably due to photooxidative damage. Y(NPQ) refers to the regulated thermal dissipation that occurs at the PSII reaction center through xantophyll cycle being induced by light and the proton gradient in the thylakoid membranes [46]. The increases in the Y(NPQ) values on infected leaflets may be associated with their low ability to regulate thermal dissipation thus causing damage to the photosynthetic apparatus. The fraction of light energy that is heat- and fluorescence-dissipated (constitutive losses), mainly when PSII reaction centers are closed, is indicated by Y(NO) [46]. In addition, the *S. sclerotiorum*-induced photooxidative damages can also be inferred by the progressive increases in Y(NO) values which suggests that the photoprotective mechanisms became ineffective [46]. Such increases in Y(NO) values were accompanied by dramatic decreases in ETR values at advanced stages of fungal infection which may be due to the cell wall degrading enzymes and oxalic acid produced by *S. sclerotiorum* [47,44]. In line with the results from the present

study, the PSII activity on tobacco leaves was found to be compromised during *S. sclerotiorum* infection [45]. In the present study, however, photochemical damages were greatly reduced by Zn and Cu phosphite. The F_v/F_m values range between 0.75 and 0.85 for most plant species under non-stress conditions [48]. For leaflets of phosphite-sprayed plants, the positive effect of both Zn and Cu phosphites to constrain the photooxidative damages caused by *S. sclerotiorum* infection was observed since the the F_v/F_m values suffered less impact. Potassium phosphite sprays reduced the size of bleeding canker of horse chestnut, caused by *Pseudomonas syringae* pv. *aesculi*, and preserved the photosynthetic machinery as evidenced by the higher values of F_v/F_m and chlorophyll concentrations [22]. Potassium phosphite also reduced the colonization of the stem tissue of pine plants by hyphae of *Fusarium circinatum*, thus mitigating fungal damage to the photosynthetic machinery [18].

Concomitantly to decreases in the F_v/F_m, Y(II) and ETR values and increases in the Y(NPQ) and Y(NO) values, concentration of photosynthetic pigments was negatively affected by *S. sclerotiorum* infection as the lesions in the leaflets expanded and the photosynthetic machinery was negatively affected. The reduction in the concentration of photosynthetic pigments may be a result of oxalic acid action on host tissue maceration, chloroplasts degeneration and the action of cell wall degradation enzymes [47,49,44]. The concentration of photosynthetic pigments was kept higher for the leaflets of plants sprayed with Zn and Cu phosphites in comparison to non-sprayed leaflets as well as the F_v/F_m, Y(II) and ETR values were greater preserving, at a certain extent, the photochemical performance and, consequently, lowering the *S. sclerotiorum*-induced damages to the photosynthetic apparatus.

In the present study, Zn and Cu phosphites appeared to have a direct mode of action by inhibiting mycelial growth of *S. sclerotiorum* even though an indirect action cannot be ruled out. The Zn and Cu phosphite sprays did not affect the photosynthetic

performance of non-inoculated plants. The *S. sclerotiorum* infection dramatically decreased photosynthesis and caused photochemical dysfunctions by inducing biochemical limitations rather than diffusive ones, but physiological impairments were greatly constrained by phosphites, especially Zn. Based on our findings, the preventative application of phosphites may represent a feasible alternative for white mold management in common bean.

Acknowledgments

Professor F. A. Rodrigues thanks the Conselho Nacional de Desenvolvimento Científico e Tecnológico (CNPq) for his fellowship. Ms. I. R. F. Fagundes-Nacarath was supported by CNPq. We thank EMBRAPA Soybean for providing the isolate of *Sclerotinia sclerotiorum* used in this study. This study was supported by grants from CAPES, CNPq and FAPEMIG to Prof. F. A. Rodrigues.

References

[1] G. Boland, R. Hall, Index of plant hosts of *Sclerotinia sclerotiorum*, Can. J. Plant Pathol. 16 (1994) 93–108.

[2] H.F. Schwartz, S.P. Singh, Breeding common bean for resistance to diseases: a review, Crop Sci. 53 (2013) 1832–844.

[3] J.R. Steadman, White mold – a serious yield – limiting disease of bean, Plant Dis. 67 (1983) 346–350.

[4] L.H. Purdy, *Sclerotinia sclerotiorum*: History, diseases and symptomatology, host ranges, geographic distribution and impact, Phytopathology. 69 (1979) 875–880.

[5] R.F. Vieira, T.J. Paula Júnior, H. Teixeira, J.E.S. Carneiro, White mold management in common bean by increasing within-row distance between plants, Plant Dis. 94 (2010) 361–367.

[6] P.N. Miklas, L.D. Porter, J.D. Kelly, J.R. Myers, Characterization of white mold disease avoidance in common bean, Eur. J. Plant Pathol. 135 (2013) 525–543.

[7] S.P. Singh, H.F. Schwartz, Breeding common bean for resistance to diseases: A review, Crop Sci. 50 (2010) 2199–2223.

[8] R.F. Vieira, T.J. Paula Júnior, J.E.S. Carneiro, H. Teixeira, T.F.N. Queiroz, Management of white mold in type III common bean with plant spacing and fungicide, Trop. Plant Pathol. 37 (2012) 95–101.

[9] F. Zhou, H.J. Liang, Y.L. Di, H. You, F.X. Zhu, Stimulatory effects of sublethal doses of dimethachlon on *Sclerotinia sclerotiorum*, Plant Dis. 98 (2014) 1364–1370.

[10] J.P. Clarkson, K. Phelps, J.M. Whipps, C.S. Young, J.A. Smith, M. Watling, Forecasting sclerotinia disease on lettuce: Toward developing a prediction model for carpogenic germination of sclerotia, Phytopathology 94 (2004) 268–279.

[11] M.S. Lehner, T.J. Paula Júnior, R.A. Silva, R.F. Vieira, J.E.S. Carneiro, G. Schnabel, E.S.G. Mizubuti, Fungicide sensitivity of *Sclerotinia sclerotiorum*: A thorough assessment using discriminatory dose, EC_{50}, high-resolution melting analysis, and description of new point mutation associated with thiophanate-methyl resistance, Plant Dis. 99, (2015) 1537–1543.

[12] M.F. Machinandiarena, M.C. Lobato, M.L. Feldman, G.R. Daleo, A.B. Andreu, Potassium phosphite primes defense responses in potato against *Phytophthora infestans*, J. Plant Physiol. 169 (2012) 1417–1424.

[13] R.J.D. Dalio, F. Fleischmann, M. Humez, W. Osswald, Phosphite protects *Fagus sylvatica* seedlings towards *Phytophthora plurivora* via local toxicity, priming and facilitation of pathogen recognition, PLoS ONE 9 (2014) e87860.

[14] J.E. Adaskaveg, W. Hao, H. Förster, Postharvest strategies for managing phytophthora brown rot of citrus using potassium phosphite in combination with heat treatments, Plant Dis. 99 (2015) 1477–1482.

[15] M. Reuveni, D. Sheglov, Y. Cohen, Control of moldy-core decay in apple fruits by β-aminobutyric acids and potassium phosphites, Plant Dis. 87 (2003) 933–936.

[16] E.F. Sharaf, A.A. Farrag, Induced resistance in tomato plants by IAA against *Fusarium oxysporum* f. sp. *Lycopersici*, Pol. J. Microbiol. 53 (2004) 111–116.

[17] M.C. Lobato, F.P. Olivieri, G.R. Daleo, A.B. Andreu, Antimicrobial activity of phosphites against different potato pathogens, J. Plant Dis. Prot. 117 (2010) 102–109.

[18] A. Cerqueira, A. Alves, H. Berenguer, B. Correia, A. Gomez-Cadenas, J.J. Diez, P. Monteiro, G. Pinto, Phosphite shifts physiological and hormonal profile of Monterey pine and delays *Fusarium circinatum* progression, Plant Physiol. Biochem. 114 (2017) 88–99.

[19] M. Reuveni, Post-infection applications of K_3PO_3, potassium phosphite and dimethomorph inhibit development of downy mildew caused by *Plasmopara viticola* on grapevines, J. Small Fruit Vitic. 5 (1997) 27–38.

[20] T.J. Jackson, T. Burgess, I. Colquhoun, G.E.S. Hardy, Action of the fungicide phosphite on *Eucalyptus marginata* inoculated with *Phytophthora cinnamomic*, Plant Pathol. 49 (2000) 147–154.

[21] L. Eshraghi, J. Anderson, N. Aryamanesh, B. Shearer, J. Mccomb, G.E.S. Hardy, P.A. O'Brien, Phosphite primed defence responses and enhanced expression of defence genes in *Arabidopsis thaliana* infected with *Phytophthora cinnamomic*, Plant Pathol. 60 (2011) 1086–1095.

[22] G.C. Percival, J.M. Banks, Phosphite-induced suppression of *Pseudomonas* bleeding canker (*Pseudomonas syringae* pv. *aesculi*) of horse chestnut (*Aesculus hippocastanum* L.), Urban For. Urban Green. 37 (2015) 7–20.

[23] R.B. Clark, Characterization of phosphates in intact maize roots, J. Agric. Food Chem. 23 (1975) 458–460.

[24] Y.S. Bae, G.R. Knudsen, Effect of sclerotial distribution pattern of *Sclerotinia sclerotiorum* on biocontrol efficacy of *Trichoderma harzianum*, Appl. Soil. Ecol. 35 (2007) 21–24.

[25] F.X.R. Vale, E.I. Fernandes Filho, J.R. Liberato, QUANT: a software plant disease severity assessment. in: Close, R., Braithwaite, M., Havery, I., (Eds.), Proceedings of the 8th International Congress of Plant Pathology. New Zealand, 2003, pp. 105.

[26] K. Oxborough, N.R. Baker, An instrument capable of imaging chlorophyll *a* fluorescence from intact leaves at very low irradiance and at cellular and subcellular levels of organization, Plant Cell Environ. 20 (1997) 1473–1483.

[27] D.M. Kramer, G. Johnson, O. Kiirats, G.E. Edwards, New fluorescence parameters for the determination of Q_A redox state and excitation energy fluxes, Photosynth. Res. 79 (2004) 209–218.

[28] N.R. Baker, Chlorophyll fluorescence: A probe of photosynthesis *in vivo*. Annu. Rev. Plant Biol. 59 (2008) 89–113.

[29] A.R. Wellburn, The spectral determination of chlorophylls *a* and *b*, as well as total carotenoids, using various solvents with spectrophotometers of different resolution, J. Plant Physiol. 144 (1994) 307–313.

[30] L. Araujo, W.M.S. Bispo, V.S. Rios, S.A. Fernandes, F.A. Rodrigues, Induction of the phenylpropanoid pathway by acibenzolar-*S*-methyl and potassium phosphite increases mango resistance to *Ceratocystis fimbriata* infection, Plant Dis. 99 (2015) 447–459.

[31] A.C.A. Monteiro, M.L.V. Resende, T.C.T. Valente, P.M. Ribeiro Junior, V.F. Pereira, J.R. Costa, J.A.G. Silva, Manganese phosphite in coffee defence against *Hemileia vastatrix*, the coffee rust fungus: biochemical and molecular analyses, J. Phytopathol. 164 (2016) 1043–1053.

[32] S.J.C. Gadaga, M.S. Abreu, M.L.V. Resende, P.M. Ribeiro Júnior, Phosphites for the control of anthracnose in common bean, Pesq. Agropec. Bras. 52 (2017) 36–44.

[33] M. King, W. Reeve, M.B. Van Der Hoek, N. Williams, J. McComb, P.A. O'Brien, G.E. Hardy, Defining the phosphite-regulated transcriptome of the plant pathogen *Phytophthora cinnamomic*, Mol. Genet. Genomics. 284 (2010) 425–435.

[34] D.D. Burra, O. Berkowitz, P.E. Hedley, J. Morris, S. Resjö, F. Levander, E. Liljeroth, E. Andreasson, E. Alexandersson, Phosphite-induced changes of the transcriptome and secretome in *Solanum tuberosum* leading to resistance against *Phytophthora infestans*, BMC Plant Biol. 14 (2014) 254–271.

[35] C.G. Díaz, R.B. Bassanezi, C.V. Godoy, D.B. Lopes, A. Bergamin Filho, Quantificação do efeito do crestamento bacteriano comum na eficiência fotossintética e na produção do feijoeiro, Fitopatol. Bras. 26 (2001) 71–76.

[36] P. Liu, B. Li, M. Lin, G. Chen, X. Ding, Q. Weng, Phosphite-induced reactive oxygen species production and ethylene and ABA biosynthesis mediate the control of *Phytophthora capsici* in pepper (*Capsicum annuum*), Funct. Plant Biol. 43 (2016) 563–574.

[37] L.R. Polanco, F.A. Rodrigues, K.J.T. Nascimento, M.F.A. Cruz, C.R.S. Curvelo, F.M. DaMatta, F.X.R. Vale, Photosynthetic gas exchange and antioxidative system in common bean plants infected by *Colletotrichum lindemuthianum* and supplied with silicon, Trop. Plant Pathol. 39 (2014) 35–42.

[38] F.A. Rodrigues, L.R. Polanco, H.S.S. Duarte, R.S. Resende, F.X.R. Vale, Photosynthetic gas exchange in common bean submitted to foliar sprays of potassium silicate, sodium molybdate and fungicide and infected with *Colletotrichum lindemuthianum*, J. Phytopathol. 163 (2014) 554–559.

[39] W.C. Jesus Junior, F.X.R. Vale, C.A. Martinez, R.R. Coelho, L.C. Costa, B. Hau, L. Zambolim, Effects of angular leaf spot and rust on leaf gas exchange and yield of common bean (*Phaseolus vulgaris*), Photosynthetica 39 (2001) 603–606.

[40] D. Debona, K.J.T. Nascimento, J.G.O. Gomes, C.E. Aucique-Pérez, F.A. Rodrigues, Physiological changes promoted by a strobilurin fungicide in the rice-*Bipolaris oryzae* interaction, Pestic. Biochem. Physiol. 10 (2015) 8–16.

[41] M.B. Bermúdez-Cardona, J.A. Wordell Filho, F.A. Rodrigues, Leaf gas exchange and chlorophyll *a* fluorescence in maize leaves infected with *Stenocarpella macrospora*, Phytopathology 105 (2015) 26–34.

[42] R.L. Guimaraes, H.U. Stotz, Oxalate production by *Sclerotinia sclerotiorum* deregulates guard cells during infection, Plant Physiol. 136 (2004) 3703–3711.

[43] G. Godoy, J.R. Steadman, M.B. Dickman, R. Dam, Use of mutants to demonstrate the role of oxalic acid in pathogenicity of *Sclerotinia sclerotiorum* on *Phaseolus vulgaris*, Physiol. Mol. Plant Pathol. 37 (1990) 179–191.

[44] S.G. Cessna, V.E. Sears, M.B. Dickman, P.S. Low, Oxalic acid, a pathogenicity factor for *Sclerotinia sclerotiorum*, suppresses the oxidative burst of the host plant, Plant Cell. 12 (2000) 2191–2199.

[45] C. Yang, Z. Zhang, H. Gao, M. Liu, X. Fan, Mechanisms by which the infection of *Sclerotinia sclerotiorum* (Lib.) de Bary affects the photosynthetic performance in tobacco leaves, BMC Plant boil. 14 (2014) 1–11.

[46] C. Klughammer, U. Schreiber, Complementary PSII quantum yield calculated from simple fluorescence parameters measured by PAM fluorometry and saturation pulse method, PAM Application Notes 1 (2008) 27–35.

[47] D.F. Bateman, S.V. Beer, Simultaneous production and synergistic action of oxalic acid and polygalacturonase during pathogenesis by *Sclerotium rolfsii*, Phytopathology 55 (1965) 204–211.

[48] H.R. Bolhar-Nordenkampf, S.P. Long, N.R. Baker, G. Oquist, U. Schreiber, E.G. Lechner, Chlorophyll fluorescence as probe of the photosynthetic competence of leaves in the field: a review of current instrumentation, Funct. Ecol. 3 (1989) 497–514.

[49] V.N. Tariq, P. Jeffries, Changes occurring in chloroplasts of *Phaseolus* following infection by *Sclerotinia*: A cytochemical study, J. Cell Sci. 75 (1985) 195–295.

Table 1

Analysis of variance of the effects of foliar treatments (FT), plant inoculation (PI), evaluation time (ET) and their interactions for lesion area (LA), white mold severity (WMS), leaf gas exchange parameters (net CO_2 assimilation rate (A), stomatal conductance to water vapor (g_s), internal to ambient CO_2 concentration ratio (C_i) and the transpiration rate (E)), chlorophyll *a* fluorescence parameters (maximum PSII quantum efficiency (F_v/F_m), photochemical yield (Y(II)), yield for dissipation by down-regulation (Y(NPQ)) and yield for non-regulated dissipation (Y(NO)) and electron transport rate (ETR) as well as concentrations of chlorophyll *a*+*b* (Chl *a*+*b*) and carotenoids (Car).

Variables	FT	PI	ET	FT × PI	FT × ET	PI × ET	FT × PI × ET
WMS	<0.001	-	<0.001	-	<0.001	-	-
LA	<0.001	-	<0.001	-	<0.001	-	-
A	<0.001	<0.001	<0.001	<0.001	<0.001	<0.001	<0.001
g_s	0.001	<0.001	<0.001	0.001	0.038	<0.001	0.127
C_i	0.099	0.001	<0.001	0.008	0.062	0.012	0.038
E	<0.001	<0.001	<0.001	<0.001	0.327	<0.001	0.018
F_v/F_m	<0.001	<0.001	<0.001	<0.001	<0.001	<0.001	<0.001
Y(II)	<0.001	<0.001	<0.001	<0.001	0.616	<0.001	0.236
Y(NPQ)	0.801	<0.001	0.010	0.092	0.127	0.077	0.053
Y(NO)	<0.001	<0.001	<0.001	<0.001	0.049	<0.001	0.484
ETR	<0.001	<0.001	<0.001	<0.001	0.403	<0.001	0.750
Chl *a*+*b*	0.003	<0.001	<0.001	0.007	0.012	<0.001	0.004
Car	0.181	0.025	<0.001	0.024	0.206	0.010	0.231

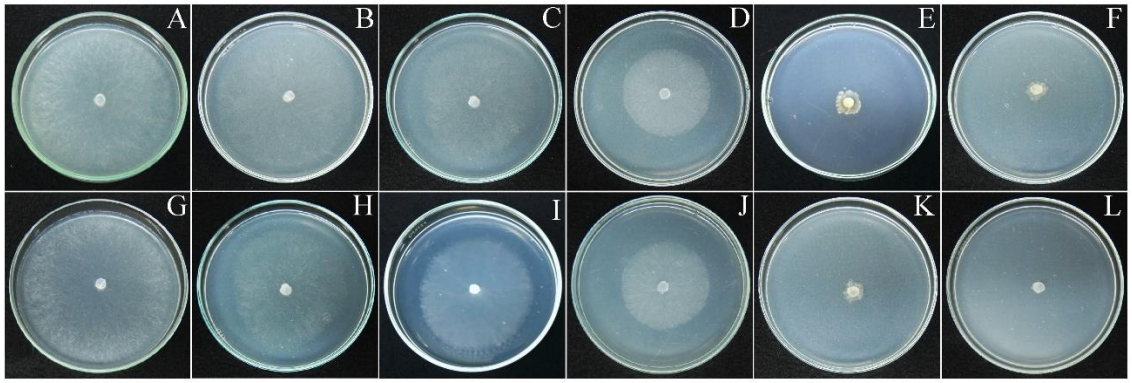

Fig. 1. Mycelial growth of *Sclerotinia sclerotiorum* in Petri dishes containing potato dextrose agar medium amended with 0 (A and G), 0.625 (B and H), 1.25 (C and I), 2.5 (D and J), 5 (E and K) and 10 mL L^{-1} (F and L) of zinc (B-F) or copper (H-L) phosphites.

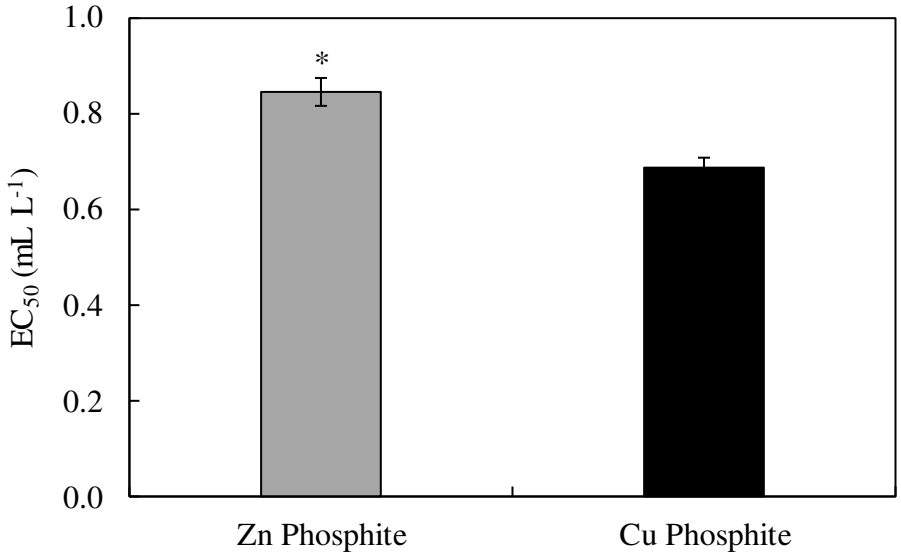

Fig. 2. Effective concentration (EC_{50}) of zinc (Zn) and copper (Cu) phosphites that inhibited 50% of the mycelial growth of *Sclerotiorum sclerotiorum*. Means followed by an asterisk are significantly different ($P \leq 0.05$) according to Tukey's test. Bars represent the standard error of the means. $n = 4$.

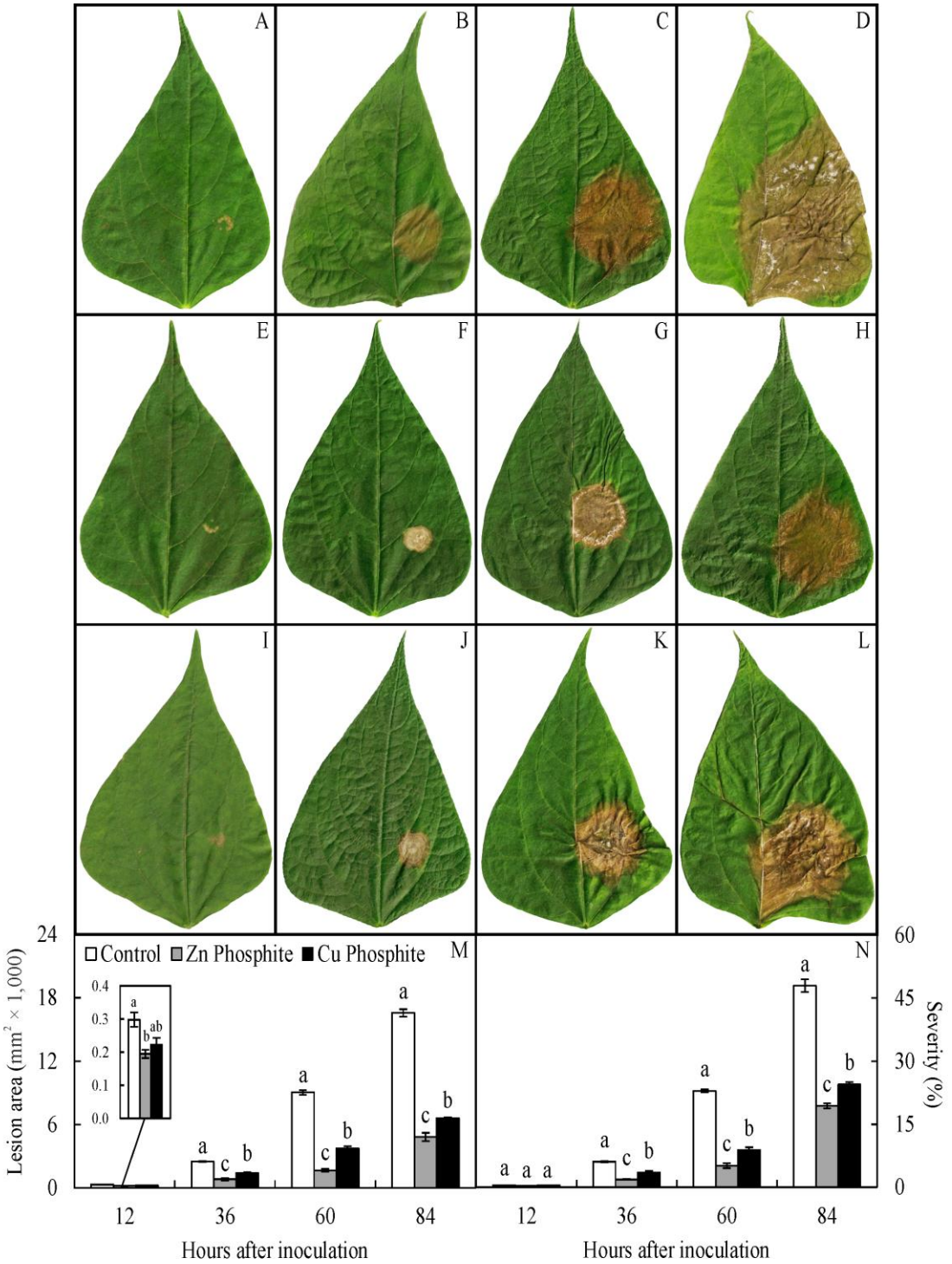

Fig. 3. White mold symptoms at 12 (A, E and I), 36 (B, F and J), 60 (C, G and K) and 84 hours after inoculation (D, H and L), lesion area (M) and severity (N) evaluated on the leaflets of common bean sprayed with water and inoculated with *Sclerotinia sclerotiorum* (A-D), inoculated leaflets sprayed with zinc phosphite (E-H) and inoculated leaflets sprayed with copper phosphite (I-L). Means from each treatment, at

each evaluation time, followed by different letters are significantly different ($P \leq 0.05$) according to Tukey's test. Bars represent the standard error of the means. $n = 4$.

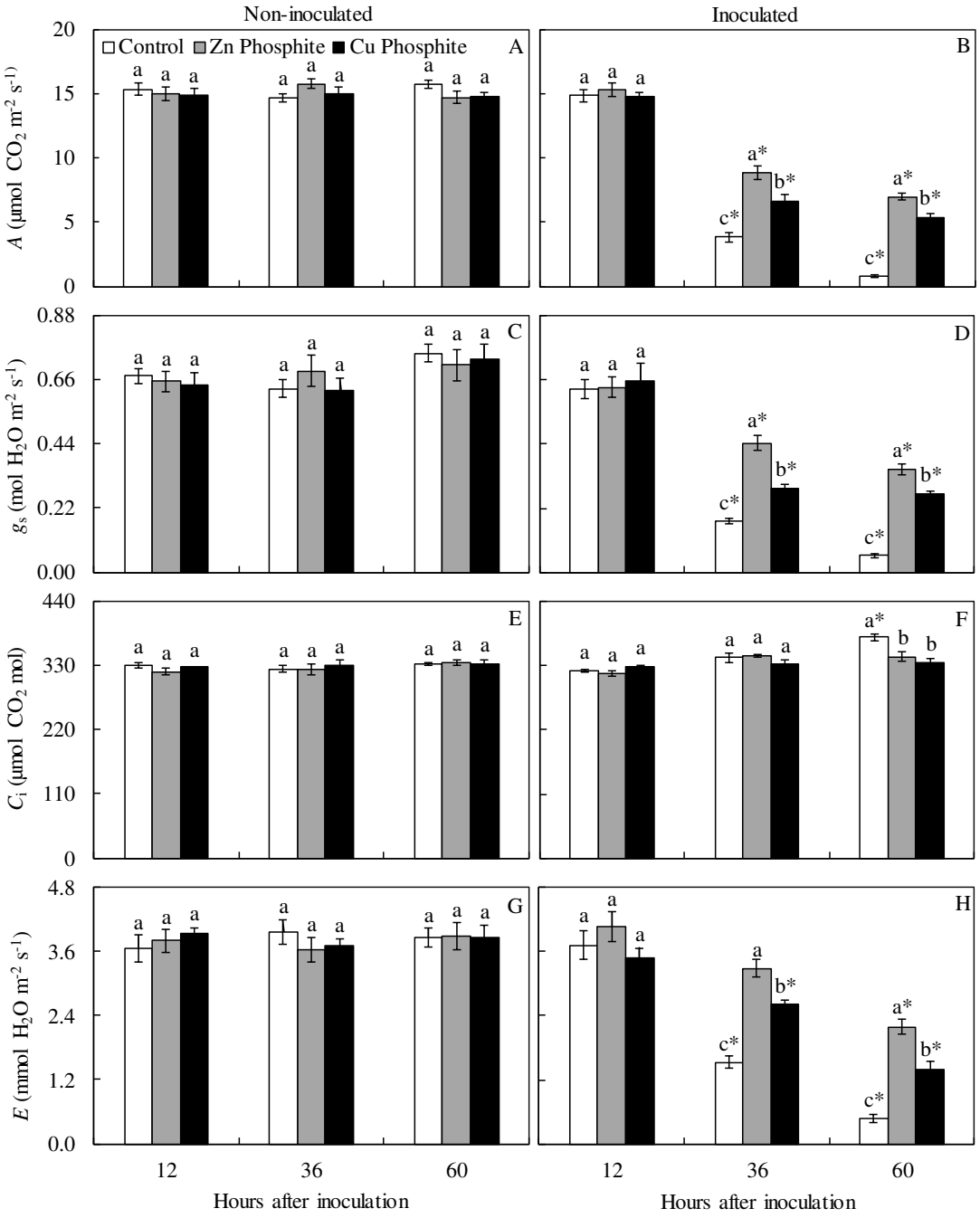

Fig. 4. Leaf gas exchange parameters: net carbon assimilation rate (A) (A and B), stomatal conductance to water vapor (g_s) (C and D), internal CO_2 concentration (C_i) (E and F) and transpiration rate (E) (G and H) determined on the leaflets of common bean

plants that were non-inoculated (A, C, E and G) or inoculated (B, D, F and H) with *Sclerotinia sclerotiorum* and sprayed with water (control treatment) or with zinc (Zn) or copper (Cu) phosphites. For each evaluation time, means from each treatment followed by different letters and for non-inoculated and inoculated plants for each treatment followed by an asterisk (*) are significantly different ($P \leq 0.05$) according to Tukey's test. Bars represent the standard error of the means. $n = 4$.

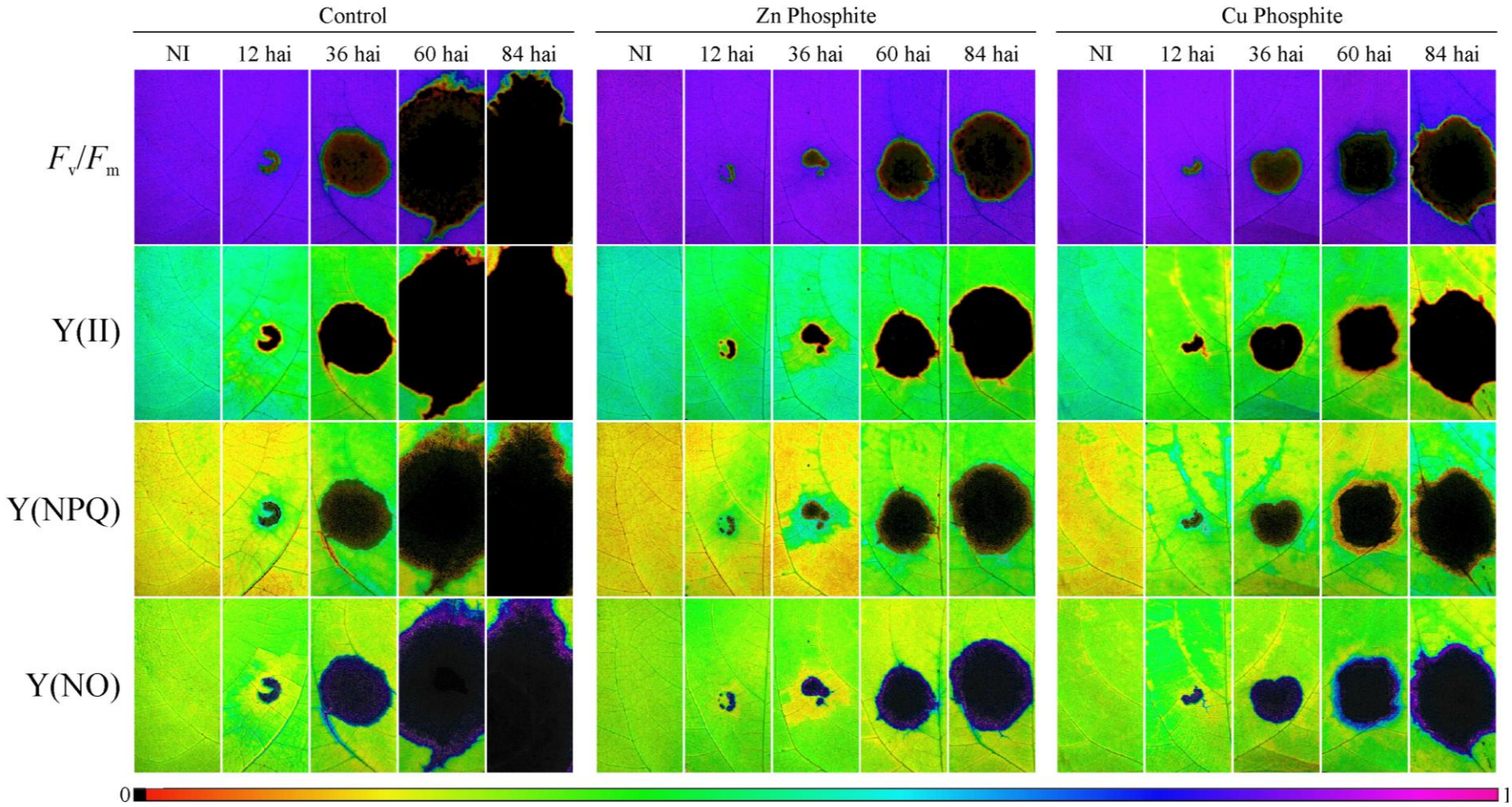
Control
Zn Phosphite
Cu Phosphite
NI
12 hai
36 hai
60 hai
84 hai
F_v/F_m
Y(II)
Y(NPQ)
Y(NO)
0
1

Fig. 5. Images of chlorophyll *a* fluorescence parameters: maximum PSII quantum efficiency (F_v/F_m), photochemical yield (Y(II)), yield for dissipation by down-regulation (Y(NPQ)) and yield for non-regulated dissipation (Y(NO)) determined on the leaflets of common bean plants that were non-inoculated or inoculated with *Sclerotinia sclerotiorum* and sprayed with water (control treatment) or with zinc (Zn) or copper (Cu) phosphites.

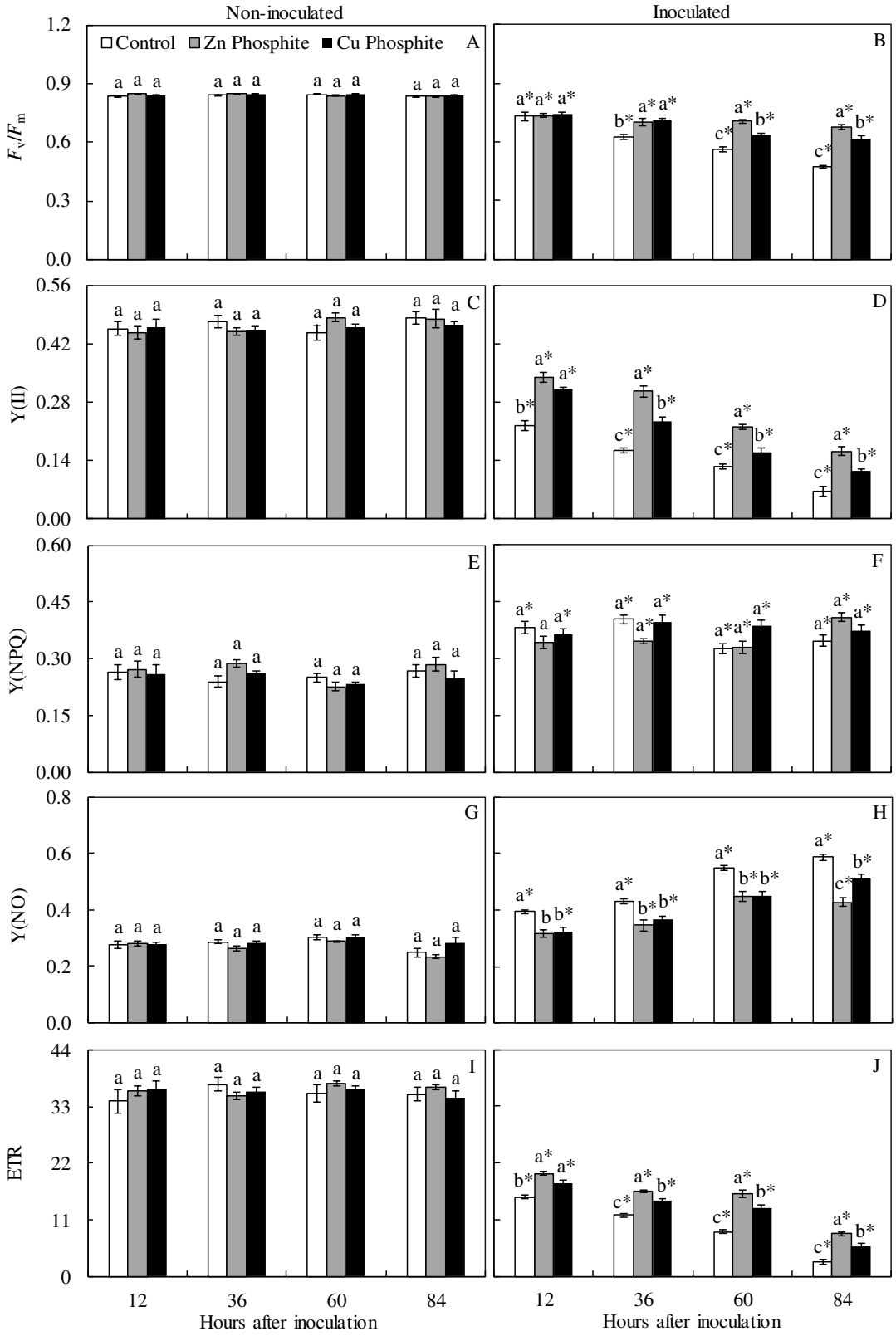

Fig. 6. Chlorophyll *a* parameters: variable-to-maximum chlorophyll *a* fluorescence ratio (F_v/F_m) (A and B), photochemical yield (Y(II)) (C and D), yield for dissipation by down-regulation (Y(NPQ)) (E and F), yield for non-regulated dissipation (Y(NO) (G

and H) and electron transport rate (ETR) (I and J) determined on the leaflets of common bean plants that were non-inoculated (A, C, E, G and I) or inoculated (B, D, F, H and J) with *Sclerotinia sclerotiorum* and sprayed with water (control treatment) or with zinc (Zn) or copper (Cu) phosphites. For each evaluation time, means from each treatment followed by different letters and for non-inoculated and inoculated plants for each treatment followed by an asterisk (*) are significantly different ($P \leq 0.05$) according to Tukey's test. Bars represent the standard error of the means. $n = 4$.

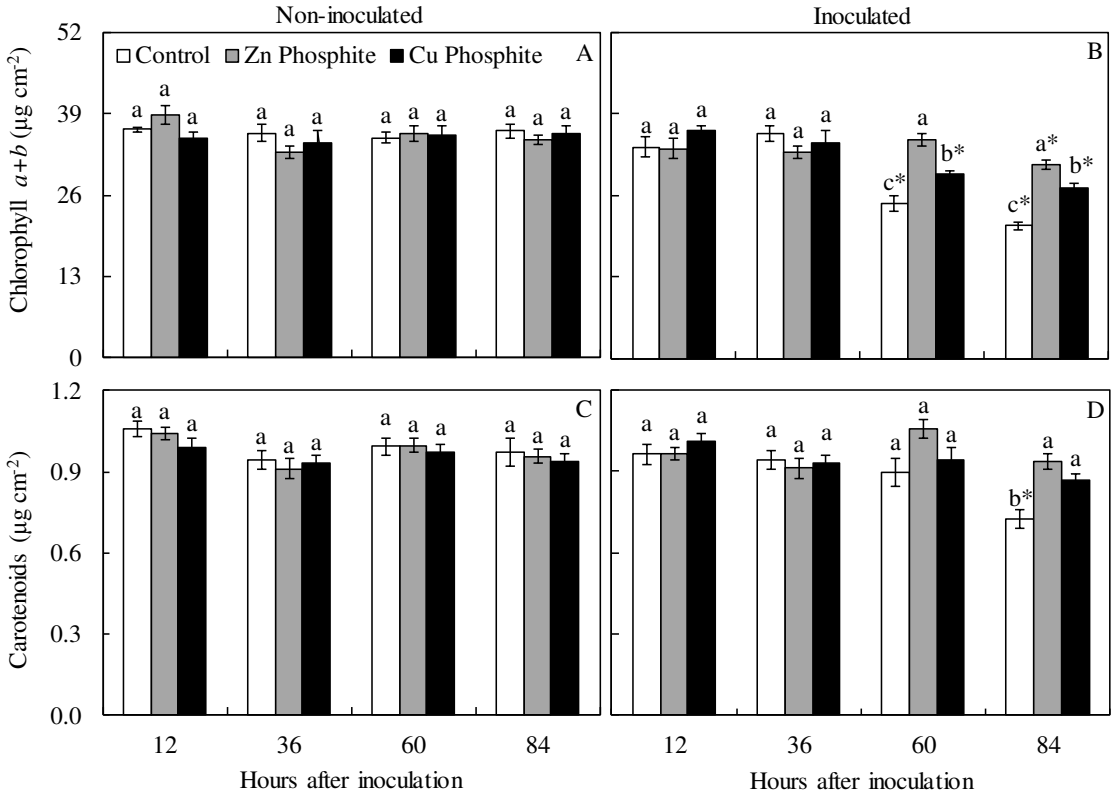

Fig. 7. Concentrations of chlorophyll *a* + *b* (A and B) and carotenoids (C and D) determined in the leaflets of common bean plants that were non-inoculated (A and C) or inoculated (B and D) with *Sclerotinia sclerotiorum* and sprayed with water (control treatment) or with zinc (Zn) or copper (Cu) phosphites. For each evaluation time, means from each treatment followed by different letters and for non-inoculated and inoculated

plants for each treatment followed by an asterisk (*) are significantly different ($P \leq 0.05$) according to Tukey's test. Bars represent the standard error of the means. $n = 4$.

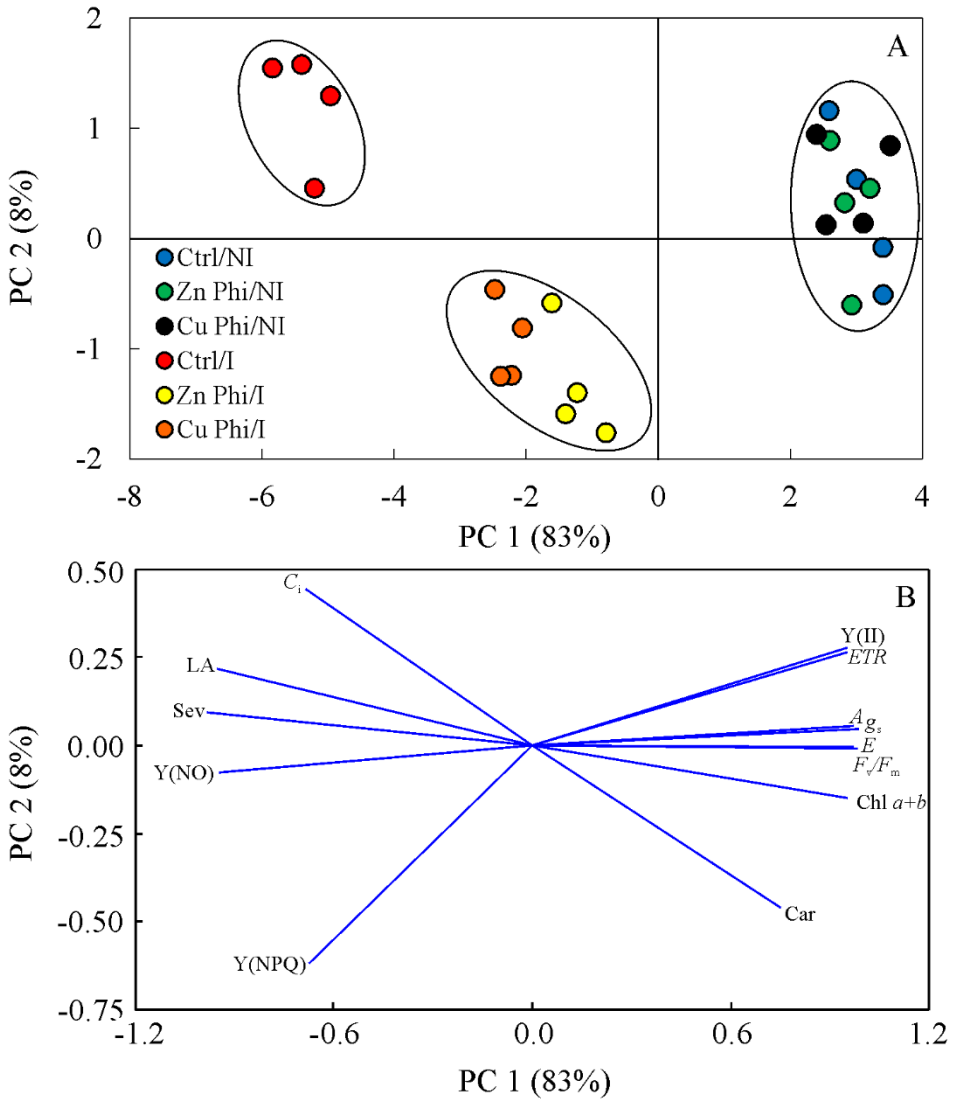

Fig. 8. Score plot (a) and loading values (b) of principal component analysis comparing lesion area (LA), white mold severity (WMS), leaf gas exchange parameters (net CO_2 assimilation rate (A), stomatal conductance to water vapor (g_s), internal to ambient CO_2 concentration ratio (C_i) and the transpiration rate (E)), chlorophyll *a* fluorescence parameters (maximum PSII quantum efficiency (F_v/F_m), photochemical yield (Y(II)),

yield for dissipation by down-regulation (Y(NPQ)) and yield for non-regulated dissipation (Y(NO)) and electron transport rate (ETR) as well as concentrations of chlorophyll *a* + *b* (Chl *a*+*b*) and carotenoids (Car) on the leaflets of common bean plants that were non-inoculated (NI) or inoculated (I) with *Sclerotinia sclerotiorum* and sprayed with water (Ctrl) or with zinc (Zn Phi) or copper (Cu Phi) phosphites.

CHAPTER 3

Biochemical responses of common bean to white mold potentiated by phosphites

Abstract

Considering that the mechanisms for phosphite-afforded disease control remain elusive, this study investigated whether zinc (Zn) and copper (Cu) phosphites could possible potentiate common bean resistance to white mold, caused by *Sclerotinia sclerotiorum*, through the stimulation of biochemical defense responses. Lesion area and disease severity were decreased by phosphites spray, but Zn phosphite outcompeted Cu phosphite. Histopathological observations revealed fewer fungal hyphae and less collapse of the mesophyll cells in the Zn and Cu phosphite-sprayed plants compared to non-sprayed ones. The *S. sclerotiorum*-triggered accumulation of reactive oxygen species, oxalic acid (a fungal secreted toxin) and malondialdehyde (an indicator of cellular damage) were constrained as a result of Zn and Cu phosphites sprays. Activities of antioxidant enzymes (superoxide dismutase, peroxidase, ascorbate peroxidase and glutathione-*S*-transferase at 12 hours after inoculation (hai) and catalase at 60 and 84 hai) were higher for Zn and Cu phosphites-sprayed plants than for non-sprayed ones. Activities of defense enzymes chitinase (CHI) at 12 hai, β-1,3-glucanase (GLU) and polyphenoloxidase (PPO) were higher at 12-84 hai for Zn and Cu phosphites sprayed plants, phenylalanine ammonia-lyase at 36-84 hai for the Zn phosphite sprayed ones, CHI at 12-36 hai, GLU at 12-60 hai, PPO at 36 hai and PAL and lipoxygenase at 12 hai for the Cu phosphite sprayed ones upon inoculation with *S. sclerotiorum* relative to their non-sprayed counterparts. Concentrations of total soluble phenols and lignin-thioglycolic acid derivatives were not affected by Cu phosphite spray on infected plants, but were higher and lower, respectively, for Zn phosphite sprayed plants at 60 hai compared to non-sprayed ones. Taken together, the findings from the present study shed light on the biochemical defense mechanisms involved in the Zn and Cu phosphites-mediated suppression of white mold in common bean.

Keywords: *Phaseolus vulgaris*, *Sclerotinia sclerotiorum*, antioxidant system, defense enzymes.

Introduction

Sclerotinia sclerotiorum, the causal agent of white mold, can infect more than 400 plant species, including economically important crops such as common bean, lettuce, oilseed rape, soybean and sunflower. Disease's control has been difficult due to pathogen aggressiveness and wide host range (Boland & Hall, 1994) and the long persistence of sclerotia in the soil and crop residues (Bolton *et al.,* 2006). There are no resistant cultivars available to growers and strategies commonly used for disease management include crop rotation with plants from Poaceae, healthy seeds, irrigation control, upright cultivarrs, increase of row spacing, fungicide application and the used biological control agents (Ando *et al.,* 2007; Singh & Schwartz, 2010; Vieira *et al.,* 2010, 2012; Miklas *et al.,* 2013; Zhou *et al.,* 2014). Despite fungicide application being effective, it increases production costs and also has potential negative impacts to human health, environment and living organisms as well as leads to emergence of pathogen resistance. Therefore, investigation of novel alternatives for management of white mold is urgently needed.

Phosphites, a group of inorganic salts of phosphorous acid (H_3PO_3), stand out as alternative products within integrated disease management and its use has increased in recent years (Gozzo & Faoro, 2013; Costa *et al.,* 2017). Phosphites have been shown to be particularly effective against oomycetes such as *Phytophthora infestans* in potato (Machinandiarena *et al.,* 2012; Burra *et al.,* 2014), *Phytophthora plurivora* in European beech (Dalio *et al.,* 2014), *Phytophthora capsici* in pepper (Liu *et al.,* 2016), *Phytophthora cinnamomi* in *Arabidopsis thaliana* (Eshraghi *et al.,* 2011), *Plasmopara viticola* in grape (Pereira *et al.,* 2012) and *Peronospora manshurica* in soybean (Silva *et al.,* 2011). Furthermore, some bacteria such as *Pseudomonas syringae* pv. *aesculi* in horse chestnut (Percival & Banks, 2015) and *Streptomyces scabies* in potato (Lobato *et al.,* 2010) as well as fungi including *Colletotrichum lindemuthianum* in common bean (Costa *et al.,* 2017; Gadaga *et al.,* 2017), *Alternaria alternata* in apple (Reuveni *et al.,*

2003), *Rhizoctonia solani* and *Fusarium solani* in potato (Lobato *et al.,* 2010), *Fusarium circinatum* in pine (Cerqueira *et al.,* 2017) and *Ceratocystis fimbriata* in mango (Araujo *et al.,* 2015) were affected by phosphite sprays.

The mode of action of phosphites is complex; both a direct effect through inhibited mycelial growth and an indirect one by stimulating host defense responses have been proposed to play a role (Dalio *et al.,* 2014; Costa *et al.,* 2017). Indirectly, phosphite sprays were shown to enhance multiple defense mechanisms in plants non-challenged or challenged with pathogens (Reuveni, 1997; Jackson *et al.,* 2000; Eshraghi *et al.,* 2011). The transcription of marker genes involved on many plant defense signaling pathways (*e.g.* abscisic, jasmonic and salicylic acids as well as ethylene), activity of defense enzymes, synthesis of phytoalexin and hydrolases and lignin-derived cell wall reinforcement were found to be increased in response to the pre-treatment with phosphites (Eshraghi *et al.,* 2011; Dalio *et al.,* 2014; Liu *et al.,* 2016). Moreover, phosphites triggered oxidative burst, accumulation of phenolic compounds, cytoplasmic aggregation and phenol production in the host cells surrounding those infected (Daniel & Guest, 2006). Preventative phosphite sprays reduced the lesion size of Pseudomonas bleeding canker and increased β-1,3-glucanase (GLU) and peroxidase (POX) activities in horse chestnut (Percival & Banks, 2015). In common bean, phosphites were demonstrated to be effective in anthracnose control and its effect was linked to decreased mycelial growth of *C. lindemuthianum* as well as to increased activities of superoxide dismutase, chitinase, GLU, POX, phenylalanine ammonia-lyase and polyphenol oxidase and greater concentrations of total soluble phenols (TSP) and lignin-thioglycolic acid (LTGA) derivatives (Silva *et al.,* 2015; Costa *et al.,* 2017; Gadaga *et al.,* 2017). Despite these reports, to the best of our knowledge, information about the effect of phosphites for the white mold control in common bean and the defense mechanisms putatively activated by them are still missing in the literature.

Therefore, this study aimed to investigate whether zinc (Zn) and copper (Cu) phosphites could be effective in white mold control. In addition, biochemical assays (activities of antioxidant and defense enzymes, concentrations of reactive oxygen species, oxalic acid, TSP and LTGA derivatives) were performed to elucidate whether phosphites possibly potentiates common bean´s defense mechanisms against *S. sclerotiorum* infection.

Material and methods

Plant growth

Five seeds of common bean from cultivar Pérola, susceptible to *S. sclerotiorum*, were sown in plastic pots of 2 liters containing 2 kg of Tropstrato® substrate (Vida Verde, Mogi Mirim, São Paulo, Brazil) composed of a mixture of pine bark, peat and expanded vermiculite (1:1:1). Each pot was thinned to three seedlings seven days after emergence. Plants were kept in a greenhouse (30 ± 5ºC temperature, 65 ± 5% relative humidity and 900 ± 15 µmol photons m^{-2} s^{-1} natural photosynthetically active radiation). Plants were fertilized weekly with 100 mL of a modified nutrient solution based on Clark (1975) as it follows: 0.8 mM KNO_3, 0.069 mM $NH_4H_2PO_4$, 1 mM NH_4NO_3, 1 mM $Ca(NO_3).4H_2O$, 0.9 mM KCl, 0.6 mM $MgSO_4$ $7H_2O$, 0.5 µM $CuSO_4$ $5H_2O$, 2 µM $ZnSO_4$ $7H_2O$, 19 µM H_3BO_3, 7 µM $MnCl_2$ $4H_2O$, 0.6 µM Na_2MoO_4 $4H_2O$, 60 µM $FeSO_4$ $7H_2O$ and 90 µM disodium ethylenediaminetetraacetic acid (EDTA). Plants were watered with deionized water as needed.

Inoculum production, inoculation procedure and treatments

The isolate CMES 1465 of *S. sclerotiorum* obtained from common bean, kindly provided by EMBRAPA Soybean (Londrina, Paraná State, Brazil), was used for plant inoculation. The isolate was preserved as sclerotia; for their production, carrots were

washed, peeled, cut in cubes of approximately 1 × 1 × 1 cm, transferred to Erlenmeyer flasks and autoclaved at 121°C for 20 min (Bae and Knudsen, 2007). For inoculum production, a sclerotium was transferred to each Petri dish containing potato dextrose agar (PDA) medium and kept in a growth chamber (20°C and 12 h photoperiod) for seven days.

The leaflets of the third leaf, from the base to the top, of each plant (V3 growth stage) were inoculated with a plug (5 mm in diameter) of PDA medium obtained from the edge of three-days-old colony of *S. sclerotiorum*. Each PDA plug was placed between the main vein and the edge of the leaflet and gently pressed with the forefinger. Inoculated plants were transferred to a plastic mist growth chamber (MGC) inside a greenhouse for the duration of the experiment. The MGC was made of wood (2 m wide, 15 m high and 5 m long) and covered with 100 µm thick transparent plastic. The temperature inside the MGC ranged from 20 ± 2°C (day) to 17 ± 2°C (night). The relative humidity was maintained at 92 ± 3% using a misting system with nozzles (model NEB-100; KGF Co.) that sprayed mist every 30 min above the plant canopy. The relative humidity and temperature were measured with a thermohygrograph (TH-508; Impac). The maximum natural photon flux density at plant canopy height was approximately 900 µmol m^{-2} s^{-1}.

At 48 h before *S. sclerotiorum* inoculation, plants were sprayed with water (control treatment), zinc (Zn) phosphite (5 mL L^{-1}, Phytogard® Zn (40% P_2O_5 and 10% Zn), Stoller do Brazil S.A., Cosmópolis, Brazil) or copper (Cu) phosphite (2.5 mL L^{-1}, Strong (20% P_2O_5 and 4% Cu), Giro Produtos Agrícolas LTDA, Machado, Brazil). Plants were sprayed using a CO_2 pressurized backpack sprayer equipped with a flat fan nozzle (XR 110 02®, Teejet, Glendale Heights, IL, USA) at a 200,000-Pa pressure to deliver a spray volume of 200 L ha^{-1}.

Quantification of lesion area (LA) and white mold severity (WMS)

Inoculated leaflets of each plant were collected at 12, 36, 60 and 84 h after inoculation (hai) to determine LA by its measurement in two perpendicular directions using a digital paquimeter. In addition, leaflets were scanned at 300 dpi resolution and the obtained images were further processed using the software QUANT (Vale *et al.,* 2003) to quantify WMS.

Light microscopy

A total of 30 of leaflets fragments (≈ 5 mm) were obtained from plants of each replication at 84 hai. The fragments were carefully transferred to glass vials containing 10 ml of fixative composed of 3% (v/v) glutaraldehyde and 2% (v/v) paraformaldehyde in 0.1 mol L^{-1} sodium cacodylate buffer (pH 7.2). Vials were covered with aluminum foil and stored at 4°C for 1 month until being processed for microscopic observations. Leaflets fragments collected were subsequently dehydrated through a graded alcohol series (10, 30, 50, 70, 85, 95 and 100%) and then embedded in methacrylate resin (Historesin, Leica Microsystems®, Nussloch/Heidelberg, Germany) (Araujo *et al.,* 2015; Hawerroth *et al.,* 2017). The fragments were placed in a vacuum chamber for 2 h during the pre-infiltration and infiltration steps twice a day, respectively, for 3 weeks for a better resin infiltration. The fragments were stored at 4°C after each vacuum procedure. Six blocks of resin, each one containing two leaflets fragments, were obtained for each treatment. Thirty-six longitudinal and transversal serial sections (4 μm thick), which were cut from each block using a Leica RM 2245 rotary microtome (Leica Microsystems®), were randomly divided and placed on three glass slides and stained with 1% toluidine blue in 2% sodium borate buffer for 1 min. The images were digitally obtained using a Carl Zeiss Axio Imager A1 microscope in the bright-field mode.

Biochemical assays

For all biochemical assays, the third leaves, from base to the top, of each plant per replication of each treatment were collected at 12, 36, 60 and 84 hai. Leaf samples were kept in liquid nitrogen during sampling and then stored at -80°C until further analysis.

Determination of antioxidant enzymes activities

To determine the activities of ascorbate peroxidase (APX) (EC 1.11.1.11), catalase (CAT) (EC 1.11.1.6), glutathione-*S*-transferase (GST) (EC 2.5.1.18), peroxidase (POX) (EC 1.11.1.7) and superoxide dismutase (SOD) (EC 1.15.1.1), a total of 0.2 g of leaf tissue was ground into a fine powder with liquid nitrogen in a mortar and pestle. The fine powder was homogenized in a 2 ml solution containing 50 mM potassium phosphate buffer (pH 6.8), 0.1 mM EDTA, 1 mM phenylmethyl-sulphonyl fluoride (PMSF) and 2% (w/v) polyvinylpyrrolidone (PVP). The homogenized material was centrifuged at 12,000 × *g* at 4°C for 15 min and the supernatant was used for enzyme determination. SOD activity was determined by measuring its ability to inhibit the photochemical reduction of nitroblue tetrazolium (NBT) as described by Beauchamp & Fridovich (1971) by adding 50 µl of the crude enzyme extract to 1.95 ml of a mixture containing 50 mM potassium phosphate buffer (pH 7.8), 13 mM methionine, 75 µM NBT, 0.1 mM EDTA and 2 µM riboflavin. Samples were light-exposed for 10 min and the production of formazan blue, resulting from the photoreduction of NBT, was measured at 560 nm and the samples kept in the dark for 10 min served as a blank. One unit of SOD was defined as the amount of enzyme necessary to inhibit NBT photoreduction by 50%. Activity of CAT was determined after addition of 50 µl of the crude enzyme extract to 1.95 ml of a reaction mixture containing 50 mM potassium phosphate buffer (pH 7.0) and 20 mM hydrogen peroxide (H_2O_2) (Havir & McHale, 1989). The absorbance was recorded at 240 nm for 1 min. POX activity was assayed by determining the pyrogallol oxidation as proposed by Kar & Mishra (1976). The reaction

was started after the addition of 15 µl of the crude enzyme extract to 1.98 ml of a reaction mixture containing 25 mM potassium phosphate (pH 6.8), 20 mM pyrogallol and 20 mM H_2O_2. The activity was determined through the absorbance of colored purpurogallin recorded for 1 min at 420 nm (Chance & Maehly, 1955). The GST activity was determined using the methodology proposed by Habig *et al.* (1974). In total, 150 µl of the crude enzyme extract was added to 1.35 ml of the mixture containing 50 mM potassium phosphate buffer (pH 6.5) and 50 mM reduced glutathione (GSH). The reaction was initiated after the addition of 500 µl of 30 mM 1-chloro-2,4-dinitrobenzene and the absorbance was measured at 340 nm over 3 min. APX activity assay followed that described by Nakano & Asada (1981). A total of 15 µl of the crude enzyme extract was added to 1.98 ml of a mixture containing 50 mM phosphate buffer (pH 7.0), 1 mM H_2O_2 and 1 mM sodium ascorbate. The rate of ascorbate oxidation was measured by recording the absorbance at 290 nm for 1 min. Enzyme activity was expressed in a protein-basis whose concentration was determined according to the method of Bradford (1976).

Determination of defense enzymes activities

To determine the activities of *β*-1,3-glucanases (GLU) (EC 3.2.1.39), chitinase (CHI) (EC 3.2.1.14), lipoxygenase (LOX) (EC 1.13.11.12), phenylalanine ammonia-lyase (PAL) (EC 4.3.1.5) and polyphenoloxidase (PPO) (EC 1.10.3.1), a total of 0.2 g of leaf tissue was ground into a fine powder with liquid nitrogen using a mortar and pestle. The fine powder was homogenized in 2 ml of a solution containing 50 mM potassium phosphate buffer (pH 6.8), 1 mM EDTA, 1 mM PMSF and 2% (w/v) PVP. Then, the homogenate was centrifuged at 12,000 × *g* for 15 min at 4°C, the supernatant was collected and used to determine the GLU, CHI, PAL, PPO and LOX activities. GLU activity was determined according to the method of Lever (1972). First, 20 µl of the

crude enzyme extract was added to a reaction mixture containing 50 mM sodium acetate buffer (pH 5.0) and laminarin (1 mg ml^{-1}). Next, the reaction mixture was incubated in a Thermo Mixer (Eppendorf, Hamburg, Germany) at 45°C for 1 h. Then, 500 µl of the reaction mixture was added to 1.5 ml of dinitrosalicylic acid (DNS) and incubated at 100°C for 15 min. The reaction was stopped in ice bath until the solution reached 25°C. The amount of reducing sugars released was calculated with a calibration curve using glucose (Sigma-Aldrich, São Paulo, Brazil) as a standard and the absorbance was measured at 540 nm (Miller, 1959). A similar procedure was used for the control samples, but the first incubation was excluded. CHI activity was determined according to the method of Harman *et al.* (1993). The reaction was started with the addition of 20 µl of the crude enzyme extract to 1980 µl of a reaction mixture containing 50 mM sodium acetate buffer (pH 5.0) and 0.1 mM *p*-nitrophenyl-b-D-N-N'-diacetylchitobiose. Next, the reaction mixture was incubated at 37°C for 2 h and the reaction was stopped by adding 500 µl of 0.2 M sodium carbonate. The control samples received 500 µl of 0.2 M sodium carbonate immediately after the addition of the crude enzyme extract to the reaction mixture. The final product released by CHI was measured at 410 nm. PAL activity was assayed following the method proposed by Guo *et al*. (2007) with some modifications. Firstly, the reaction was started by adding 100 µl of crude enzyme extract to 0.9 ml of a reaction mixture containing 40 mM sodium borate buffer (pH 8.8) and 20 mM *L*-phenylalanine. The reaction mixture was incubated at 30°C for 1 h. The reaction was stopped by adding 50 µl of 6 N HCl. For the control samples, HCl was added before incubation. The absorbance of the *trans*-cinnamic acid derivatives was recorded at 290 nm (Zucker, 1965). PPO activity was assayed following the colorimetric determination of pyrogallol oxidation according to the method of Kar & Mishra (1976) with some modifications. The reaction was started after the addition of 15 µl of the crude enzyme extract to 985 µl of a reaction mixture containing 25 mM

potassium phosphate buffer (pH 6.8) and 20 mM pyrogallol. Immediately after the reaction was initiated, the absorbance was determined at 420 nm for 1 min at 25°C. LOX activity was assayed according to the method described by Axelrod *et al.* (1981). The reaction was started after the addition of 10 µl of the crude enzyme extract to 900 µl of 50 mM sodium phosphate buffer (pH 6.8) and 15 µl of 10 mM sodium linoleate substrate. Then, the reaction mixture was incubated at 25°C for 4 min. The absorbance of the product released by the LOX during 1 min was measured at 234 nm.

Determination of malondialdehyde (MDA) concentration

Oxidative damage in the leaf cells was assessed based on lipid peroxidation and expressed as equivalents of MDA according to Cakmak & Horst (1991). A total of 100 mg of leaf tissue was ground into a fine powder using a mortar and pestle with liquid nitrogen and homogenized in 2 ml of 0.1% (w/v) trichloroacetic acid (TCA) solution in ice bath and the homogenate was centrifuged at 12,000 × *g* for 15 min at 4°C. After centrifugation, 0.5 ml of the supernatant was added to 1.5 ml of TBA solution (0.5% in 20% TCA) and held for 30 min in a boiling water bath at 95°C. After this period, the reaction was stopped in ice bath. The samples were centrifuged at 9,000 × *g* for 10 min and the absorbance of the supernatant was read at 532 nm and discounting the non-specific absorbance at 600 nm (Heath & Packer, 1968).

Determination of superoxide (O_2^-) concentration

A total of 0.2 g of leaf tissue was ground into a fine powder in a mortar and pestle with liquid nitrogen. The fine powder was homogenized in 2 ml of a solution containing 100 mM sodium phosphate buffer (pH 7.2) and 1 mM sodium diethyl dithiocarbamate (SDD). The homogenate was centrifuged at 22,000 × *g* for 20 min at 4°C. After centrifugation, 0.1 ml of the supernatant was reacted with 1.9 ml of a solution

containing 100 mM sodium phosphate buffer (pH 7.2), 1 mM SDD and 0.25 mM NBT. The O_2^- concentration was determined by subtracting the absorbance of the final product from the initial absorbance at 540 nm (Chaitanya & Naithani, 1994).

Determination of hydrogen peroxide (H_2O_2) concentration

A total of 0.2 g of leaf tissue was ground into a fine powder in liquid nitrogen and homogenized in 2 ml of a mixture containing 50 mM potassium phosphate buffer (pH 6.5) and 1 mM hydroxylamine. The homogenate was centrifuged at 10,000 × *g* for 15 min at 4°C (Kuo & Kao, 2003) and the supernatant was used as the crude extract. A total of 100 µl of the supernatant was then added to a reaction mixture containing 100 µM ferric ammonium sulphate ($FeNH_4[SO_4]$), 25 mM sulphuric acid, 250 µM xylenol orange and 100 mM sorbitol in a final volume of 2 ml (Gay & Gebicki, 2000). After 30 min of dark incubation at room temperature, the absorbance of the samples was determined at 560 nm. Blanks were prepared under the same conditions and subtracted from the samples. A standard curve for H_2O_2 (Sigma-Aldrich, São Paulo, Brazil) was used to determine the H_2O_2 concentration.

Determination of oxalic acid (OA) concentration

A catalytic kinetic spectrophotometric method (Liu *et al.*, 2015) was used to determine OA concentration. A total of 0.2 g of leaf tissue was ground into in 0.9% NaCl solution and homogenized were centrifuged at 1,000 × *g* for 10 min. A total of 100 µL aliquot of the supernatant, 120 µL sulphuric acid (1 M) and 40 µL methylene blue were mixed and distilled sterile water was added to achieve a final volume of 980 mL. The mixture was heated in water bath (40°C) for 5 min and 20 µL of 0.1 M potassium dichromate was added to the tube. After 5 min, 200 µL sodium carbonate (2 M) was added to terminate the reaction and the absorbance was measured at 660 nm and recorded as A_s.

Absorbance at 660 nm was read again and recorded as A_b when the aliquot of the supernatant was replaced with water. The difference between A_s and A_b ($\Delta A = A_s - A_b$) corresponded to the OA concentration. A calibration curve was generated by measuring ΔA for OA concentrations ranging from X to Y.

Determination of the concentrations of total soluble phenolics (TSP) and lignin-thioglycolic acid (LTGA) derivatives

A total of 100 mg of leaf tissue was ground into a fine powder with liquid nitrogen using a mortar and pestle and homogenized in 1 ml of a solution containing 80% (v/v) methanol. Next, the crude extract was shaken at 300 rpm at 25°C for 2 h. Subsequently, the mixture was centrifuged at 17,000 × *g* for 30 min. The methanolic extract was collected and used to determine the TSP concentration and the pellet was maintained at 20°C to further determine the LTGA derivatives concentration. The TSP concentration was assayed following the methodology proposed by Zieslin & Ben-Zaken (1993) adapted by Rodrigues *et al.* (2005). The reaction was started after the addition of 150 µL of methanolic extract to 750 µL of 0.2 M Folin-Ciocalteu phenol reagent and incubated at 25°C for 5 min. The next step was the addition of 0.1 M sodium carbonate to the solution, which was maintained at 25°C for 10 min. Afterwards, 1 mL of deionized water was also added to the mixture and the solution was incubated at 25°C for 1 h. The TSP concentration was calculated based on a calibration curve using catechol (Sigma-Aldrich, São Paulo, Brazil) as a standard and the absorbance was read at 725 nm. For the determination of the LTGA derivatives concentration, the pellet was resuspended in 1.5 mL of deionized water and homogenized and centrifuged at 12,000 × *g* for 15 min. Afterwards, the supernatant was discarded and the pellet was dried at 65°C for 12 h. The alcohol-insoluble dry residue was used to determine the concentration of LTGA derivatives as described by Barber & Ride (1988). The

absorbance of the LTGA derivatives in the supernatant was read at 280 nm and the concentration was determined from a calibration curve using lignin, alkali and 2-hydroxypropyl ether (Sigma-Aldrich. São Paulo, Brazil) as standards.

Experimental design and data analysis

A 3 × 2 factorial experiment, consisting of three foliar treatments (FT) [water (control treatment), Zn and Cu phosphites] and two plant inoculation (PI) conditions (non-inoculated or inoculated plants), was arranged in a completely randomized design with four replications. Each replication corresponded to a plastic pot containing three plants. The experiment was repeated. Data were subjected to analysis of variance (ANOVA) and means were compared based on Tukey's test ($P \leq 0.05$). For LA and WMS, ANOVA was considered to be a 3 × 4 factorial experiment with three FT and four evaluation times (ET) (12, 36, 60 and 84 hai). For biochemical assays, a 3 × 2 × 4 factorial experiment consisting of three FT, two PI and four ET (12, 36, 60 and 84 hai) was considered for ANOVA. Principal components analysis (PCA) technique was used to determine the relationship among the variables studied. Data were analyzed using the Minitab software (version 18; Minitab Corporation).

Results

Analysis of variance

The factors FT and ET and their interaction were significant for LA and WM. Most of the factors and double interactions were significant for the variables, whereas FT × PI × ET interaction was significant for the activities of APX, CHI, GST, LOX, PAL, POX and SOD as well as for the concentrations of OA, O_2^-, H_2O_2 and TSP (Table 1).

LA and WMS

LA and WMS were significantly reduced by the Zn and Cu phosphites sprays at 36, 60 and 84 hai (Fig. 1). Decreases of 47-70% and 23-60% in LA and of 33-67% and 8-49% in WMS were observed for Zn and Cu phosphite sprays, respectively.

Light microscopy

In contrast to the non-inoculated leaflet tissue (Fig. 2A, B and C), hyphae of *S. sclerotiorum* massively colonized the epidermal cells and the intercellular spaces causing severe tissue damage in the leaflets tissue obtained from plants non-sprayed with phosphites (Fig. 2D, E and F). Mesophyll cells were collapsed and host tissues were hard to be recognized, with exception of the xylem vessels that remained undamaged (Fig. 2D and F). By contrast, even though some degree of cells disorganization was seen in tissues of the Zn (Fig. 2G, H and I) and Cu phosphite-sprayed leaflets (Fig. 2J, K and L), the amount of fungal hyphae and the extension of collapsed cells were greatly reduced indicating that *S. sclerotiorum* colonization was constrained, which was particularly evident for the Zn phosphite spray.

Antioxidant enzymes activities

Activities of SOD, CAT, POX, APX and GST in the non-inoculated plants were not influenced by phosphite spray regardless of the sampling time (Fig. 3A, C, E, G and I). For the inoculated plants, activities of SOD, POX, APX and GST were significantly higher by 39 and 57%, 63 and 80%, 34 and 53%, and 42 and 39% at 12 hai and those of CAT by 36-60% and 40-42% at 60 and 84 hai for Zn and Cu phosphites, respectively, in comparison to the control (Fig. 3B, D, F, H and J). On the other hand, Zn and Cu phosphite-sprayed plants displayed lower activities of SOD (16-30%), POX (27-46%), APX (21-41%) and GST (15-34%) at 60 and 84 hai compared to the control, but such

activities were higher for the Cu phosphite than for the Zn phosphite-sprayed plants (Fig. 3B, F, H and J).

Activities of SOD (46-82%), APX (58-97%) and GST (80-118%) increased at 60 e 84 hai for inoculated plants and of POX (36-177%) at 36, 60 and 84 hai for non-inoculated ones (Fig. 3B, F, H and J). By contrast, the inoculated plants showed lower activities of CAT (23-48%) at 60 and 84 hai than their non-inoculated counterparts (Fig. 3D). For the Zn and Cu phophite-sprayed plants, increases in the activities of SOD (27-51%) and APX (41-92%) at 12 and 84 hai, of GST (28-45%) at 12, 60 and 84 hai and of POX (36-101%) at 12, 36, 60 and 84 hai were observed in response to *S. sclerotinia* infection (Fig. 3B, F, H and J). CAT activity of *S. sclerotiorum*-infected and Cu phosphite-sprayed plants was significantly decreased by 26% at 84 hai and was not affected in the Zn phosphite-treated plants (Fig. 3D).

Defense enzymes activities

Regardless of sampling time, activities of CHI, GLU, PAL, PPO and LOX for the non-inoculated plants were not affected by Zn and Cu phosphites (Fig. 4A, C, E, G and I). The Zn phosphite-sprayed and inoculated plants showed higher activities of CHI (29%) at 12 hai, PAL (161-221%) at 36, 60 and 84 hai, GLU (26-51%) and PPO (48-115%) at 12, 36, 60 and 84 hai compared to the control plants (Fig. 4B, D, F and H). The Cu phosphite spray also increased activities of LOX (64%) at 12 hai, PPO (68%) at 36 hai, CHI (26-67%) at 12 and 36 hai and GLU (30-61%) at 12, 36 and 60 hai compared to the control treatment (Fig. 4B, D, H and J). The Cu phosphite sprayed resulted in higher activities of CHI (29-64%) at 12, 36 and 60 hai, PAL (239%) and LOX (84%) at 12 hai compared to the Zn phosphite spray, whereas higher activities of GLU (31%) at 84 hai, PAL (61-200%) and PPO (15-107%) at 36, 60 and 84 hai were observed in the latter spray than in the Cu phosphite one (Fig. 4B, D, F, H and J). However, inoculated plants

from the control treatment showed higher activities of CHI (46-251%) and LOX (55-114%) at 60 and 84 hai than their Zn and Cu phosphite-treated counterparts (Fig. 4B and J).

While GLU, PAL and PPO activities were not affected on inoculated plants, there were significant increases in the activities of CHI (29-336%) at 36, 60 and 84 hai and LOX (44-96%) at 60 and 84 hai for the control plants (Fig. 4B, D, F, H and J). CHI activity was increased at 12, 60 and 84 hai for the Zn phophite-sprayed plants (28-44%) and at 12, 36 and 60 hai for the Cu phosphite-sprayed ones (50-143%) relative to their non-inoculated counterparts (Fig. 4B). Increases in the activities of GLU (19-79%) throughout sampling time and PAL (71-556%) at 12, 36 e 60 hai were obtained for inoculated and Zn and Cu phosphites-sprayed plants, respectively, compared with the non-inoculated plants (Fig. 4D and F). Increases in the PPO activity throughout sampling time for the Zn phosphite (56-108%) and at 12 and 36 hai for the Cu phosphite (37-77%) were observed in response to *S. sclerotiorum* infection (Fig. 4H). LOX activity for the Cu phosphite-sprayed and inoculated plants was increased by 86% at 12 hai compared with their non-inoculated counterparts, whereas pathogen infection did not affect LOX activity for the Zn phosphite-sprayed plants (Fig. 4J).

Concentrations of OA, O_2^-, H_2O_2, MDA, TSP and LTGA derivatives

Neither the non-inoculated plants throughout sampling times nor the inoculated ones at 12 and 36 hai showed difference for the concentrations of OA, O_2^-, H_2O_2, MDA, TSP and LTGA derivatives as a result of phosphites spray (Fig. 5). Concentrations of OA, O_2^-, H_2O_2, MDA and LTGA derivatives were significantly lower by 24 and 46%, 50 and 64%, 36 and 41%, 35 and 31%, and 30 and 18% at 60 and 84 hai, respectively, for the inoculated and Zn phosphite-sprayed plants relative to their non-sprayed counterparts (Fig. 5B, D, F, H and L). Conversely, TSP concentration was significantly increased by

21% at 60 hai for the Zn phosphite-sprayed plants compared to the control treatment (Fig. 5J). The Cu phosphite-sprayed plants displayed concentrations of OA, O_2^- and MDA that were significantly lower by 17 and 32%, 33 and 32%, and 5 and 9% at 60 and 84 hai, respectively, and by 28% for H_2O_2 at 84 hai compared to the control treatment (Fig. 5B, D, F, and H).

There were significant increases of 61 and 144%, 105 and 318%, 80 and 125% and 52 and 119% in the concentrations of OA, O_2^-, H_2O_2, MDA at 60 and 84 hai, of 59% in the TSP concentration at 84 hai and of 29, 62 and 77% in the LTGA derivatives concentration at 36, 60 and 84 hai, respectively, in response to *S. sclerotiorum* infection (Fig. 5A-L). Concentrations of OA, H_2O_2, MDA and LTGA derivatives at 84 hai were significantly higher by 24, 31, 39 and 58%, respectively, and 23% for TSP at 60 hai for Zn phosphite-sprayed and inoculated plants relative to their non-inoculated counterparts (Fig. 5B, F, H, J and L). For the Cu phosphite-sprayed plants, *S. sclerotiorum* infection resulted in significant increases in the concentrations of LTGA derivatives (24-87%) at 36, 60 and 84 hai, OA (40-54%), O_2^- (39-178%) and H_2O_2 (57-70%) at 60 and 84 hai, and MDA (67%) and TSP (89%) at 84 hai (Fig. 5B, D, F, H and J).

Principal component analysis (PCA)

To gain further insights of the Zn and Cu phosphite-triggered biochemical changes, the dataset was subjected to PCA of the two first PCs, which explained the major variance of the dataset (Fig. 6, PC1 and PC2 covered 72 and 14% of the total variance, respectively). For the non-inoculated plants, PCA showed that Zn and Cu phosphite-sprayed plants were clustered together with those of the control suggesting, therefore, that phosphites did not affect the metabolism of non-infected plants (Fig. 6A). By contrast, inoculated plants displayed substantial adjustments on their metabolim. The Zn and Cu phosphite-sprayed plants as well as those from the control were clustered

separately indicating that the Zn and Cu phosphites affected differently plant metabolism in order to increase host resistance to white mold. The first PC, which had positive scores for LA, WMS, SOD, POX, APX, GST, CHI, PPO, LOX, OA, O_2^-, H_2O_2, MDA, TSP and LTGA derivatives (which were clustered together) displayed negative correlations with CAT, GLU and PAL (Fig. 6B).

Discussion

This study brings new insights at the biochemical level of the indirect effect of the Zn and Cu phosphites in common bean resistance to white mold. It was showed that the Zn and Cu phosphites were able to reduce both LA and WMS indicating, therefore, their potential in constraining *S. sclerotiorum* infection in common bean leaflets. Several studies have demonstrated the potential of phosphites in plant disease control through a direct action on the pathogen as well as by stimulating host defense responses (King *et al.,* 2010; Lobato *et al.,* 2010; Burra *et al.,* 2014; Dalio *et al.,* 2014; Araujo *et al.,* 2015; Liu *et al.,* 2016; Cerqueira *et al.,* 2017; Costa *et al.,* 2017; Gadaga *et al.,* 2017). Despite being less fungitoxic, Zn phosphite outcompeted Cu phosphite in disease control, suggesting that other mechanisms besides direct action may be involved in suppressing white mold symptoms. Histopathological analysis revealed severe disorganization of the leflets tissue; mesophyll cells were collapsed and abundantly colonized by *S. sclerotiorum* hyphae. Consistently with these findings, in *S. sclerotiorum*-infected soybean leaves, fungal hyphae were demonstrated to grow through the epidermal cell walls, into the intercellular space and along vascular tissue, collapsing mesophyll cells and causing severe ultrastructural damage (Davidson *et al*., 2016). Although histological damage was not prevented on common bean leaflets sprayed with Zn or Cu phosphites, fungal colonization was greatly constrained since fewer hyphae and less tissue disorganization was observed.

Oxidative burst, an accumulation of reactive oxygen species (ROS), including O_2^- and H_2O_2, at the pathogen's infection site represents one of the earliest biochemical changes in response to the challenger's recognition (Apostol *et al.,* 1989; Lamb *et al.,* 1997; Cessna *et al.,* 2000; Yarden *et al.,* 2014). Manipulation of ROS balance by *S. sclerotiorum* has been shown to be essential for fungal successful infection. Initially, the fungus is able to suppress ROS accumulation to prevent host defense mechanisms and then triggers ROS production to induce oxidative stress to the host cells to favor colonization. Such changes are thought to be chiefly due to the fungus-secreted OA, a key toxin essential for *S. sclerotiorum* pathogenicity (Godoy *et al.,* 1990; Cessna *et al.,* 2000; Willian *et al.,* 2011; Zhou *et al.,* 2013). Consistent with these reports, in the present study common bean plants non-sprayed with phosphites displayed significant increases in O_2^- and H_2O_2 generation from 60 hai onwards stemmed from *S. sclerotiorum* infection, which was related to the higher OA concentration. *Sclerotinia sclerotiorum*-triggered oxidative stress was confirmed by the increases in MDA, an indicator of cellular damage, which may be is related to the direct action of OA in membrane destabilization, which was also suggested to occur in the soybean genotypes 1511/99 and Meli that showed increased levels of ROS and MDA upon *S. sclerotiorum* infection (Malencic *et al.,* 2010).

The Zn and Cu phosphites sprays themselves were not able to trigger ROS production in the non-inoculated plants supporting observations made for potato plants sprayed with potassium (K) phosphite without being infected by *P. infestans* (Machinandiarena *et al.,* 2012). Although concentrations of O_2^-, H_2O_2, MDA and OA were increased for the inoculated and Zn or Cu phosphite-sprayed plants from 60 hai onwards, such concentrations were lower than those from the non-sprayed plants. These findings are in disagreement with those found in the K phosphite-sprayed *A. thaliana* leaves, which showed increased H_2O_2 production in attempted sites of *P. cinnamomi*

penetration and in cells close to the infected ones at 24 hai (Eshraghi *et al.,* 2011). *Arabidopsis thaliana* and potato plants that were sprayed with K phosphite and infected by *P. palmivora* and *P. infestans*, respectively, also displayed increases in O_2^- and H_2O_2 concentrations at early stages of pathogen infection (Daniel & Guest, 2006; Machinandiarena *et al.,* 2012). Although the hypothesis that the Zn and Cu phosphites may have induced a localized ROS accumulation cannot be ruled out; it seems more plausible to assume that, for the common bean-*S. sclerotiorum* interaction, phosphites rather than inducing early generation of ROS, were involved in mitigating oxidative stress at late (from 60 hai onwards) stages of the fungal infection.

SOD represents the front line of plant protection against ROS. This enzyme is responsible for O_2^- removal from the cells converting it in H_2O_2 and O_2 (Malencic *et al.,* 2010). In the present study, irrespective of phosphite spray, higher activity of SOD was observed for inoculated plants, which was most likely due to O_2^- production as a result of fungal infection, especially from 60 hai onwards. Induction of SOD upon *S. sclerotiorum* infection has been reported in many of its hosts (Malencic *et al.,* 2004; Feng *et al.,* 2005; Malencic *et al.,* 2010; Leite *et al.,* 2014). On the other hand, SOD activity at early (12 hai) stages of *S. sclerotiorum* infection was higher in the Zn and Cu phosphite-sprayed plants. It is well-established that *S. sclerotiorum* benefit itself from ROS that are generated in the host cells during its infection to favor its colonization process (Cessna *et al.,* 2000). Therefore, early increases of SOD activity as a result of the Zn and Cu phosphite sprays may be an strategy to restrict fungal colonization through ROS removal. By contrast, at late stages of fungal infection, phosphite sprays by suppressing white mold symptoms is believed to have limited *S. sclerotiorum*-triggered O_2^- production, explaining the lower activities of SOD observed in such treatments when compared with the non-sprayed plants.

Removal of the H_2O_2 excess generated spontaneously or by O_2^- dismutation via SOD requires the action of enzymes such as CAT, POX, APX and GST. In the present study, activities of POX, APX and GST were increased, whereas those of CAT were reduced, in the *S. sclerotiorum*-infected common bean leaflets, especially for plants from the control treatment. Leite *et al.* (2014) also showed for common bean-*S. sclerotiorum* interaction increases in the activities of SOD, POX, APX and reductions in those of CAT stemmed from fungal infection. The inoculated and Zn or Cu phosphite-sprayed plants displayed higher activities of CAT, POX, APX and GST at 12 hai, but activities of POX, APX and GST were lower relative to their non-treated counterparts. These findings suggest that phosphite-mediated resistance of common bean to white mold may be due to early increases in the activities of antioxidant enzymes. The early containment of *S. sclerotiorum* infection by phosphites may explain the lower H_2O_2 generation observed later supporting, therefore, the lower activities of antioxidant enzymes recorded from 60 hai owards compared to plants from the control treatment. Similarly, activities of most antioxidant enzymes were not potentiated by silicon, though this element was able to enhance wheat resistance to leaf blast (Debona *et al.,* 2014). In rice, the study of the effect of azoxystrobin in the antioxidant enzymes and oxidative stress-related metabolites in plants that were inoculated with *Bipolaris oryzae* revealed that fungicide relieved oxidative stress by limiting brown spot development rather than activating the antioxidant system. By contrast, the reduction in anthracnose symptoms in common bean as a result of phosphite sprays was attributed to increased activities of SOD and POX (Costa *et al.,* 2017).

Some studies have demonstrated that phosphite sprays affect the levels of TSP and LTGA derivatives (Ávila *et al.,* 2011; Leite *et al.,* 2014; Costa *et al.,* 2017; Gadaga *et al.,* 2017). The findings of the present study showed that TSP and LTGA derivatives were not affected by the Cu phosphite spray. For the Zn phosphite, on the other hand,

higher and lower concentrations of TSP and LTGA derivatives, respectively, were observed in the *S. sclerotiorum*-infected common bean plants at 60 hai in comparison to the control treatment. For the common bean-*C. lindemuthianum* interaction, concurrent decreases in TSP and increases in LTGA derivatives were reported (Polanco *et al.,* 2012). Although cell wall strengthening constraints pathogen colonization, some phenolic compounds produced quickly are highly toxic to pathogens (Campos *et al.,* 2004). Thus, the increases in TSP content for the Zn phosphite-treated plants are believed to play a role in suppressing white mold in common bean. Consistently with these findings, spraying K and manganese (Mn) phosphites aiming to protect common bean against anthracnose revealed that they were able to increase TSP levels without changing those of LTGA derivatives (Gadaga *et al.,* 2017). By contrast, increases in both LTGA derivatives and TSP were observed in the K phosphite-treated and *C. lindemuthianum*-infected common bean plants (Costa *et al.,* 2017).

CHI and GLU catalyze the hydrolysis of chitin and β-1,3-glucan, respectively, that are found in the cell wall of fungi; in addition, they can release oligossacharides that activate host defense responses (Keen & Yoshikawa, 1983; Wu & Bradford 2003). In the present study, *S sclerotinia* infection increased CHI activity regardless of phosphite spray. However, the Zn and Cu phosphite-sprayed plants displayed higher enzyme activity at 12 hai and then it was lower relative to their non-sprayed counterparts. In contrast to CHI, GLU activity was increased only for the inoculated plants that were sprayed with the Zn and Cu phosphites suggesting its apparent contribution for common bean resistance to white mold. In agreement with these findings, K phosphite spray improved plant vitality by increasing GLU activity and reducing lesion size of Pseudomonas bleeding canker in horse chestnut (Percival & Banks, 2015). Phosphite sprays were also found to decrease anthracnose severity in common bean due to an

increase on activities of antioxidant and defense enzymes, including CHI and GLU (Costa *et al.,* 2017).

In response to *S. sclerotiorum* infection, PAL activity was increased in the Zn and Cu phosphite-sprayed plants in all sampling times and at 12 hai, respectively. In soybean, PAL play a major role in disease resistance since this enzyme converts *L*-phenylalanine to *trans*-cinnamic acid which, in turn, is a precursor of several phenolics of antimicrobial nature (Campbell & Sederoff, 1996; Dixon *et al.,* 2002; Borges *et al.,* 2012). Therefore, the higher PAL activity as a result of the Zn phosphite sprays suggests that the phenylpropanoid pathway played a role in the protection of common bean against *S. sclerotiorum*, especially by increasing TSP. Common bean plants that were sprayed with K phosphite were also found to have increased PAL activity upon *C. lindemuthianum* infection (Costa *et al.,* 2017). In another study, symptoms of downy mildew in grape and enhanced PAL activity were observed in the K phosphite-sprayed plants (Pinto *et al.,* 2012).

PPO participates of phenols oxidation, leading to quinone production in the plant tissue, which are known to be extremely toxic to pathogens (Campbell & Sederoff, 1996; Lattanzio *et al.,* 2006). In the present study, PPO activity was increased in the inoculated plants that were sprayed with Zn (all sampling times) or Cu (12 and 36 hai) phosphites, which may be related to the increased levels of TSP verified in the former at 60 hai. Accordingly, the K and Mn phosphite-afforded protection of common bean against anthracnose involved concurrent increases in the PPO activity and TSP production (Gadaga *et al.,* 2017). It seems plausible to assume, therefore, that PPO played a major role in increasing common bean resistance to white mold as a consequence of the Zn phosphite spray in the present study.

LOX activity was increased in response to *S. sclerotiorum* infection at 60 and 84 hai for the control and at 12 hai for the Cu phosphite spray. LOX is responsible for the

oxygenation of polyunsaturated fatty acids giving rise to hydroperoxides of unsaturated fatty acids that amplify specific host defenses against pathogens and may irreversibly damage plasma membrane (Hammond-Kosack & Jones, 1996). Given that LOX is involved in the jasmonic acid (JA) synthesis, a key hormone known to play a role in induced systemic resistance, particularly against necrotrophic pathogens (Pieterse *et al.,* 2009), the stimulation of the JA pathway at early stages of *S. sclerotiorum* infection by the Cu phosphite most likely had contributed for common bean resistance to white mold. Conversely, the higher LOX activity from 60 hai onwards recorded for plants from the control treatment may have favored fungal colonization by stimulating leakage of cell content as a result of lipid peroxidation of the plasma membrane, thereby explaining the higher MDA concentration for such plants.

In conclusion, it was demonstrated that Zn and Cu phosphites were able to reduce white mold symptoms giving credence to their potential as an alternative measure to be included in an integrated white mold management. The increases in the activities of antioxidant and defense enzymes as a result of phosphite sprays shed light on the biochemical defense responses which are thought to be involved, at least partially, in their effect in constraining fungal infection and *S. sclerotiorum*-induced oxidative stress.

Acknowledgments

Professor F. A. Rodrigues thanks the Conselho Nacional de Desenvolvimento Científico e Tecnológico (CNPq) for his fellowship. Ms. I. R. F. Fagundes-Nacarath was supported by CNPq. We thank EMBRAPA Soybean for providing the isolate of *Sclerotinia sclerotiorum* used in this study. This study was supported by grants from CAPES, CNPq and FAPEMIG to Prof. F. A. Rodrigues.

References

Ando K, Grumet R, Terpstra K, Kelly JD, 2007. Manipulation of plant architecture to enhance crop disease control. *CAB Reviews: Perspectives in Agriculture, Veterinary Science, Nutrition, and Natural Resources* **2**, 1–8.

Apostol I, Heinstein PF, Low PS, 1989. Rapid stimulation of an oxidative burst during elicitation of cultured plant cells. *Plant Physiology* **90**, 109–116.

Araujo L, Bispo WMS, Rios VS, Fernandes AS, Rodrigues FA, 2015. Induction of the phenylpropanoid pathway by acibenzolar-S-methyl and potassium phosphite increases mango resistance to *Ceratocystis fimbriata* infection. *Plant Disease* **99**, 447–459.

Ávila FW, Faquin V, Araujo JL, Marques DJ, Ribeiro PM, Lobato AK, Ramos SJ, Baliza DP, 2011. Phosphite supply affects phosphorus nutrition and biochemical responses in maize plants. *Australian Journal of Crop Science* **5**, 646–653.

Axelrod B, Cheesbrough TM, Laasko S, 1981. Lipoxygenases from soybeans. *Methods in Enzymology* **71**, 441–451.

Bae YS, Knudsen GR, 2007. Effect of sclerotial distribution pattern of *Sclerotinia sclerotiorum* on biocontrol efficacy of *Trichoderma harzianum*. *Applied Soil Ecology* **35**, 21–24.

Barber MS, Ride JP, 1988. A quantitative assay for induced lignification in wounded wheat leaves and its use to survey potential elicitors of the response. *Physiological and Molecular Plant Pathology* **32**, 185–197.

Beauchamp C, Fridovich I, 1971. Superoxide dismutase: improved assays and an assay applicable to acrylamide gels. *Analytical Biochemistry* **44**, 276–287.

Boland G, Hall R, 1994. Index of plant hosts of *Sclerotinia sclerotiorum*. *Canadian of Journal of Plant Pathology* **16**, 93–108.

Bolton MD, Thomma BPHJ, Nelson BD, 2006. Pathogen profile *Sclerotinia sclerotiorum* Lib. de Bary: biology and molecular traits of a cosmopolitan pathogen. *Molecular Plant Pathology* **7**, 1–16.

Borges A, Melotto M, Tsai SM, Caldas DGG, 2012. Changes in spatial and temporal gene expression during incompatible interaction between common bean and anthracnose pathogen. *Journal of Plant Physiology* **169**, 1216–1220.

Bradford MN, 1976. A rapid and sensitive method for the quantitation of microgram quantities of protein utilizing the principle of protein-dye binding. *Analytical Biochemistry* **72**, 248–254.

Burra DD, Berkowitz O, Hedley PE, Morris J, Resjö S, Levander F, Liljeroth E, Andreasson E, Alexandersson E, 2014. Phosphite-induced changes of the transcriptome and secretome in *Solanum tuberosum* leading to resistance against *Phytophthora infestans*. *BMC Plant Biology* **14**, 254–271.

Cakmak I, Horst WJ, 1991. Effect of aluminum on lipid peroxidation, superoxide dismutase, catalase, and peroxidase activities in root tips of soybean (*Glycine max*). *Physiologia Plantarum* **83**, 463–468.

Campbell MM, Sederoff RR, 1996. Variation in lignin content and composition. *Plant Physiology* **110**, 3–13.

Campos AD, Ferreira AG, Hampe MMV, Antunes IF, Brancão N, Silveira EP, Osório VA, Augustin E, 2004. Atividade de peroxidase e polifenoloxidase na resistência do feijão à antracnose. *Pesquisa Agropecuária Brasileira* **39**, 637–643.

Cerqueira A, Alves A, Berenguer H, Correia B, Gomez-Cadenas A, Diez JJ, Monteiro P, Pinto G, 2017. Phosphite shifts physiological and hormonal profile of Monterey pine and delays *Fusarium circinatum* progression. *Plant Physiology and Biochemistry* **114**, 88–99.

Cessna SG, Sears VE, Dickman MB, Low PS, 2000. Oxalic acid, a pathogenicity factor for *Sclerotinia sclerotiorum*, suppresses the oxidative burst of the host plant. *Plant Cell* **12**, 2191–2199.

Chaitanya KSK, Naithani SC, 1994. Role of superoxide lipid peroxidation and superoxide dismutase in membrane perturbation during loss of viability in seeds of *Shorea robusta* 371 Faertn. *New Phytologist* **126**, 623–627.

Chance B, Maehley AC, 1955. Assay of catalases and peroxidases. *Methods in Enzymology* **2**, 764–775.

Clark RB, 1975. Characterization of phosphates in intact maize roots, *Journal of Agricultural and Food Chemistry* **23**, 458–460.

Costa BHG, Resende MLV, Monteiro ACA, Júnior PMR, Botelho DMDS, Silva BM, 2017. Potassium phosphites in the protection of common bean plants against anthracnose and biochemical defence responses. *Journal of Phytopathology* **166**, 95–102.

Debona D, Rodrigues FA, Rios JA, Nascimento KJT, Silva LC, 2014. The effect of silicon on antioxidant metabolism of wheat leaves infected by *Pyricularia oryzae*. *Plant Pathology* **63**, 581–589.

Dalio RJD, Fleischmann F, Humez M, Osswald W, 2014. Phosphite protects *Fagus sylvatica* seedlings towards *Phytophthora plurivora* via local toxicity, priming and facilitation of pathogen recognition. *PLoS ONE* **9**, e87860.

Daniel R, Guest D, 2006. Defence responses induced by potassium phosphonate in *Phytophthora palmivora*-challenged *Arabidopsis thaliana*. *Physiological and Molecular Plant Pathology* **67**, 194–201.

Davidson AL, Blahut-Beatty L, Itaya A, Zhang Y, Zheng S, Simmonds D, 2016. Histopathology of *Sclerotinia sclerotiorum* infection and oxalic acid function in susceptible and resistant soybean. *Plant Pathology* **65**, 878–887.

Dixon RA, Achnine L, Kota P, Liu CJ, Reddy MS, Wang L, 2002. The phenylpropanoid pathway and plant defence – a genomics perspective. *Molecular Plant Pathology* **3**, 371–390.

Eshraghi L, Anderson J, Aryamanesh N, Shearer B, Mccomb J, Hardy GES, O'Brien PA, 2011. Phosphite primed defence responses and enhanced expression of defence genes in *Arabidopsis thaliana* infected with *Phytophthora cinnamomi*. *Plant Pathology* **60**, 1086–1095.

Feng SQ, Zhang Y, Xu JW, Gan L, 2005. Activities of some defense enzymes in *Brassica napus* L. and their relations with resistance to *Sclerotinia sclerotiorum*. *Journal of Huazhong Agricultural University* **24**, 231–235.

Gadaga SJC, Abreu MS, Resende MLV, Ribeiro Júnior PM, 2017. Phosphites for the control of anthracnose in common bean. *Pesquisa Agropecuária Brasileira* **52**, 36–44.

Gay C, Gebicki JM, 2000. A critical evaluation of the effect of sorbitol on the ferric-xylenol orange hydroperoxide assay. *Analytical Biochemistry* **284**, 217–220.

Godoy G, Steadman JR, Dickman MB, Dam R, 1990. Use of mutants to demonstrate the role of oxalic acid in pathogenicity of *Sclerotinia sclerotiorum* on *Phaseolus vulgaris*. *Physiological and Molecular Plant Pathology* **37**, 179–191.

Gozzo F, Faoro F, 2013. Systemic acquired resistance (50 years after discovery): Moving from the lab to the field. *Journal of Agricultural and Food Chemistry* **61**, 12473–12491.

Guo Y, Liu L, Bi Y, 2007. Use of silicon oxide and sodium silicate for controlling *Trichothecium roseum* postharvest rot in Chine cantaloupe (*Cucumis melo* L.). *International Journal of Food Science & Technology* **42**, 1012–1018.

Habig WH, Pabst MJ, Jakoby WB, 1974. Glutathione-S-transferases. The first enzymatic step in mercapturic acid formation. *The Journal of Biological Chemistry* **249**, 7130–7139.

Hammond-Kosack KE, Jones JD, 1996. Resistance gene dependent plant defense responses. *Plant Cell* **8**, 1773–1793.

Harman GR, Hayes CK, Lorito M, Broadway RM, Pietro AD, Peterbauer C, Tronsmo A, 1993. Chitinolytic enzymes of *Trichoderma harzianum*: purification of chitobiosidase and endochitinase. *Phytopathology **83***, 313–318.

Havir EA, MChale NA, 1989. Enhanced – peroxidatic activity in specific catalase isozymes of tobacco, barley, and maize. *Plant Physiology* **91**, 812–815.

Hawerroth C, Araujo L, Rodrigues FA, 2017. Infection process of *Gaeumannomyces graminis* var. *graminis* on the roots and culms of rice. *Journal of Phytopathology* **165**, 692–700.

Heath RL, Packer L, 1968. Photoperoxidation in isolated chloroplast. I Kinetics and stoichometry of fatty acid peroxidation. *Archives of Biochemistry and Biophysics* **125**, 189–198.

Jackson TJ, Burgess T, Colquhoun I, Hardy GES, 2000. Action of the fungicide phosphite on *Eucalyptus marginata* inoculated with *Phytophthora cinnamomi*. *Plant Pathology* **49**, 147–154.

Kar M, Mishra D, 1976. Catalase, peroxidase, and polyphenol oxidase activities during rice leaf senescence. *Plant Physiology* **57**, 315–319.

Keen NT, Yoshikawa M, 1983. β-1,3-endoglucanase from soybean releases elicitor active carbohydrates from fungus cell walls. *Plant Physiology* **71**, 460–465.

King M, Reeve W, Van der Hoek MB, Williams N, McComb J, O'Brien PA, Hardy GE, 2010. Defining the phosphite-regulated transcriptome of the plant pathogen *Phytophthora cinnamomi*. *Molecular Genetics and Genomics* **284**, 425–435.

Kuo MC, Kao CH, 2003. Aluminum effects on lipid peroxidation and antioxidative enzyme activities in rice leaves. *Biologia Plantarum* **46**, 149–152.

Lamb C, Dixon RA, 1997. The oxidative burst in plant disease resistance. *Annual Review of Plant Physiology and Plant Molecular Biology* **48**, 251–275.

Lattanzio V, Lattanzio VMT, Cardinali A, 2006. Role of phenolics in the resistance mechanisms of plants against fungal pathogens and insects. *Phytochemistry* **37**, 23–67.

Leite ME, Santos JB, Ribeiro Júnior PM, Souza DA, Castro LA, Resende MLV, 2014. Biochemical responses associated with common bean defence against *Sclerotinia sclerotiorum*. *European Journal of Plant Pathology* **138**, 391–404.

Lever M, 1972. A new reaction for colorimetric determination of carbohydrates. *Analytical Biochemistry* **47**, 273–279.

Liu P, Li B, Lin M, Chen G, Ding X, Weng Q, 2016. Phosphite-induced reactive oxygen species production and ethylene and ABA biosynthesis mediate the control of *Phytophthora capsici* in pepper (*Capsicum annuum*). *Functional Plant Biology* **43**, 563–574.

Liu F, Wang M, Wen J, Yi B, Shen J, Ma C, Tu J, Fu T, 2015. Overexpression of barley oxalate oxidase gene induces partial leaf resistance to *Sclerotinia sclerotiorum* in transgenic oilseed rape. *Plant Pathology* **64**, 1407–1416.

Lobato MC, Olivieri FP, Daleo GR, Andreu AB, 2010. Antimicrobial activity of phosphites against different potato pathogens. *Journal of Plant Diseases and Protection* **117**, 102–109.

Machinandiarena MF, Lobato MC, Feldman ML, Daleo GR, Andreu AB, 2012. Potassium phosphite primes defense responses in potato against *Phytophthora infestans*. *Journal of Plant Physiology* **169**, 1417–1424.

Malencic D, Kiprovski B, Popovic M, Prvulovic D, Miladinovic J, Djordjevic V, 2010. Changes in antioxidant systems in soybean as affected by *Sclerotinia sclerotiorum* (Lib.) de Bary. *Plant Physiology and Biochemistry* **48**, 903–908.

Malencic D, Vasic D, Popovic M, Devic D, 2004. Antioxidant systems in sunflower as affected by oxalic acid. *Biologia Plantarum* **48**, 243–247.

Miklas PN, Porter LD, Kelly JD, Myers JR, 2013. Characterization of white mold disease avoidance in common bean. *European Journal of Plant Pathology* **135**, 525–543.

Miller GL, 1959. Use of dinitro salicylic acid reagent for determination of reducing sugar. *Analytical Chemistry* **31**, 426–428.

Nakano Y, Asada K, 1981. Hydrogen peroxidase is scavenged by ascorbate specific peroxidases in spinach chloroplasts. *Plant and Cell Physiology* **22**, 867–880.

Percival GC, Banks JM, 2015. Phosphite-induced suppression of *Pseudomonas* bleeding canker (*Pseudomonas syringae* pv. *aesculi*) of horse chestnut (*Aesculus hippocastanum* L.). *Urban Forestry & Urban Greening* **37**, 7–20.

Pereira VF, Resende MLV, Ribeiro Júnior PM, Regina MA, Mota RV, Vitorino LRR, 2012. Fosfito de potássio no controle do míldio da videira e características físico-químicas de uvas Merlot. *Pesquisa Agropecuária Brasileira* **47**, 1581–1588.

Pieterse CM, Leon-Reyes A, Van der Ent S, Van Wees SC, 2009. Networking by small-molecule hormones in plant immunity. *Nature Chemical Biology* **5**, 308–316.

Pinto KMS, Nascimento LC, Gomes ECS, Silva HF, Miranda J, 2012. Efficiency of resistance elicitors in the management of grapevine downy mildew *Plasmopara viticola*: epidemiological, biochemical and economic aspects. *European Journal of Plant Phytopathology* **134**, 745-754.

Polanco LR, Rodrigues FA, Nascimento KJT, Shulman P, Silva LC, Neves FW, Vale FXR, 2012. Biochemical aspects of bean resistance to anthracnose mediated by silicon. *Annals of Applied Biology* **161**, 140–150.

Reuveni M, 1997. Post-infection applications of K_3PO_3, potassium phosphite and dimethomorph inhibit development of downy mildew caused by *Plasmopara viticola* on grapevines. *Journal of Small Fruit & Viticulture* **5**, 27–38.

Reuveni M, Sheglov D, Cohen Y, 2003. Control of moldy-core decay in apple fruits by *β*-aminobutyric acids and potassium phosphites. *Plant Disease* **87**, 933–936.

Rodrigues FA, Jurick II WM, Datnoff LE, Jones JB, Rollins JA, 2005. Silicon influences cytological and molecular events in compatible and incompatible rice-*Magnaporthe grisea* interactions. *Physiological and Molecular Plant Pathology* **66**,144–159.

Silva JL, Souza PE, Alves E, Pinto JEBP, Bertolucci SKV, Freitas MLO, Andrade CCL, Resende MLV, 2015. Essential oil of *Cymbopogon flexuosus*, *Vernonia polyanthes* and potassium phosphite in control of bean anthracnose. *Journal of Medicinal Plants Research* **9**, 243–253.

Silva OC, Santos HAA, Dalla Pria M, May-De Mio LL, 2011. Potassium phosphite for control of downy mildew of soybean. *Crop Protection* **30**, 598–604.

Singh SP, Schwartz HF, 2010. Breeding common bean for resistance to diseases: A review. *Crop Science* **50**, 2199–2223.

Vale FXR, Fernandes Filho EI, Liberato JR, 2003. QUANT: a software plant disease severity assessment. in: Close, R., Braithwaite, M., Havery, I., (Eds.), Proceedings of the 8th International Congress of Plant Pathology. New Zealand, pp. 105.

Vieira RF, Paula Júnior TJ, Carneiro JES, Teixeira H, Queiroz TFN, 2012. Management of white mold in type III common bean with plant spacing and fungicide. *Tropical Plant Pathology* **37**, 95–101.

Vieira RF, Paula Júnior TJ, Teixeira H, Carneiro JES, 2010. White mold management in common bean by increasing within-row distance between plants. *Plant Disease* **94**, 361–367.

Williams B, Kabbage M, Kim HJ, Britt R, Dickman MB, 2011. Tipping the balance: *Sclerotinia sclerotiorum* secreted oxalic acid suppresses host defenses by manipulating the host redox environment. *PLOS Pathogens* **7**, e1002107.

Wu CT, Bradford KJ, 2003. Class I chitinase and *β*-1,3-glucanase are differentially regulated by wounding, methyl jasmonate, ethylene, and gibberellin in tomato seeds and leaves. *Plant Physiology* **133**, 263–273.

Yarden O, Veluchamy S, Dickman MB, Kabbage M, 2014. *Sclerotinia sclerotiorum* catalase SCAT1 affects oxidative stress tolerance, regulates ergosterol levels and controls pathogenic development. *Physiological and Molecular Plant Pathology* **85**, 34–41.

Zhou F, Liang HJ, Di YL, You H, Zhu FX, 2014. Stimulatory effects of sublethal doses of dimethachlon on *Sclerotinia sclerotiorum*. *Plant Disease* **98**, 1364–1370.

Zhou J, Sun A, Xing D, 2013. Modulation of cellular redox status by thiamine-activated NADPH oxidase confers *Arabidopsis* resistance to *Sclerotinia sclerotiorum. Journal of Experimental Botany* **64**, 3261–3272.

Zieslin N, Ben-Zaken R, 1993. Peroxidase activity and presence of phenolic substances in peduncles of rose flowers. *Plant Physiology and Biochemistry* **31**, 333–339.

Zucker M, 1965. Induction of phenylalanine deaminase by light and its relation to chlorogenic acid synthesis in potato tuber tissue. *Plant Physiology* **40**, 779–784.

Table 1. Analysis of variance of the effects of foliar treatments (FT), plant inoculation (PI), evaluation time (ET) and their interactions for lesion area (LA), white mold severity (WMS), activities of superoxide dismutase (SOD), catalase (CAT), peroxidase (POX), ascorbate peroxidase (APX), glutathione-*S*-transferase (GST), chitinase (CHI), β-1,3-glucanase (GLU), phenylalanine ammonia-lyase (PAL), polyphenoloxidase (PPO) and lipoxygenase (LOX) and for the concentrations of oxalic acid (OA), superoxide (O_2^-), hydrogen peroxide (H_2O_2) malondialdehyde (MDA), total soluble phenolics (TSP) and lignin-thioglycolic acid (LTGA) derivatives.

Variables	FT	PI	ET	FT × PI	FT × ET	PI × ET	FT × PI × ET
LA	<0.001	-	<0.001	-	<0.001	-	-
WMS	<0.001	-	<0.001	-	<0.001	-	-
SOD	0.003	<0.001	<0.001	0.148	<0.001	<0.001	<0.001
CAT	0.084	0.025	<0.001	0.844	0.059	<0.001	0.318
POX	0.005	<0.001	<0.001	0.003	<0.001	<0.001	<0.001
APX	<0.001	<0.001	<0.001	0.007	<0.001	<0.001	<0.001
GST	0.003	<0.001	<0.001	0.068	<0.001	<0.001	<0.001
CHI	<0.001	<0.001	<0.001	<0.001	<0.001	<0.001	<0.001
GLU	0.001	<0.001	0.069	<0.001	0.164	<0.001	0.125
PAL	<0.001	<0.001	<0.001	<0.001	<0.001	<0.001	<0.001
PPO	<0.001	<0.001	0.075	<0.001	0.001	0.008	0.001
LOX	<0.001	<0.001	0.062	<0.001	<0.001	0.033	<0.001
OA	<0.001	<0.001	<0.001	<0.001	<0.001	<0.001	<0.001
O_2^-	<0.001	<0.001	<0.001	<0.001	<0.001	<0.001	<0.001
H_2O_2	<0.001	<0.001	<0.001	<0.001	<0.001	<0.001	<0.001
MDA	0.012	<0.001	<0.001	<0.001	0.079	<0.001	0.036
TSP	0.119	<0.001	<0.001	<0.001	<0.001	<0.001	<0.001
LTGA	<0.001	<0.001	<0.001	0.001	0.345	<0.001	0.199

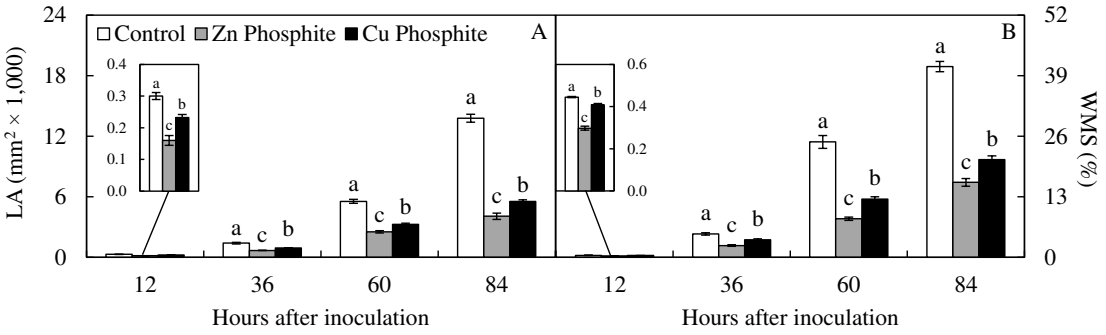

Fig. 1. Lesion area (LA) (A) and white mold severity (WMS) (B) evaluated on the

leaflets of common bean plants that were non-sprayed (control) or sprayed with zinc (Zn) or copper (Cu) phosphites and inoculated with *Sclerotinia sclerotiorum*. For each evaluation time, means from each treatment followed by different letters are significantly different ($P \leq 0.05$) based on Tukey's test. Bars represent the standard error of the means. $n = 4$.

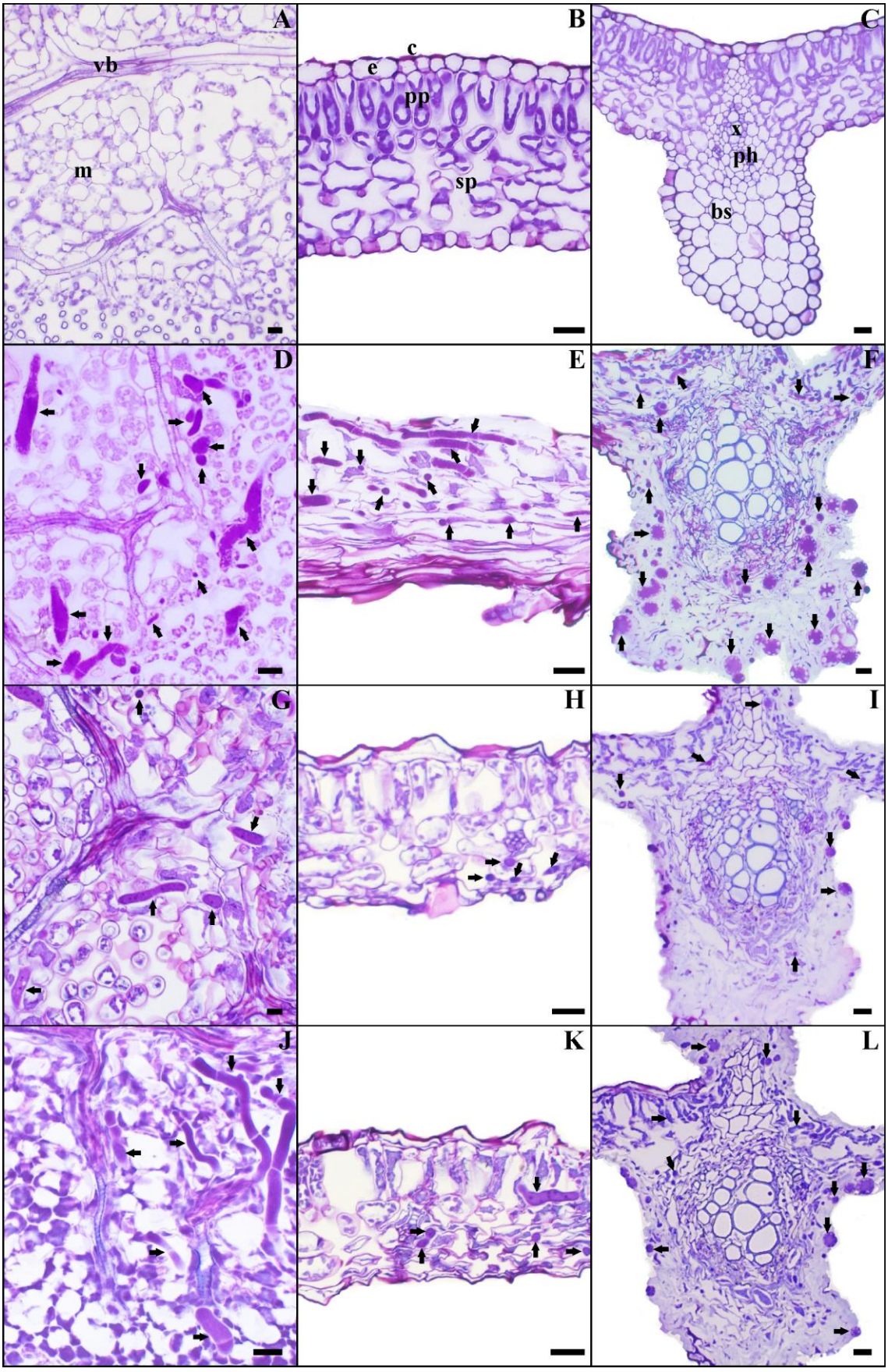

Fig. 2. Light micrographs of longitudinal (A, B, D, E, G, H, J and K) and transverse (C, F, I and L) sections of leaflets of common bean plants that were non-inoculated

(A, B and C) or inoculated with *Sclerotinia sclerotiorum* (84 hours after inoculation) and non-sprayed (control) (D, E and F) or sprayed with zinc (G, H and I) or copper (J, K and L) phosphites. Arrows represent leaflet tissue colonized by *Sclerotinia sclerotiorum* hyphae. vb: vessel bundle, m: mesophyll, c: cuticle, e: epidermal cells, pp: palisade parenchyma cells, sp: spongy parenchyma; x: xylem, ph: phloem, bs: bundle sheath. Scale bars: 20 μm.

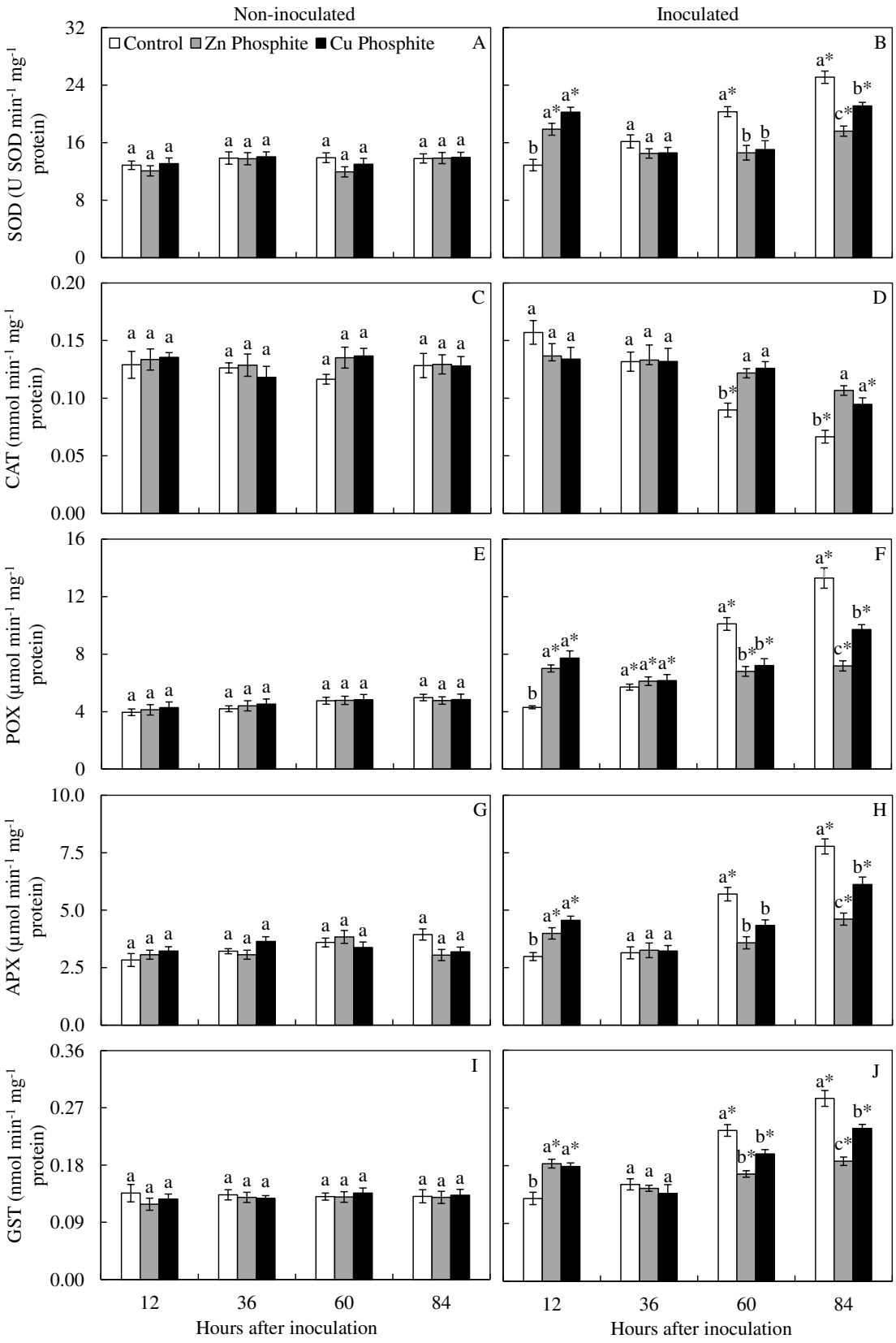

Fig. 3. Activities of superoxide dismutase (SOD) (A and B), catalase (CAT) (C and D), peroxidase (POX) (E and F), ascorbate peroxidase (APX) (G and H) and glutathione-*S*-transferase (GST) (I and J) determined on the leaflets of common bean

plants that were non-inoculated (A, C, E, G and I) or inoculated (B, D, F, H and J) with *Sclerotinia sclerotiorum* and non-sprayed (control) or sprayed with zinc (Zn) or copper (Cu) phosphites. For each evaluation time, means from each treatment followed by different letters and for non-inoculated and inoculated plants for each treatment followed by an asterisk (*) are significantly different ($P \leq 0.05$) based on Tukey's test. Bars represent the standard error of the means. $n = 4$.

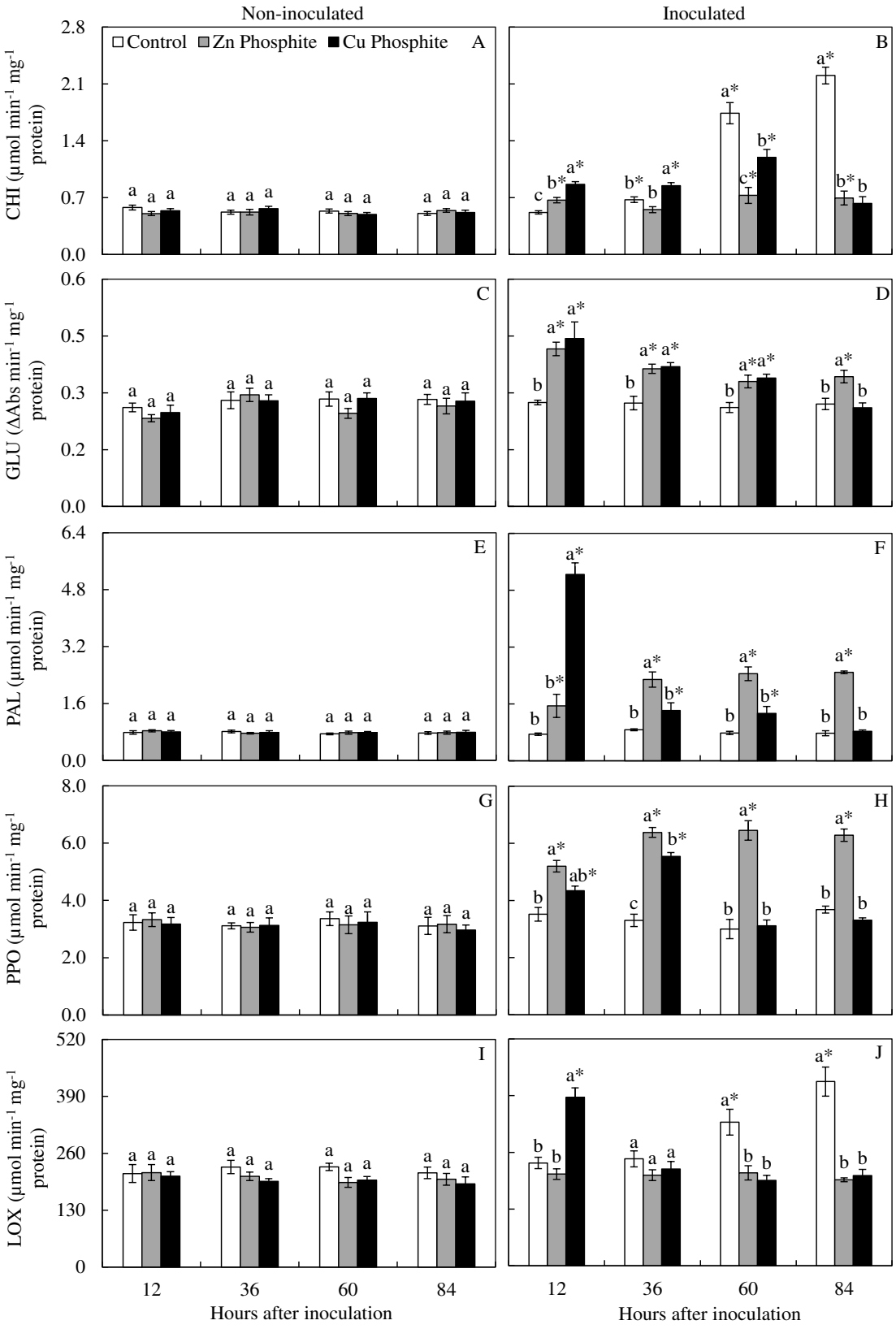

Fig. 4. Activities of chitinase (CHI) (A and B), *β*-1,3-glucanase (GLU) (C and D), phenylalanine ammonia-lyase (PAL) (E and F), polyphenoloxidase (PPO) (G and H) and lipoxygenase (LOX) (I and J) determined on the leaflets of common bean plants

that were non-inoculated (A, C, E, G and I) or inoculated (B, D, F, H and J) with *Sclerotinia sclerotiorum* and non-sprayed (control) or sprayed with zinc (Zn) or copper (Cu) phosphites. For each evaluation time, means from each treatment followed by different letters and for non-inoculated and inoculated plants for each treatment followed by an asterisk (*) are significantly different ($P \leq 0.05$) based on Tukey's test. Bars represent the standard error of the means. $n = 4$.

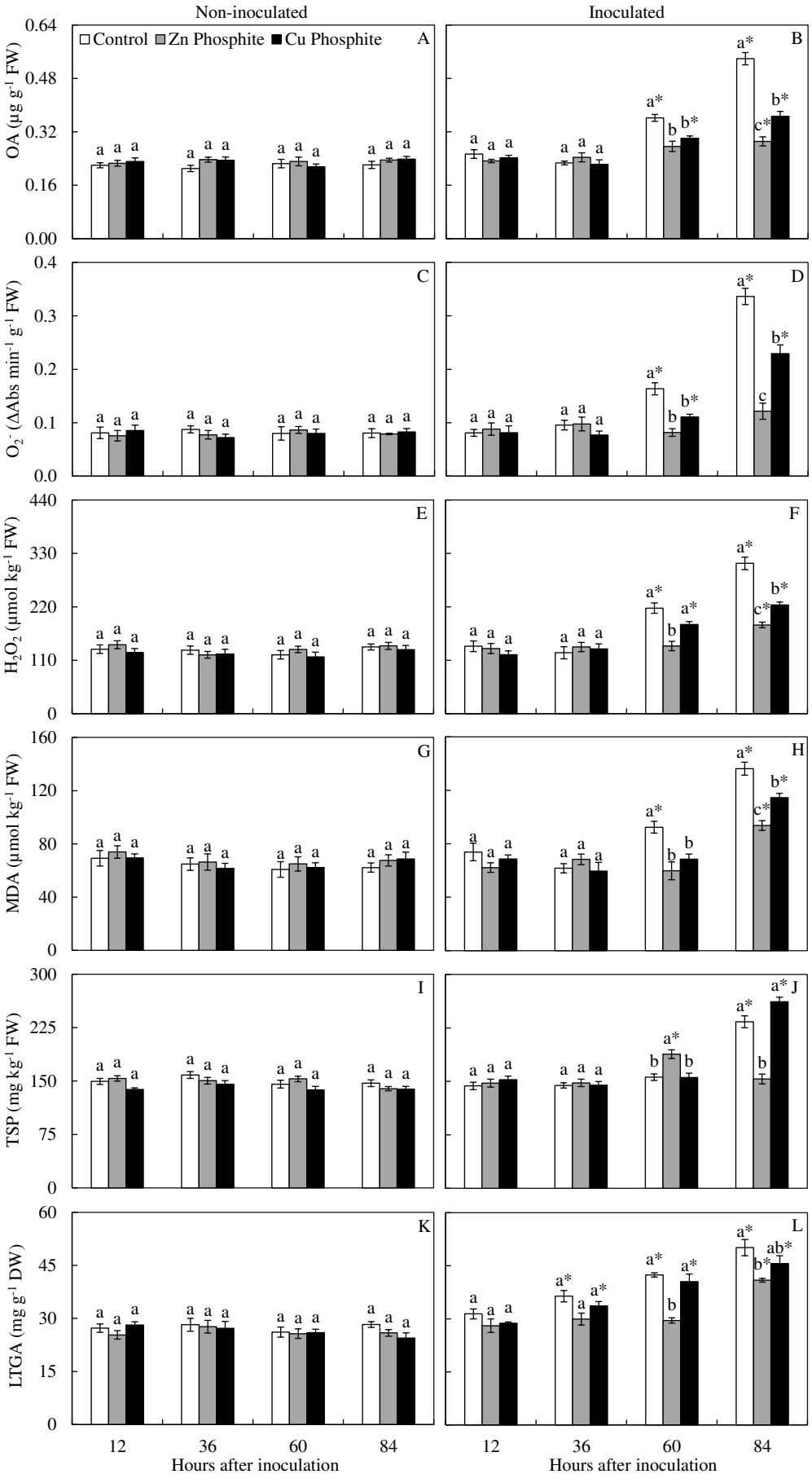
Non-inoculated
Inoculated
Control
Zn Phosphite
Cu Phosphite
A
B
C
D
E
F
G
H
I
J
K
L
OA (µg g-1 FW)
O2- (ΔAbs min-1 g-1 FW)
H2O2 (µmol kg-1 FW)
MDA (µmol kg-1 FW)
TSP (mg kg-1 FW)
LTGA (mg g-1 DW)
0.64
0.48
0.32
0.16
0.00
0.4
0.3
0.2
0.1
0.0
440
330
220
110
0
160
120
80
40
0
300
225
150
75
0
60
45
30
15
0
12
36
60
84
Hours after inoculation

Fig. 5. Concentrations of oxalic acid (OA) (A and B), superoxide (O_2^-) (C and D), hydrogen peroxide (H_2O_2) (E and F), malondialdehyde (MDA) (G and H), total soluble phenols (TSP) (I and J) and lignin-thioglycolic acid (LTGA) derivatives (K and L) determined on the leaflets of common bean plants that were non-inoculated (A, C, E, G, I and K) or inoculated (B, D, F, H, J and L) with *Sclerotinia sclerotiorum* and non-sprayed (control) or sprayed with zinc (Zn) or copper (Cu) phosphites. For each evaluation time, means from each treatment followed by different letters and for non-inoculated and inoculated plants for each treatment followed by an asterisk (*) are significantly different ($P \leq 0.05$) based on Tukey's test. FW = fresh weight and DW = dry weight. Bars represent the standard error of the means. $n = 4$.

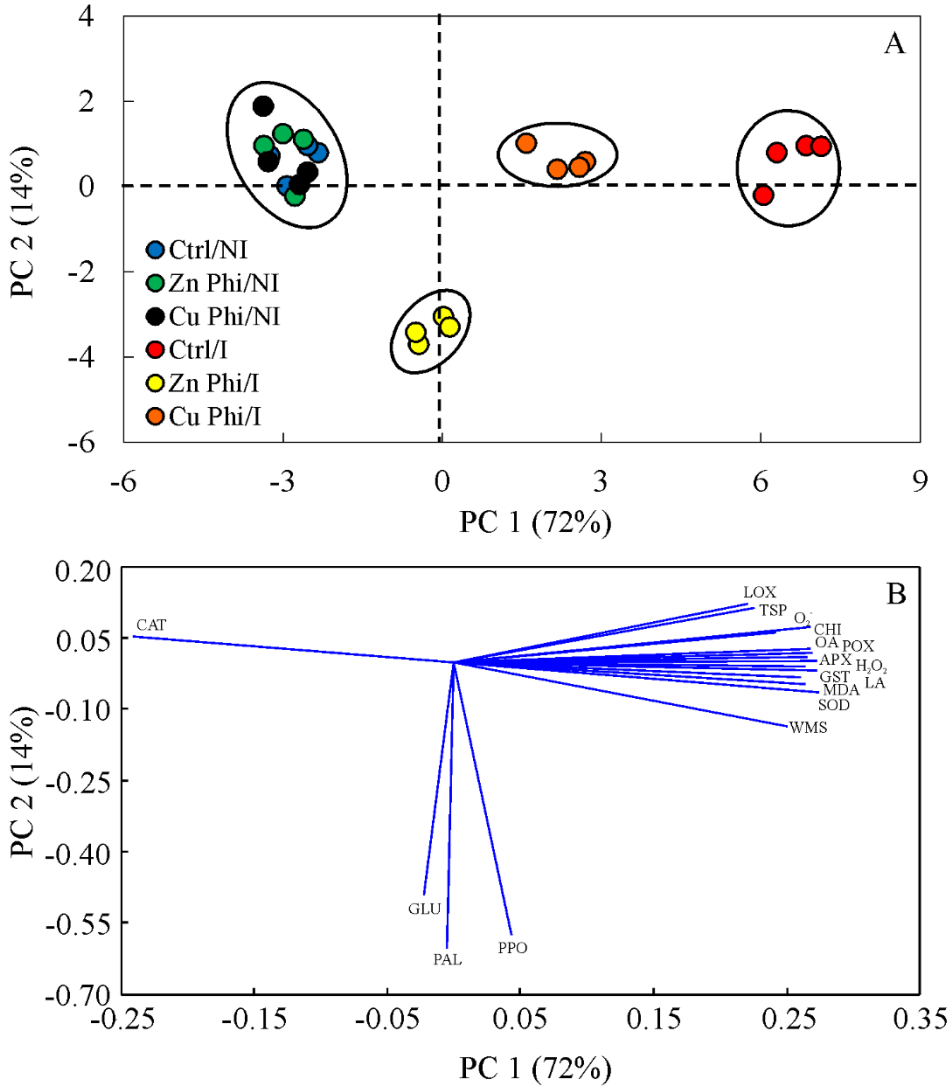

Fig. 6. Score (A) and loading (B) plots of the principal component analysis comparing lesion area (LA), white mold severity (WMS), activities of superoxide dismutase (SOD), catalase (CAT), peroxidase (POX), ascorbate peroxidase (APX), glutathione-*S*-transferase (GST), chitinase (CHI), *β*-1,3-glucanase (GLU), phenylalanine ammonia-lyase (PAL), polyphenoloxidase (PPO) and lipoxygenase (LOX) and the concentrations of oxalic acid (OA), superoxide (O_2^-), hydrogen peroxide (H_2O_2) malondialdehyde (MDA), total soluble phenols (TSP) and lignin-thioglycolic acid (LTGA) derivatives on the leaflets of common bean plants that were non-inoculated (NI) or inoculated (I) with *Sclerotinia sclerotiorum* and non-sprayed (Ctrl) or sprayed with zinc (Zn Phi) or copper (Cu Phi) phosphites.

CHAPTER 4

A set of standard area diagrams to assess white mold severity on the leaflets of common beans

Abstract

The fungus *Sclerotinia sclerotiorum* is the major pathogen affecting common beans yield worldwide and an adequate disease quantification is demanded in some trials. However, a set of standard area diagrams (SADs) to aid visual assessment of severity of white mold (SWM) is lacking. This study developed SADs consisting of eight color images of diseased leaflets with severity values that ranged from 0.4 to 53.7%. Twenty raters [10 experienced (ER) and 10 inexperienced (IR)] validated the SADs by assessing the same set of 50 images twice, the first without SADs and the second using it as an aid. The SADs significantly improved both accuracy and precision for IR as evidenced by increases from 0.86 to 0.98 in the coefficients of bias (C_b) from 0.93 to 0.98 in correlation coefficient (r) and from 0.86 to 0.96 in overall agreement [Lin's concordance correlation coefficients (ρ_c)] without and with SADs, respectively, whereas for ER only precision (r) was improved by SADs. The SWM estimates were also more reliable because inter-rater reliability (coefficient of determination, R^2) was significantly increased for both ER and IR by using SADs. Therefore, the SADs presented is thought to be a valuable tool to provide accurate, precise and reliable estimates of the SWM on common bean leaflets in epidemiological studies, evaluation of disease control methods, assessment of aggressiveness of pathogen isolates, disease resistance and other types of surveys regarding the common beans-*S. sclerotiorum* interaction.

Keywords *Phaseolus vulgaris* · *Sclerotinia sclerotiorum* · Disease assessment · Disease severity · Epidemiology · Phytopathometry

Introduction

The fungus *Sclerotinia sclerotiorum* (Lib.) de Bary, the causal agent of white mold, is one of the most devastating and cosmopolitan pathogens worldwide (Bolton et al., 2006). The pathogen has a wide range of hosts, infecting over 400 plant species from several botanical families, including economically important crops such as common beans and soybeans (Boland and Hall, 1994). The annual losses caused by *S. sclerotiorum* reach millions of dollars, causing yield losses ranging from 20 to 100% (Steadman and Boland, 2005; Bolton et al., 2006; Schwartz and Singh, 2013).

In common beans, white mold symptoms begin as wilting; afterwards, leaflets, stems and pods display water-soaked spots that are light-brown in color and soft in consistency and quickly expands forming necrotic lesions, on which a cottony fungal mycelium can be observed (Purdy, 1979; Steadman, 1983). White mold epidemics are favored by high plant density, long rainy periods, mild temperatures (< 20ºC) and high relative humidity (> 70%) (Purdy, 1979). White mold can occur at any growth stage of common beans plants, but the flowering growth stage is the most critical period for disease epidemics; at this phase, the high foliar index makes the microclimate highly favorable to *S. sclerotiorum* (Steadman, 1983).

Some control methods including chemical (Mueller et al., 2002; Vieira et al., 2012), genetic (Lehner et al., 2015), cultural and biological control (Singh and Schwartz, 2010) have been adopted for white mold management. Disease quantification plays a critical role to assess the efficacy of methods for disease control (Madden et al., 2007) and must be accurate, precise and reliable (Nutter and Schultz, 1995; Madden et al., 2007). Accuracy measures the degree of closeness between the estimates and the actual severity (Nutter and Schultz, 1995; Madden et al., 2007); precision is a measure of similarity within estimates/measurements obtained by the same rater (intra-rater

precision or reliability) (Madden et al., 2007) as well as under different conditions, raters or methods (inter-rater precision or reproductibility) (Nutter et al., 1993; Madden et al., 2007).

The standard area diagram (SAD) is a standardized method to disease quantification and it has been used as a tool to estimate disease severity, an essential variable in phytopathometry (Del Ponte et al., 2017). The use of the SADs has demonstrated that inexperienced raters are more benefited in terms of accuracy and precision when compared with estimates made without SADs (Duarte et al., 2013; Rios et al., 2013; Braido et al., 2014; González-Domínguez et al., 2014; Vieira et al., 2014; Debona et al., 2015; Dolinski et al., 2017). Data analysis of SADs efficacy can be performed by linear regression or Lin's concordant correlation coefficient (LCCC) method (Lin, 1989; Madden et al., 2007; Bock et al., 2010). The meta-analysis of 105 studies (127 SADs) over the last 25 years of the scientific impact of the SADs demonstrated that there is a current trend to use LCCC analysis (Del Ponte et al., 2017), which was suggested to be a more robust statistic than the linear regression method (Bock et al., 2010; Del Ponte et al., 2017).

The white mold intensity has been estimated mostly through incidence (Hoffman et al., 1998; Yang et al., 1999; del Río et al., 2007; Lenher et al., 2017), but severity is assessed in some cases (Madden et al., 2007). Although severity is commonly estimated using an ordinal rating scale (Hall and Phillips, 1996; Kolkman and Kelly, 2002), this method is little informative and can have a major impact on data analysis (Madden et al., 2007). Some studies regarding the efficacy of measures for white mold control, aggressiveness of *S. sclerotiorum* isolates and other aspects of the disease in different hosts have been performed through pathogen inoculation on the leaflets under controlled conditions (Lenher et al., 2016; Arfaoui et al., 2016). SADs have been

employed to assess the resistance of soybean cultivars to white mold, but such SADs were not validated (Garcia and Juliatti, 2012). The lack of a standardized and validated method for disease quantification may result in inaccurate disease assessment, thus leading to mistaken conclusions and recommendations, with catastrophic consequences for the growers (Madden et al., 2007).

Considering that some experiments have been carried out under controlled conditions by inoculating common beans leaflets with *S. sclerotiorum*, and the lack of SADs to assess the severity of white mold (SWM), the present study aimed: i) to develop SADs to quantify SWM in common bean leaflets and ii) to determine the effect of SADs and rater experience in accuracy, precision and reliability of the estimates of SWM.

Materials and methods

Plant growth

A total of five seeds of common beans from cultivar Pérola, susceptible to *S. sclerotiorum*, were sown in plastic pots of 2 liters containing 2 kg of Tropstrato® substrate (Vida Verde, Mogi Mirim, São Paulo, Brazil) composed of a mixture of pine bark, peat and expanded vermiculite (1:1:1). Each pot was thinned to three seedlings seven days after emergence. Plants were kept in a greenhouse (30 ± 5ºC, 65 ± 5% relative humidity and natural photosynthetically active radiation of 900 ± 15 µmol photons m^{-2} s^{-1}). Plants were fertilized weekly with 100 ml of a modified nutrient solution based on Clark (1975) as it follows: 0.8 mM KNO_3, 0.069 mM $NH_4H_2PO_4$, 1 mM NH_4NO_3, 1 mM $Ca(NO_3).4H_2O$, 0.9 mM KCl, 0.6 mM $MgSO_4$ $7H_2O$, 0.5 µM $CuSO_4$ $5H_2O$, 2 µM $ZnSO_4$ $7H_2O$, 19 µM H_3BO_3, 7 µM $MnCl_2$ $4H_2O$, 0.6 µM Na_2MoO_4 $4H_2O$, 60 µM $FeSO_4$ $7H_2O$ and 90 µM disodium ethylenediaminetetraacetic acid (EDTA). Plants were watered with deionized water as needed.

Inoculum production and inoculation procedure

The isolate CMES 1465 of *S. sclerotiorum* obtained from common bean, provided by EMBRAPA Soybean (Londrina, Paraná State, Brazil), was used to inoculate the plants. The isolate was preserved as sclerotia; for their production, carrots were washed, peeled, cut in cubes of approximately 1 × 1 × 1 cm, transferred to Erlenmeyer flasks and autoclaved at 121°C for 20 min (Bae and Knudsen, 2007). For inoculum production, a sclerotium was transferred to each Petri dish containing potato-dextrose-agar (PDA) medium and kept in a growth chamber (20°C and 12 h photoperiod).

The three leaflets of the third leaf, from the base to the top, of each plant (V3 growth stage) were inoculated with a plug (5 mm in diameter) of PDA medium obtained from the edge of seven-days-old colony of *S. sclerotiorum*. Each PDA plug was placed between the main vein and the edge of each leaflet and gently pressed with the forefinger. Inoculated plants were transferred to a plastic mist growth chamber inside a greenhouse for the duration of the experiments. The temperature inside the MGC ranged from 20 ± 2°C (day) to 17 ± 2°C (night) and the relative humidity was kept at 92 ± 3% using a misting system spraying mist every 30 min above the plant canopy. A thermohygrograph (TH-508; Impac) was used to measure both relative humidity and temperature. At plant canopy height, the maximum natural photon flux density was approximately 900 µmol $m^{-2}s^{-1}$.

Development and evaluation of the SADs

A total of 150 leaflets, with a range of white mold severities, were collected at 12, 24, 36, 48, 72 and 84 hours after inoculation (hai) and individually scanned to obtain images with a resolution of 300 dpi. These images were processed and the actual SWM was determined using QUANT software (Vale et al., 2003). The minimum and

maximum SWM on the leaflets were obtained and following increases approximately linear, six additional, intermediate values of SWM, were established for a set of eight images. The common beans leaflets that contained the respective SWM were used as templates to obtain the diagrams that comprised the SADs. The typical symptoms of necrosis were included on the SADs.

Each image of the 50 white mold-diseased leaflets set was inserted as an individual slide in a Microsoft Powerpoint file for evaluation. The same images were assessed by a group of 20 raters (10 inexperienced and 10 experienced). Raters that received previous formal training and practice in SWM assessment and were familiar with the white mold symptoms were classified as experienced. Raters had no formal training or familiarity with white mold symptoms were considered as the inexperienced ones. A total of 50 digital images of the white mold-diseased leaflets, in a random order, were projected for 15 s for each group. In the first assessment, the raters did not use the SADs as an aid to estimate SWM. Two weeks later, the same raters made a second assessment using the SADs as an aid to estimate SWM using the same set of images. To evaluate each leaflet, the rater compared its image with the SADs to obtain a new SWM estimate. Before performing both evaluations, the raters received the information to consider only the symptoms of necrosis of the lesions and visually estimated the percentage of diseased area related to total leaflet area for each image.

Data analyses

The agreement between the estimated and the actual white mold severity for each rater, based on the data obtained during the SADs validation, was determined using the Lin's concordance correlation coefficient (LCCC) (ρ_c) (Lin, 1989). The analysis was

performed separately using the data obtained with and without the use of the SADs for both inexperienced and experienced raters.

Considering both accuracy and precision of the ρ_c analysis, it was used to assess the fit of pairs of observations to the line of concordance (45°) as follow: $\rho_c = C_b \, . \, r$. In this case, C_b equals the bias correction factor that measures how far the best-fit line deviates from 45° and is a measure of bias or accuracy while the r equals the correlation coefficient between the estimated severity (Y) and the actual severity (X), which measures, in this case, the precision of the best-fit line. C_b is the bias correction factor and is derived from the following equation: $C_b = 2/[(\upsilon + 1/\upsilon + \mu^2)]$, where $\upsilon = \sigma_y / \sigma_x$, and σ_y and σ_x are the standard deviations of Y and X, respectively, and where $\mu = (\mu_y - \mu_x) / \sqrt{(\sigma_y \, . \, \sigma_x)}$ and μ_y and μ_x are the mean values of Y and X, respectively. The term υ measures the difference between actual and estimated values of the SADS, which is defined by the difference in the slopes of the two lines. Equal slopes would have a υ of 1. The term μ is a reflection of a location shift relative to the SADs, primarily reflecting height differences in the lines. Equal heights would have a μ of 0. A perfectly accurate measurement occurs when the points are on the concordance line (*e.g.*, $r = 1$, $C_b = 1$ [$\upsilon = 1$, $\mu = 0$] and thus, $\rho_c = 1$) (Bock et al., 2010; Nita et al., 2003).

The differences between the means (i.e., with SADS minus without SADS) for all parameters analyzed (r, C_b, υ, μ and ρ_c) were calculated and an equivalence test was used to test their significance (Yi et al., 2008; Bardsley and Ngugi, 2013; Yadav et al., 2013). The equivalence test was used to calculate the 95% confidence intervals (CIs) for each statistic (the difference between the means) by bootstrapping using the percentile method (with an equivalence test, the null hypothesis is the converse of H_0, *e.g.,* the null hypothesis is non-equivalence). All analyses were based on 2,000 balanced bootstrap samples using and the 95% CIs that were calculated on the difference between the

means of the groups. If the CIs spanned zero, there was no significant difference (P = 0.05). Precision was also determined using analysis of the absolute error (estimated SWM minus actual SWM).

The coefficient of determination (R^2) from linear regression analyses of relationships between severity estimates for all pairs of raters was used to determine the inter-rater reliability of the estimates (Nutter and Schultz, 1995). All statistical analyses were performed using R (R Core Team 2013). The epi.ccc function of the epiR package (Stevenson, 2012) was used to obtain LCC statistics. The built-in boot.sample R function was used for the hypothesis test.

Results

White mold symptoms on common beans leaflets began as water-soaked spots; as lesions expanded, light-brown-colored spots that were soft in consistency formed quickly (Fig. 1). Moreover, a mycelial fungal growth with cottony appearance developed on lesions and intense chlorosis were observed on leaflets displaying high SWM (~ 40%). SADs developed in the present study was comprised of eight color white mold-diseased common beans leaflet images, each of a known severity value ranging from 0.4 to 53.7% (Fig. 2).

The estimated approached the actual SWM severity, based on the Lin's concordance analysis, by using SADs regardless of the raters´ experience. Independently of the raters´s category, the relationship between estimated and actual SWM was linear. A significant improvement for most bias and accuracy statistics of Lin's concordance correlation coefficient (C_b, ρ_c and r) for inexperienced raters and only for r for experienced raters was achieved by using SADs (Table 1). The scale and location shift (υ and μ) were not significantly improved by SADs regardless of the raters´ category.

By using SADs, the proportion of raters with υ values between 0.90 and 1.10 and with μ values between -0.10 and 0.26 increased from 25 to 80% and from 40 to 95%, respectively indicating, therefore, the occurrence of repeatability.

Accuracy (C_b) was significantly increased when inexperienced raters used SADs (Table 1). Accuracy for inexperienced raters ranged from 0.68 to 0.95 (mean of 0.86) and from 0.97 to 1.00 (mean of 0.98) without and with SADs, respectively. The proportion of raters with accuracy > 0.95 was increased from 65 to 100% with the use of SADs (Fig. 3c).

Precision (r) ranged from 0.82 to 0.97 (mean of 0.93) and from 0.94 to 0.98 (mean of 0.96) for inexperienced and experienced raters, respectively, without using SADs (Table 1). On the other hand, both inexperienced [0.94 to 0.99 (mean of 0.98)] and experienced raters [0.97 to 0.99 (mean of 0.98)] had their precision improved by using SADs. A gain in precision was obtained by using SADs considering that the proportion of raters with r > 0.95 was 65 and 95% without and with its use, respectively (Fig. 3d).

The use of SADs significantly improved agreement (ρ_c), which combines measures of both accuracy and precision, for inexperienced raters (Table 1). For inexperienced raters not using SADs, ρ_c ranged from 0.61 to 0.95 (mean of 0.81), but with its use, ρ_c ranged from 0.93 to 0.99 (mean of 0.96). The proportion of raters with a ρ_c value > 0.90 (55 and 100% without and with the SADs aid, respectively) increased due to an improvement on ρ_c (Fig. 3e).

The increase in precision was reflected in the reduction in absolute errors when raters used SADs, and was particularly evident for inexperienced raters (Fig. 4) When estimates were made without SADs, 70% of the raters had error > 15% at least in one estimate. When SADs were used as an aid to estimate SWM, the errors were consistently < 11%.

The inter-rater reliability was greatly improved by using SADs regardless of the raters´s experience (Table 2). The R^2 values ranged from 0.57 to 0.92 (mean of 0.77) and from 0.58 a 0.93 (mean of 0.83) for inexperienced and experienced rates, respectively, not using SADs. On the other hand, R^2 ranged from 0.84 to 0.97 (mean of 0.92) and from 0.90 to 0.97 (mean of 0.95), respectively, for inexperienced and experienced raters that used SADs. A total of 90% of the rater pairwise comparisons had R^2 <0.90 without the use of SADs while 16% of the pairwise comparisons had R^2 < 0.90 using it indicating, therefore, a gain in inter-rater reliability irrespective of the rater´s experience (Fig. 3f).

Without SADs, experienced raters had less bias and better accuracy, precision, agreement and inter-rater reliability (C_b, r, ρ_c and R^2, respectively) compared to inexperienced raters (Table 2). However, when the experienced raters used SADs, only the inter-rater reliability (R^2) was significantly improved compared to inexperienced raters. Although estimates of severity were improved with the SADs aid for most raters regardless of their experience, the biggest reduction in bias and gains in accuracy, precision, agreement and inter-rater reliability were obtained for inexperienced raters (Fig. 5).

Discussion

Previous studies have demonstrated that the use of SADs improves accuracy and precision of estimates of disease severity, including soybean frogeye leaf spot (Debona et al., 2015), peach rust (Dolinski et al., 2017), wheat blast (Rios et al., 2013), tomato powdery mildew (Lage et al., 2015), corn leaf blight (Vieira et al., 2014), orange citrus canker (Braido et al., 2014) and loquat scab (González-Domínguez et al., 2014). In spite of white mold intensity under field conditions has been usually assessed based on

incidence, mostly of the experiments performed under controlled conditions, when *S. sclerotiorum* is inoculated on leaves, has quantified disease severity, even though SADs has not been developed to this specific purpose. To the best of the authors' knowledge, this is the first report of SADs developed and validated to estimate SWM on common beans leaflets. The SADs from the present study were proved to improve accuracy, precision and reliability of the estimates of SWM, being a valuable tool to be used in further studies that require disease quantification.

SADs herein proposed have eight color images of diseased leaflets, a similar number that has been used for SADs developed to assess other diseases (Debona et al., 2015; González-Domínguez et al., 2015; Vieira et al., 2014). Based on SADs that were validated previously (Debona et al., 2015; González-Domínguez et al., 2015; Rios et al., 2013), the eight levels of severity of the SADs from the present study followed linear increases. SADs had severities that ranged from 0.4 to 53.7%; above the latter value leaflet abscission was observed. Accordingly, SADs developed, but not validated, for assessment of white mold in soybean had a maximum severity of 50% (Garcia and Juliatti, 2012). Therefore, the range of severity represented in the SADs from the present study is believed to be quite adequate to obtain accurate and fast estimates of SWM on common bean leaflets.

It was observed that irrespective of the rater experience, most raters overestimated SWM on common beans leaflets in the absence of SADs. Despite raters that did not use SADs as an aid underestimated disease severity in some studies (Duarte et al., 2013; González-Domínguez et al., 2014), overestimation is a more common phenomenon (Debona et al., 2015; Dolinski et al., 2017), consistently with the results from the present study. It was also observed a tendency of overestimation when raters used SADs, but overestimates were greatly reduced in comparison to the absence of SADs,

corroborating with previous findings (Lenz et al., 2010; Capucho et al., 2011; Yadav et al., 2013; Domiciano et al., 2014). Aiming to reduce errors of the estimates of disease severity, computer-based training of the raters and use of SADs have been suggested to improve the accuracy of disease estimates (Nutter and Schultz, 1995). The results from the present study showed that SADs decreased absolute errors of the estimates, which was particularly evident for the inexperienced raters.

The parameters scale shift (υ) and location shift (μ) were not significantly improved with the use of SADs regardless of the rater experience. This result probably occurred because even when SADs were not adopted, the slope and height of the plotted line approached the concordance line, supporting the results found for SADs proposed to quantify loquat scab severity (González-Domínguez et al., 2014). On the other hand, the equivalence test showed that other measurements of accuracy and precision (r, C_b and ρ_c) were all improved by using SADs for the inexperienced raters, whereas for the experienced raters only precision (r) was improved with the use of SADs. Indeed, inexperienced raters had greater gains in accuracy and precision with the use of SADs. Inexperienced raters have been shown to be more benefited by the use of SADs than inexperienced raters (Duarte et al., 2013; Rios et al., 2013; Braido et al., 2014; González-Domínguez et al., 2014; Vieira et al., 2014; Debona et al., 2015; Dolinski et al, 2017). Interestingly, the inter-rater coefficient of determination (R^2) was significantly improved with the used of SADs as an aid irrespective of the rater experience. Without using the SADs, R^2 was lower than 0.90 for 90% of the inter-rater pairwise comparisons, whereas in the presence of the SADs 84% of the inter-rater pairwise comparisons displayed R^2 higher than 0.90, indicating that SADs increased the uniformity of the assessments. Similarly, SADs proposed and validated in other studies improved accuracy, precision and reliability of the estimates of disease severity (Braido

et al., 2014; González-Domínguez et al., 2014; Vieira et al., 2014; Debona et al., 2015; Dolinski et al., 2017).

The accuracy and precision of disease estimates are affected by rater experience regardless of the use of SADs (Yadav et al., 2013; Debona et al., 2015; Dolinski et al., 2017). The findings from the present study showed that experienced raters were more accurate and precise than the inexperienced raters when SADs were not used as indicated by significant differences between the two groups for the statistics of the parameters C_b, r and ρ_c. With the use of SADs, however, such differences were negligible, evidencing that SADs made the inexperienced raters as accurate and precise as the experienced raters confirming, therefore, previous reports (Yadav et al., 2013; González-Domínguez et al., 2014).

The SADs from the present study were demonstrated to improve accuracy, precision and reliability of the estimates of SWM on common bean leaflets. Therefore, they should be a valuable tool for epidemiological studies, evaluation of the efficacy of methods for white mold control, evaluation of aggressiveness of *S. sclerotiorum* isolates, disease resistance and other studies regarding common bean- *S. sclerotiorum* interaction.

Acknowledgements

Professor F. A. Rodrigues thanks the Conselho Nacional de Desenvolvimento Científico e Tecnológico (CNPq) for his fellowship. Ms. I. R. F. Fagundes-Nacarath was supported by CNPq. We thank EMBRAPA Soybean for providing the isolate of *Sclerotinia sclerotiorum* used in this study. This study was supported by grants from CAPES, CNPq and FAPEMIG to Prof. F. A. Rodrigues.

References

Arfaoui, A., El Hadrami, A., Adam L. R., Daayf, F., 2016. Pre-treatment with calcium enhanced defense-related genes' expression in the soybean's isoflavones pathway in response to *Sclerotinia sclerotiorum*. Physiol. Mol. Plant Pathol. 93, 12–21.

Bae, Y. S., Knudsen, G. R., 2007. Effect of sclerotial distribution pattern of *Sclerotinia sclerotiorum* on biocontrol efficacy of *Trichoderma harzianum*. Appl. Soil. Ecol. 35, 21–24.

Bardsley, S. J., Ngugi, H. K., 2013. Reliability and accuracy of visual methods used to quantify severity of foliar bacterial spot symptoms on peach and nectarine. Plant Pathol. 62, 460–474.

Bock, C. H., Poole, G., Parker, P. E., Gottwald, T. R., 2010. Plant disease severity estimated visually, by digital photography and image analysis, and by hyperspectral imaging. Crit. Rev. Plant Sci. 29, 59–107.

Boland, G., Hall, R., 1994. Index of plant hosts of *Sclerotinia sclerotiorum*. Can. J. Plant Pathol. 16, 93–108.

Bolton, M. D., Thomma, B. P., Nelson, B. D., 2006. *Sclerotinia sclerotiorum* (Lib.) de Bary: biology and molecular traits of a cosmopolitan pathogen. Mol. Plant Pathol. 7, 1–16.

Braido, R., Gonçalves-Zuliani, A. M. O., Nocchi, P. T. R., Belasque Júnior, J., Janeiro, V., Bock, C. H., Nunes, W. M. C., 2014. Development and validation of standard area diagrams as assessment aids for estimating the severity of citrus canker on unripe oranges. Plant Dis. 98,1543–1550.

Capucho, A. S., Zambolim, L., Duarte, H. S. S., Vaz, G. R. O., 2011. Development and validation of a standard area diagram set to estimate severity of leaf rust in *Coffea arabica* and *C. canephora*. Plant Pathol. 60, 1144–1150.

Clark, R. B., 1975. Characterization of phosphatase of intact maize roots. J. Agric. Food Chem. 23, 458–460.

Debona, D., Nascimento, K. J. T., Rezende, D., Rios, J. A., Bernardeli, A. M. A., Silva, L. C., Rodrigues, F. A., 2015. A set of standard area diagrams to assess severity of frogeye leaf spot on soybean. Eur. J. Plant Pathol. 142, 603–614.

Del Ponte, E. M., Pethybridge, S. J., Bock, C., Michereff, S. J., Machado, F. J., Spolti, P., 2017. Standard area diagrams for aiding severity estimation: scientometrics, pathosystems and methodological trends in the last 25 years. Phytopathology. 10, 1161–1174.

Del Río, L. E., Bradley, C. A., Henson, R. A., Endres, G. J., Hanson, B. K., McKay, K., Halvorson, M., Porter, P. M., Le Gare, D. G., 2007. Impact of sclerotinia stem rot on yield of canola. Plant Dis. 91, 191–194.

Dolinski, M. A., Duarte, H. S. S., Silva, J.B., May De Mio, L. L., 2017. Development and validation of a standard area diagram set for assessment of peach rust. Eur. J. Plant Pathol. 148, 817–824.

Domiciano, G. P., Duarte, H. S. S., Moreira, E. N., Rodrigues, F. A., 2014. Development and validation of a set of standard area diagrams to aid in estimation of spot blotch severity on wheat leaves. Plant Pathol. 63, 922–928.

Duarte, H. S. S., Zambolim, L., Capucho, A. S., Nogueira Júnior, A. F., Rosado, A. W. C., Paul, P. A., Cardoso, C. R., Mizubuti, E. S. G., 2013. Development and

validation of a set of standard area diagrams to estimate severity of potato early blight. Eur. J. Plant Pathol. 137, 249–257.

Gamer, M., Lemon, J., Fellows, I., 2012. irr: Various Coefficients of Interrater Reliability and Agreement. R Package Version 0.84.

Garcia, R. Á., Juliatti, F. C., 2012. Avaliação da resistência da soja a *Sclerotinia sclerotiorum* em diferentes estádios fenológicos e períodos de exposição ao inóculo. Trop. Plant Pathol. 37, 196–203.

González-Domínguez, E., Martins, R. B., Del Ponte, E. M., Michereff, S. J., García-Jiménez, J., Armengol, J., 2014. Development and validation of a standard area diagram set to aid assessment of severity of loquat scab on fruit. Eur. J. Plant Pathol. 139, 413–422.

Hall, R., Phillips, L. G., 1996. Evaluation of parameters to assess resistance of white bean to white mold. Annu. Rep. Bean Improv. Coop. 39, 306–307.

Hoffman D. D., Hartman, G. L., Mueller D. S., Leitz, R. A., Nickell, C. D., Petersen, W. L., 1998. Yield and seed quality of soybean cultivars infected with *Sclerotinia sclerotiorum*. Plant Dis. 82, 826–829.

Kolkman, J. M., Kelly, J. D., 2002. Agronomic traits affecting resistance to white mold in common bean. Crop Sci. 42, 693–699.

Lage, D. A. C., Marouelli, W. A., Duarte, H. S. S., Café-Filho, A. C., 2015. Standard area diagrams for assessment of powdery mildew degree on tomato leaves and leaflets. Crop Prot. 67, 26–34.

Lehner, M. S., Lima, R. C., Carneiro, J. E. S., Paula Júnior, T. J., Vieira, R. F., Mizubuti, E. S. G., 2016. Similar aggressiveness of phenotypically and genotypically distinct isolates of *Sclerotinia sclerotiorum*. Plant Dis. 100, 360–366.

Lehner, M. S., Paula Júnior, T. J., Hora Júnior, B. T., Teixeira, H., Vieira, R. F., Carneiro, J. E. S., Mizubuti, E. S. G., 2015. Low genetic variability in *Sclerotinia sclerotiorum* populations from common bean fields in Minas Gerais State, Brazil, at regional, local and micro-scales. Plant Pathol. 64, 921–931.

Lehner, M. S., Pethybridge, S. J., Meyer, M. C., Del Ponte, E. M., 2017. Meta-analytic modelling of the incidence-yield and incidence-sclerotial production relationships in soybean white mould epidemics. Plant Pathol. 66, 460–468.

Lenz, G., Balardin, R. S., Corte, G. D., Marques, L. N., Debona, D., 2010. Diagrammatic scale for assessment of rice brown spot severity. *Ciência Rural*, *40*, 752–758 (in Portuguese).

Lin, L. I. K., 1989. A concordance correlation coefficient to evaluate reproducibility. Biometrics. 45, 255–268.

Madden, L. V., Hughes, G., van den Bosch, F., 2007. The study of plant disease epidemics. St. Paul: APS Press. 421 pp.

Mueller, D., Dorrance, A., Derksen, R., Ozkan, E., Kurle, J., Grau, C., Gaska, J., Hartman, G., Bradley, C., Pedersen, W., 2002. Efficacy of fungicides on *Sclerotinia sclerotiorum* and their potential for control of Sclerotinia stem rot on soybean. Plant Dis. 86, 26–31.

Nita, M., Ellis, M. A., Madden, L. V., 2003. Reliability and accuracy of visual estimation of phomopsis leaf blight of strawberry. Phytopathology. 93, 995–1005.

Nutter, F. W., Gleason, M. L., Jenco, J. H., Christians, N. L., 1993. Assessing the accuracy, intra-rater repeatability, and inter-rater reliability of disease assessment systems. Phytopathology. 83, 806–812.

Nutter, F. W., Schultz, P. M., 1995. Improving the accuracy and precision of disease assessments: selection of methods and use of computer-aided training programs. Can. J. Plant Pathol. 17, 174–184.

Purdy, L. H., 1979. *Sclerotinia sclerotiorum*: History, diseases and symptomatology, host ranges, geographic distribution and impact. Phytopathology. 69, 875–880.

Rios, J. A., Debona, D., Duarte, H. S. S., Rodrigues, F. A., 2013. Development and validation of a standard area diagram set to assess blast severity on wheat leaves. Eur. J. Plant Pathol. 136, 603–611.

Schwartz, H. F., Singh, S. P., 2013. Breeding common bean for resistance to diseases: a review. Crop Sci. 53, 1832–1844.

Shrout, P. E., Fleiss, J. L., 1979. Intraclass correlations: uses in assessing rater reliability. Psychol Bull. 86, 420–428.

Singh, S. P., Schwartz, H. F., 2010. Breeding common bean for resistance to diseases: A review. Crop Sci. 50, 2199–2223.

Steadman, J. R., 1983. White mold – a serious yield – limiting disease of bean. Plant Dis. 67, 346–350.

Steadman, J. R., Boland, G., 2005. White mold. In: Schwartz, H. F., Steadman, J. R., Hall, R., Forster, R. L. (Eds.), Compendium of Bean Diseases, second ed. Phytopathology. 44–46.

Stevenson, M., 2012. Epir: An R Package for the Analysis of Epidemiological Data. R package version 0.9–43.

Vale, F. X. R., Fernandes Filho, E. I., Liberato, J. R., 2003. QUANT: a software plant disease severity assessment. In: Close, R., Braithwaite, M., Havery, I. (Eds.), Proceedings of the 8th International Congress of Plant Pathology (pp. 105). New Zealand.

Vieira, R. A., Mesquini, R. M., Silva, C. N., Hata, F. T., Tessmann, D. J., Scapim, C. A., 2014. A new diagrammatic scale for the assessment of northern corn leaf blight. Crop Prot. 56, 55–57.

Vieira, R. F., Paula Júnior, T. J., Carneiro, J. E. S., Teixeira, H., Queiroz, T. F. N., 2012. Management of white mold in type III common bean with plant spacing and fungicide. Trop. Plant Pathol. 37, 91–101.

Yadav, N. V., Vos, S. M., Bock, C. H., Wood, B. W., 2013. Development and validation of standard area diagrams to aid assessment of pecan scab symptoms on fruit. Plant Pathol. 62, 325–35.

Yang, X. B., Lundeen, P., Uphoff, M. D., 1999. Soybean varietal response and yield loss caused by *Sclerotinia sclerotiorum*. Plant Dis. 83, 456–461.

Yi, Q., Wang, P. P., He, Y., 2008. Reliability analysis for continuous measurements: equivalence test for agreement. Stat. Med. 27, 2816–2825.

Table 1 Effect of the use of a set of standard area diagrams (SADs) as an assessment aid on bias, precision and agreement of estimates of severity of white mold (SWM) on common bean leaflets made by raters with or without experience in SWM assessment.

Experience	LCC statistic	Means		95% CI[a] of the difference between means
		No SADs	With SADs	
Inexperienced	Scale shift (v)[b]	1.08	1.05	-0.159, 0.120
	Location shift (μ)[c]	0.30	0.15	-0.363, 0.100
	Bias correction factor (C_b)[d]	0.86	0.98	**0.062, 0.181**
	Correlation coefficient (r)[e]	0.93	0.98	**0.022, 0.080**
	Concordance coefficient (ρ_c)[f]	0.81	0.96	**0.088, 0.231**
	Inter-rater coefficient of determination (R^2)[g]	0.77	0.92	**0.117, 0.182**
Experienced	Scale shift (v)	1.03	1.04	-0.046, 0.073
	Location shift (μ)	0.12	0.18	-0.038, 0.148
	Bias correction factor (C_b)	0.97	0.98	-0.008, 0.031
	Correlation coefficient (r)	0.96	0.98	**0.011, 0.026**
	Concordance coefficient (ρ_c)	0.94	0.96	-0.008, 0.031
	Inter-rater coefficient of determination (R^2)	0.83	0.95	**0.005, 0.053**

[a] Bootstrap calculated difference between means and confidence intervals (CIs). If the CIs embrace zero, difference is not significant at the 5% level. Bold numbers represent significance of the difference.
[b] Scale or slope shift (systematic bias) relative to the perfect relationship (1 = perfect relation between x and y).
[c] Location or height shift (constant bias) relative to the perfect relationship (0 = perfect relation between x and y).
[d] Bias correction factor that measures how far the best-fit line deviates from a line at 45°. No deviation from the 45° line occurs when $C_b = 1$. C_b is calculated from v and μ and is a measure of accuracy.
[e] Correlation coefficient (r) that measures precision.
[f] Lin's concordance correlation coefficient (ρ_c) combines both precision (r) and accuracy (C_b) ($\rho_c = r.C_b$) to measure agreement with the actual value (Lin, 1989).
[g] Mean coefficients of determination estimated from pairwise comparisons of assessments by visual raters.

Table 2 Effect of rater experience on the bias, precision and overall agreement of estimates of severity of white mold made by ten raters either unaided or aided by a standard area diagram set (SADs).

Experience	LCC statistic	Means		95% CI[a] of the difference between means
		Inexperienced	Experienced	
No SADs	Scale shift (v)[b]	1.08	1.03	-0.218, 0.150
	Location shift (μ)[c]	0.30	0.12	-0.485, 0.148
	Bias correction factor (C_b)[d]	0.86	0.97	**0.041, 0.171**
	Correlation coefficient (r)[e]	0.93	0.96	**0.009, 0.064**
	Concordance coefficient (ρ_c)[f]	0.81	0.94	**0.052, 0.207**
	Inter-rater coefficient of determination (R^2)[g]	0.77	0.83	**0.020, 0.084**
SADs	Scale shift (v)	1.05	1.04	-0.048, 0.033
	Location shift (μ)	0.15	0.18	-0.062, 0.113
	Bias correction factor (C_b)	0.98	0.98	-0.018, 0.007
	Correlation coefficient (r)	0.98	0.98	-0.003, 0.016
	Concordance coefficient (ρ_c)	0.96	0.96	-0.019, 0.020
	Inter-rater coefficient of determination (R^2)	0.92	0.95	**0.014, 0.039**

[a] Bootstrap calculated difference between means and confidence intervals (CIs). If the CIs embrace zero, difference is not significant at the 5% level. Bold numbers represent significance of the difference.

[b] Scale or slope shift (systematic bias) relative to the perfect relationship (1 = perfect relation between x and y).

[c] Location or height shift (constant bias) relative to the perfect relationship (0 = perfect relation between x and y).

[d] Bias correction factor that measures how far the best-fit line deviates from a line at 45°. No deviation from the 45° line occurs when $C_b = 1$. C_b is calculated from v and μ and is a measure of accuracy.

[e] Correlation coefficient (r) that measures precision.

[f] Lin's concordance correlation coefficient (ρ_c) combines both precision (r) and accuracy (C_b) ($\rho_c = r.C_b$) to measure agreement with the actual value (Lin, 1989).

[g] Mean coefficients of determination estimated from pairwise comparisons of assessments by visual raters.

Fig. 1 Symptoms of white mold on common bean leaflets inoculated with *Sclerotinia sclerotiorum*.

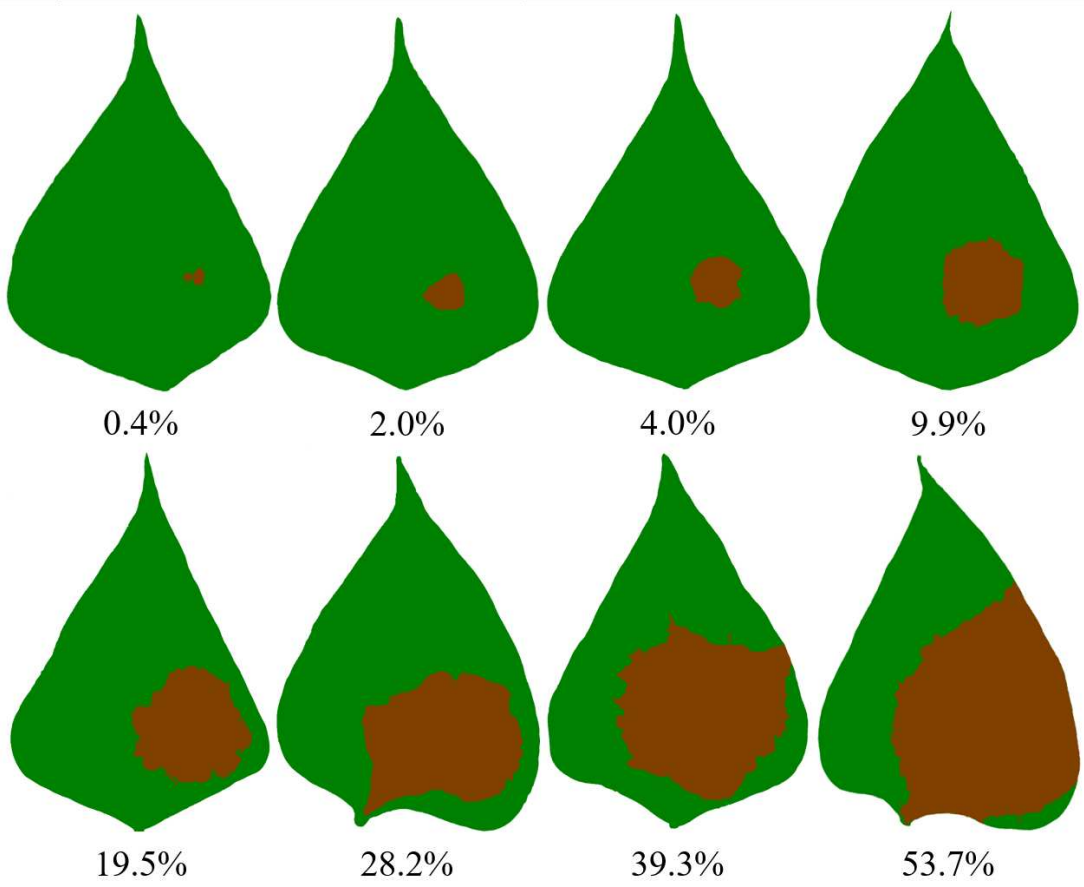

Fig. 2 Set of standard area diagrams (SADs) developed as an aid for assessment of white mold severity on common beans leaflets. Values represent the percentage (%) of the leaflet area showing white mold symptoms.

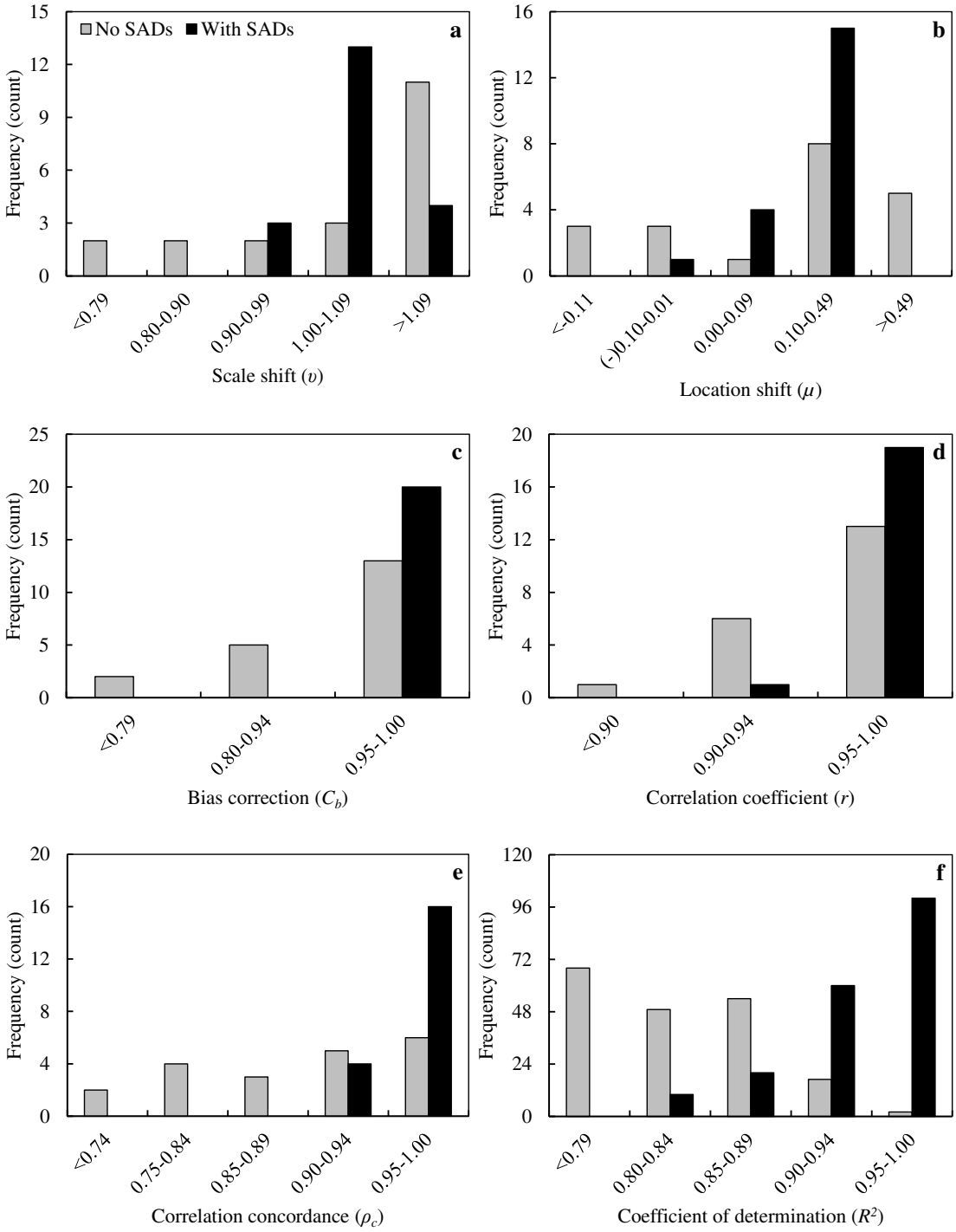

Fig. 3 Frequency of bias, precision and agreement and inter-rater reliability without and with use of a set of standard area diagrams (SADs) as an assessment aid by 20 raters who assessed 50 images of white mold-diseased common bean leaflets. (a) Scale shift (or systematic bias, υ), (b) location shift (or constant bias, μ), (c) bias

correction factor (C_b), (d) correlation coefficient (r), (e) Lin's concordance correlation coefficient (ρ_c), and (f) coefficient of determination (R^2).

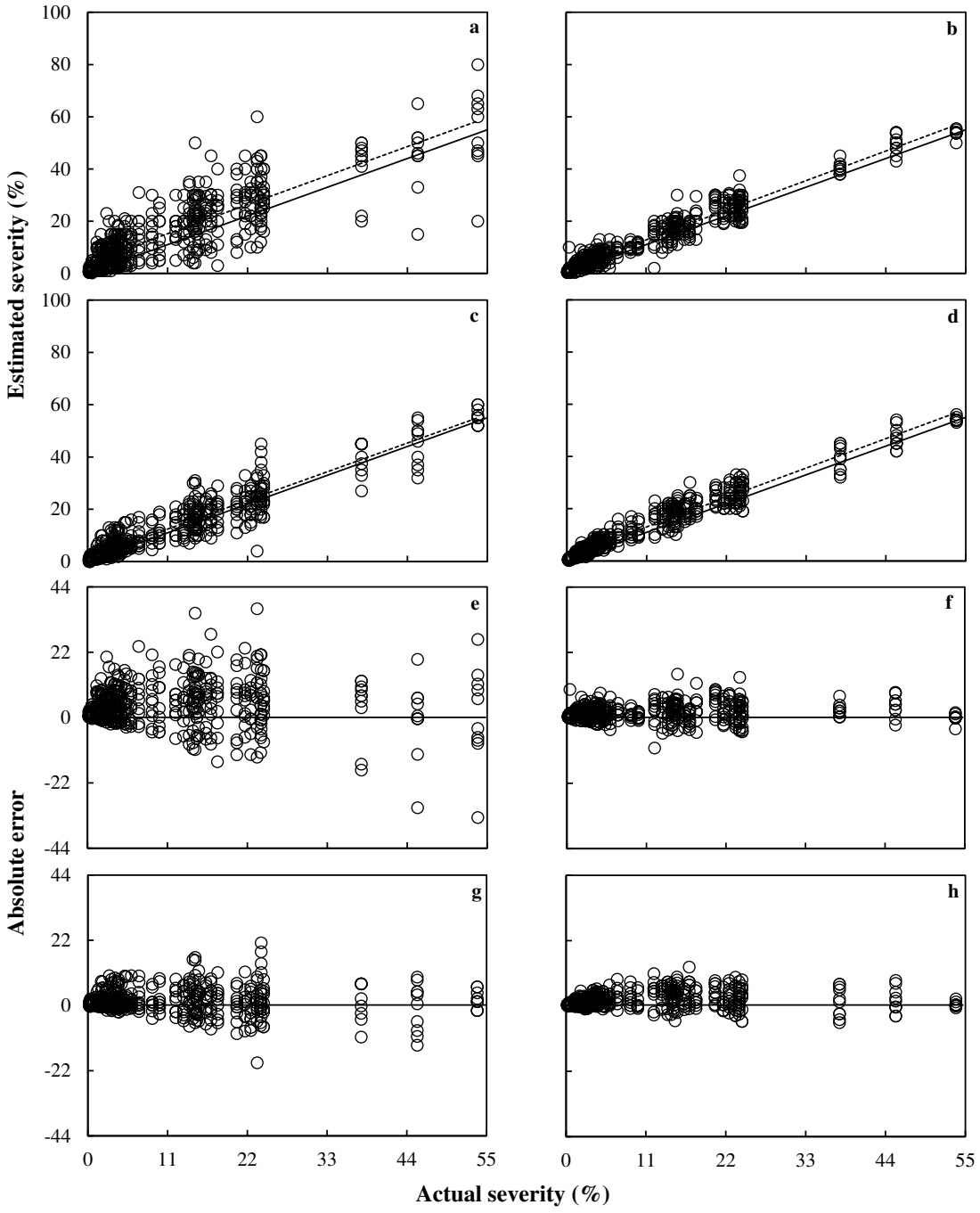

Fig. 4 Relationship between actual and estimated severity of white mold assessed on 50 common bean leaflets by (a, b) ten inexperienced and (c, d) ten experienced raters, and absolute errors (estimated severity minus actual severity) for each of (e, f)

ten inexperienced and (g, h) experienced raters (a, c, e, g) without and (b, d, f, h) with the use of a standard area diagram set (SADs). In (a-d), the solid line represents the best-fit linear regression line, whereas the dotted line is the concordance line, which represents perfect agreement between actual and estimated severity (slope of 1, intercept of 0).

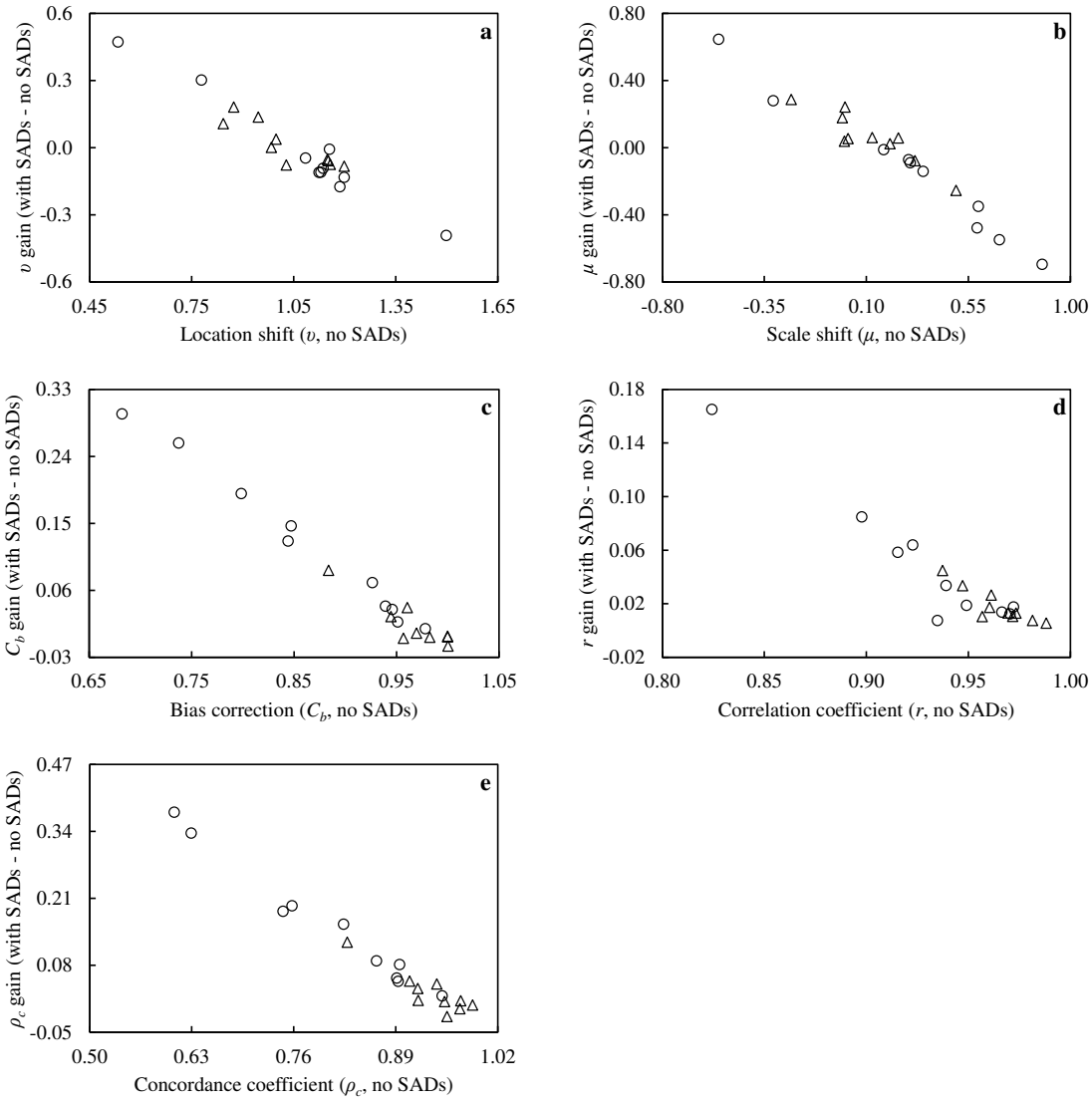

Fig. 5 The relationship between gain [difference between the estimate with and without use of a set of standard area diagrams (SADs)] for measures of (a) location shift (or systematic bias, υ), (b) scale shift (or constant bias, μ), (c) bias correction

factor (C_b), (d) correlation coefficient (r), and (e) Lin's concordance correlation coefficient (ρ_c) of visual severity estimates made by 10 inexperienced (*circles*) and 10 experienced (*triangles*) raters for a set of 50 images of white mold-diseased common bean leaflets.